Ozonation of Chloridazon Metabolites: Identification of Oxidation Products and Reaction Pathways

Zur Erlangung des akademischen Grades eines

DOKTORS DER NATURWISSENSCHAFTEN

(Dr. rer. nat.)

Fakultät für Chemie und Biowissenschaften
Karlsruher Institut für Technologie (KIT) - Universitätsbereich
genehmigte

DISSERTATION

von

Diplom-Lebensmittelchemikerin

Nina Jane Schatz

aus Reutlingen

Dekan: Prof. Dr. Martin Bastmeyer
Referent: Prof. Dr. Sabine E. Kulling
Korreferent: Prof. Dr. Dr. Manfred Metzler
Tag der mündlichen Prüfung: 19.10.2012

The following thesis was completed in the Department of Analysis and Water Quality at the Technologiezentrum Wasser (TZW) Karlsruhe in co-operation with the Department of Safety and Quality of Fruit and Vegetables at the Max Rubner-Institut (MRI) Karlsruhe and the Department of Chemistry and Biosciences at the Karlsruher Institut für Technologie (KIT) between June 2009 and September 2012.

Contents

List of Abbreviations v
Zusammenfassung vii
1 Background 1
1.1 Application of ozone in drinking water treatment 1
1.1.1 Drinking water sources 1
1.1.2 Drinking water treatment 2
1.2 Ozone and ozone reactions 4
1.2.1 Reactions with carbon-carbon double bonds 6
1.2.2 Reactions with carbon-nitrogen double bonds 8
1.2.3 Reactions with amines 10
1.2.4 Reactions with aldehydes 11
1.2.5 Reactions with carbon-hydrogen bonds 12
1.3 Pesticides 13
1.3.1 Tolylfluanid 14
1.3.2 Chloridazon 15
1.3.3 Legal situation 16
2 Objective 18
3 Materials and Methods 19
3.1 Materials 19
3.1.1 Chemicals 19
3.1.2 Consumables 20
3.1.3 Equipment 21
3.2 Methods 21
3.2.1 Ozonation 21
3.2.2 Stock solutions 25
3.2.3 Determination of TOC 25
3.2.4 Determination of $SAC_{254\ nm}$ and $SAC_{436\ nm}$ 25
3.2.5 HPLC-DAD-Q-ToF-MS 26
3.2.6 HPLC-MS/MS 27
3.2.7 GC-MS 29
3.2.8 IC-CD 29
3.2.9 Fraction collection 30
3.2.10 Syntheses 32
3.2.10.1 (2-Methyl)-4,5-dihydroxy-pyridazine-3-one 32
3.2.10.2 5-Amino-4-hydroxy-pyridazine-3-one 32

4 Results and discussion 34
4.1 Identified oxidation products of DPC in MilliQ water 34
4.1.1 Pyridazine-3,4,5-trione (OP 2) 35
4.1.2 6-Azauracil (OP 4) 37
4.1.3 OPs derived from 6-azauracil 39
4.1.3.1 N-(Nitrosocarbamoyl)-2-oxoacetamide (OP IV) 40
4.1.3.2 5-Hydroxyhydantoin (OP I) 42
4.1.3.3 Parabanic acid (OP III) 43
4.1.3.4 Oxaluric acid (OP II) and small organic compounds 44
4.1.3.5 1,2,4-Triazinane-3,5,6-trione (OP V) 46
4.1.4 1,2-Dihydro-1,2,4-triazine-3,6-dione (OP 3) 47
4.1.5 Summary and discussion of the oxidation pathway of DPC 50
4.2 Development and application of an SPE enrichment method 52
4.2.1 Sample preparation 52
4.2.2 Method development 52
4.2.2.1 Selection of SPE material 52
4.2.2.2 Optimization of enrichment parameters 53
4.2.2.3 Influence of sample volume and concentration 54
4.2.3 Method validation 56
4.2.3.1 Compound stability 56
4.2.3.2 Recovery, RSD, LOD and LOQ 57
4.2.3.3 Determination of matrix effects 58
4.2.4 Validated SPE method 60
4.2.5 Application and determination of 6-azauracil formation 61
4.2.5.1 Formation in drinking water 61
4.2.5.2 Formation in river water 62
4.2.5.3 Formation in environmentally relevant concentrations 64
4.2.6 Summary and discussion of the SPE method and application 65
4.3 Identified oxidation products of M-DPC in MilliQ water 65
4.3.1 M-OA-HEA (OP 3) 67
4.3.2 CM-MHAA (OP 1) 70
4.3.3 2-Methyl-pyridazine-3,4,5-trione (OP 6) 72
4.3.4 5-Amino-4-hydroxy-pyridazine-3-one (OP 7) 73
4.3.5 1-Methyl-6-azauracil (OP 8) 74
4.3.6 2-Methyl-4-chloro-5-amino-pyridazine-3,6-dione (OP 9) 76
4.3.7 Desphenyl-chloridazon (OP 10) 76
4.3.8 Small organic compounds 77

4.3.9 Oxidation products of M-DPC identified in drinking water 78
4.3.10 Summary and discussion of the oxidation pathway for M-DPC 81
5 Summary 83
6 Glossary 86
7 References 89
8 Appendix 99
8.1 Water parameters 99
8.2 Supplementary information to the results section 100
List of Publications 105
List of Conference Contributions 105
Curriculum Vitae 107
Acknowledgements 109

List of Abbreviations

ALARA	As low as reasonably achievable
AOP	Advanced oxidation process
Arb. U.	Arbitrary units
AU	Absorption units
CD	Conductivity detector
CID	Collision induced dissociation
DAD	Diode array detector
DBE	Double bond equivalent
DBP	Disinfection by-product
DMS	N,N-dimethylsulfamide
DOC	Dissolved organic carbon
DOM	Dissolved organic matter
DPC	Desphenyl-chloridazon (5-amino-4-chloro-pyridazine-3-one)
DW	Drinking water
EI	Electron impact
EIC	Extracted ion chromatogram
GC	Gas chromatography
HPLC	High performance liquid chromatography
IC	Ion chromatography
LOD	Limit of detection
LOQ	Limit of quantification
m/z	Mass versus charge
M-DPC	Methyl-desphenyl-chloridazon (2-methyl-5-amino-4-chloro-pyridazine-3-one)
MQ	MilliQ water
MS	Mass spectrometry
OP	Oxidation product
ppm	Parts per million
Q-ToF	Quadrupole time-of-flight
SAC	Spectral absorption coefficient
SPE	Solid-phase extraction

TIC	Total ion chromatogram
TOC	Total organic carbon
UV/VIS	Ultraviolet visible spectroscopy

Zusammenfassung

Die Identifizierung von Oxidationsprodukten (OPs), die während der Trinkwasseraufbereitung mit Ozon aus organischen Mikroverunreinigungen entstehen, ist ein aktuelles Forschungsgebiet. Der Aufklärung von Oxidationsprodukten wird seit 2007 eine erhöhte Aufmerksamkeit zuteil, als die Umwandlung eines nicht-relevanten Fungizid Metaboliten in eine kanzerogene Substanz entdeckt wurde.

In der vorliegenden Arbeit wurden erstmalig die OPs der Metaboliten Desphenyl-chloridazon (DPC) und Methyl-desphenyl-chloridazon (M-DPC) des Herbizides Chloridazon untersucht. Hierbei lag der Fokus auf der Strukturaufklärung und der Relevanz für die Wasseraufbereitung. Für die Identifizierung der OPs wurden bekannte Ozonungsmechanismen auf die Strukturen von DPC und M-DPC übertragen. Die Analyse von ozonten Proben wurde mit modernen analytischen Methoden wie HPLC-DAD-Q-ToF-MS, GC-MS und IC-CD durchgeführt.

Bei der Ozonung von DPC wurden sechs OPs detektiert, von denen vier OPs in ihrer Struktur aufgeklärt werden konnten. Eines dieser OPs wurde als 6-Azauracil identifiziert. Ein Bildungsmechanismus, der über die ersten Schritte des Criegee-Mechanismus abläuft, wurde postuliert. Allerdings entsteht nach der Öffnung des Ozonids durch den Angriff des primären Amins an der Ketogruppe ein neues 1,2,4-Triazin-Ringsystem. Für 6-Azauracil werden eine Vielzahl adverser Effekte für Mensch und Umwelt beschrieben. So werden zum Beispiel Enzyme, die an der RNA-Basen-Synthese beteiligt sind, gehemmt. Um spurenanalytische Untersuchungen von DPC und 6-Azauracil in Trinkwasser zu ermöglichen, wurde eine SPE-Methode etabliert und validiert. Die Bildung von 6-Azauracil unter umweltrelevanten DPC-Konzentrationen (10 µg/L) und wasserwerksüblichen Ozondosen (0,5 mg/L) konnte bestätigt werden. Die maximale molare Bildung von 6-Azauracil, bezogen auf die DPC-Ausgangskonzentration, lag bei 3,6 % (0,3 µg/L). Bei einem Überschuss an Ozon wird 6-Azauracil weiter oxidiert. Auch dieser Oxidationspfad wurde bis zur Mineralisierung aufgeklärt.

Für M-DPC wurden zehn OPs identifiziert und – basierend auf der Position des Primärangriffs des Ozons – in drei Gruppen eingeteilt. Der Hauptreaktionsweg erfolgt über den Angriff von Ozon an der C-C-Doppelbindung und führt u.a. zur Öffnung des Pyridazinringes. Nebenreaktionswege führen über die Oxidation der C-N-Doppelbindung zu einem chlorierten OP und über die Oxidation der Methylgruppe zu weiteren OPs, unter anderem auch zu DPC. Ein Überschuss an Ozon führt zur weiteren Oxidation der identifizierten OPs und der Bildung von Karbonsäuren. Für alle identifizierten OPs wurden Reaktionsmechanismen postuliert, die ihre Bildung erklären.

1 Background

Over the last decades, a stable trend in the use of pesticides, pharmaceuticals or other industrial chemicals could be observed. Most of these compounds undergo natural transformation processes in the environment. This quite often results in the formation of mostly less active but more polar metabolites. Due to their high polarity and often increased stability, the metabolites are able to reach groundwaters and contaminate them. The improved sensitivity of analytical instruments in recent years has resulted in a steady increase in the number of detectable pollutants in groundwater. As almost 70 % of German drinking water is gained from groundwater, its ongoing pollution is critically observed.

Waters used for drinking water preparation undergo various treatment steps, such as chlorination or ozonation. Due to these disinfection steps, the formation of disinfection by-products (DBPs), some showing genotoxic or cytotoxic potential, has become an area of research over the last decades. In general, the treatment of water with ozone leads to a lower formation of halogenated DBPs compared to the treatment with chlorine. In Germany, treatment with ozone is quite often employed when drinking water is obtained from surface water or water influenced by surface water (for example riverbank filtrate). Due to the lack of knowledge regarding the identification of oxidation products (OPs) formed during ozonation, a surge in publications can be observed in this area in the last years. The scientific results clearly demonstrate that OPs formed during ozonation can have adverse effects on human health.

To provide an insight into the different aspects of the problem this chapter will give an overview on basic drinking water treatment steps and on the application of ozone in drinking water treatment. It will explain mechanisms involved when ozone attacks different chemical structures, group different pesticides and finally highlight the problem arising when pesticides are transformed through biotic or abiotic as well as through anthropogenic processes like ozonation.

1.1 Application of ozone in drinking water treatment

1.1.1 Drinking water sources

In Germany, there are approximately 6400 water suppliers [1]. Hence, the water supply in Germany, compared to that of other countries such as France, Great Britain or Italy, consists of rather small entities. Half of the water suppliers are situated in the south of Germany (Baden-Württemberg and Bavaria) [2]. Approximately 70 % of the water suppliers produce under 0.5 million m^3 water annually, which represents only 7 % of the total drinking water

production [1]. With a production of over 10 million m^3 per year about 100 water suppliers provide 50 % of the total water amount. The annual water production volume in Germany ranges around 5.4 billion m^3 [1]. The waters used for drinking water preparation come from different sources. Groundwater fills underground openings in the earth´s crust and follows gravity. It is generated through percolated rainfall which usually has a long seepage way and residence time underground. Spring water is groundwater which appears through free incline, although it differs from “real” groundwater regarding its formation mechanism, its nature and its form of catchment. Artificially recharged groundwater, also known as infiltration water, is groundwater which is enriched through artificial percolation of, for example, surface water via basins, suction wells or horizontal percolation lines. Riverbank filtrate is surface water that naturally infiltrates via riverbanks and riverbeds. Surface water is water from standing or flowing above-ground water especially from reservoirs, lakes and rivers, but also from seawater. The composition of surface waters strongly differs depending on time of year and location, and in particular on the type and utilization of the catchment area [3].

Compared to other European countries such as Great Britain, Spain or Poland that produce drinking water mainly from surface water [4], Germany produces 66 % from groundwaters and 8 % from spring waters which together make up 74 % of the total drinking water production [1,5]. Surface water, impounding bank filtrate and artificially recharged ground-water account for the remaining percentage. Due to the passage through the atmosphere, the soil and sediment, naturally found waters are impure and differ in parameters such as pH value, water hardness or buffering capacity depending on their geological origin [3].

1.1.2 Drinking water treatment

When possible, natural waters used for drinking water abstraction should meet the legal requirements for drinking waters. Because waters of this quality are not available everywhere in sufficient quantities, it is necessary to treat waters in several steps (as specified in the German standard DIN 2000) before distributing it as drinking water [6]. The requirements for treatment steps are described in the worksheet W 202 of the German Technical and Scientific Association for Gas and Water (DVGW) [7].

The aims of these treatment processes can generally be divided into two categories. The first is the removal of unwanted compounds from the water; examples here are de-ironing or desalination. The second is the supplementation of compounds to achieve a specific pH value or a specific corrosion behavior. The treatment processes can also be grouped depending on the mechanism behind each process. Basically, they can be assigned to three major groups, namely physical, chemical and biological processes [3]. The physical and chemical processes can again be subdivided, although a strict classification is not always

possible. Treatment steps include sedimentation and flotation, in which the separation of pollutants and water is achieved through their different densities. During flocculation, a method based on chemical and physical mechanisms, chemicals (mostly aluminum or ferric salts) are added to waters and cause finely dispersed colloids to aggregate, allowing them to be removed [8,9]. Through aeration, volatile compounds such as carbon dioxide, hydrogen sulfide, methane, halogenated hydrocarbons and substances affecting odor or taste are removed [3]. To remove small particles from waters various membranes can be employed. These differ in terms of their porosity and thus in the size of particles that are removed [10,11]. Activated carbon is applied to remove dissolved organic, mostly unpolar, water constituents [9]. Artificially recharged groundwater undergoes a complex treatment process, which can consist of mechanical removal of particular substances in the water/soil contact zone, sorption of substances to the biomass formed in the same zone, biodegradation of nutrient matter through algae biomass and bacteria, and ion exchange with silt in the ground [3]. The division of the chemical treatment steps can be made in neutralization (with the aim of pH adjustment according to the Drinking Water Ordinance), ion exchange (with the aim of desalination and removal of water hardness) and oxidation (with the aim of making pollutants more polar and more easily biodegradable) [3,9].

In drinking water production, oxidative treatment steps are used to modify and subsequently remove inorganic compounds such as iron, manganese or ammonium [12]. Furthermore, ozonation can reduce the formation of chlorinated organic substances in a subsequent chlorination step [13]. Besides objectionable coloration, caused through chromophores present in humic substances of waters such as artificially impounded surface water, odor and flavor can be removed in this treatment step. Not only natural impurities but also anthropogenic compounds such as pesticides or pharmaceuticals can also be reduced in concentration. To prevent microbial recontamination of the distribution network the ozonation step is usually not the last step in drinking water treatment but is followed by either a biological filtration step or a disinfection step with for example chlorine. In Germany, ozone, calcium hypochlorite, hydrogen peroxide, sodium peroxodisulfate, potassium peroxomono-sulfate and oxygen can be used as oxidizing agents in drinking water preparation [14-16]. The application of a combination of ozone and hydrogen peroxide, resulting in the formation of OH-radicals with an even greater oxidizing potential compared to ozone, is known as advanced oxidation process (AOP) but is not widespread in Germany [17].

Ozone can be used not only as oxidizing agent but also as a disinfectant [14]. Ozone is the only chemical oxidizing agent that is capable of killing parasites under economically practicable working conditions. Hence, it is of special interest to ensure the hygienic water quality when using surface waters for drinking water preparation [13]. Regarding the

formation of halogenated DBPs through the application of chlorine or chlorine dioxide, the use of ozone as alternative disinfectant is of growing interest in the US [18]. The maximum application dose for ozone is restricted to 10 mg/L and the residual ozone after application must not exceed 0.05 mg/L [14]. Depending on the raw water type, applied ozone concentrations vary, but usually are in a range of 0.2 mg/L to 1 mg/L [12].

In the last decade, the pollution of surface and groundwaters with pharmaceutically active compounds has been studied throughout the world [19]. Due to significant progress in analytical instrumentation, substances belonging to the classes of analgesics and anti-inflammatory drugs [20-22], antibiotics [23,24], beta blockers [25], blood lipid regulators [26], oral contraceptives [27,28] and contrast media [29,30] could be detected in the aquatic environment in the ng/L to µg/L level. More recently an increasing number of small and polar micropollutants have been detected in waters, which has again enhanced the demand for more effective techniques for their removal. Oxidation through treatment with ozone seems a promising technique for this and thus is the subject of intense research [31-33].

1.2 Ozone and ozone reactions

The ozone molecule, consisting of three oxygen atoms, is depicted in Figure 1.1 and can be described as a resonance hybrid of structures with an obtuse angle (116°45´ ± 30´) and two oxygen-oxygen bonds of equal length (1.278 ± 0.002 Å) [34]. Based on this structure, ozone can act as a 1,3-dipole, a nucleophile or an electrophile during reactions [35]. Furthermore, ozone is a strong oxidizing agent with a normal potential of 2.1 eV [36].

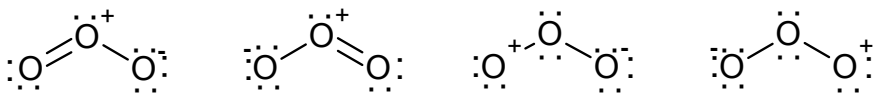

Figure 1.1: Proposed structures for the ozone molecule [34].

Investigations regarding the decomposition of ozone in water have revealed a complex mechanism that involves the formation of hydroxyl radicals, which are among the most reactive oxidizing agents in water and show short half-life times in the range of microseconds [37-39]. Figure 1.2 shows the basic cyclic chain mechanism and the species involved in the decomposition of ozone. Hydroxide ions can function as initiator of ozone decomposition, resulting essentially in the formation of hydroxyl radicals via several intermediates.

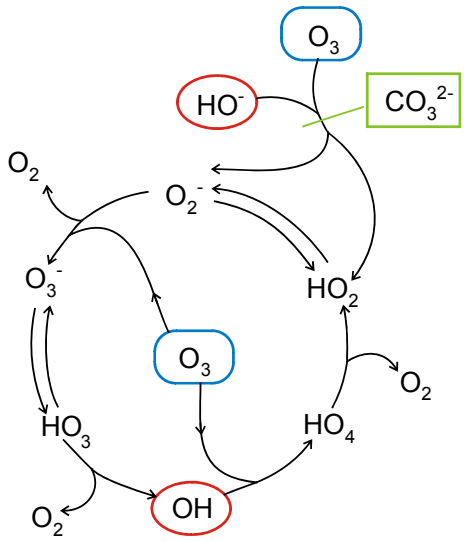

Figure 1.2: Proposed cyclic chain mechanism for the decomposition of ozone initiated by hydroxide ions in aqueous solutions in which carbonate functions as a inhibitor [modified from 40-43].

Based on the fact that ozone decomposes to radicals, organic pollutants can be oxidized in two ways, either through the direct oxidation by ozone or through the attack of hydroxyl radicals. These two pathways differ in their selectivity. The radicals are highly reactive and attack most organic compounds in an unspecific way [40,42,43]. Hence, the hydroxyl radicals will also react with compounds occurring naturally in the water matrix. Ozone, on the other hand, is highly selective with regard to reaction sites in molecules. It shows high reactivity towards activated aromatic compounds, unsaturated aliphatic molecules and compounds with hetero atoms such as nitrogen and sulfur [44-47]. An increase in pH value, temperature and dissolved organic matter (DOM) content results in a shift of the predominant way towards radical reactions, whereas an increase in carbonate concentrations leads to a shift towards ozone reactions [40,41,48]. It is possible to determine whether waters favor ozone or radical reactions by the R_{ct} value, which is defined as the ratio of radicals to ozone concentrations [49].

The following sections describe known ozonation mechanisms which can provide valuable assistance in the elucidation of OPs formed during ozonation and in some cases can help to predict reaction pathways. Three possible reaction sites for the attack of ozone on organic systems can be differentiated and will be described. The first possible pathway includes a cleavage of carbon-carbon or carbon-nitrogen double bonds. The second includes substitution of hydrogen atoms from aromatic rings, and the third includes oxididation of substituents of side chains of the aromatic ring [35,50,51]. Additional information can be found in literature regarding reactions of sulfides, triple bonds or ethers but will not be included in the following description as they are not of relevance for the present work [52].

1.2.1 Reactions with carbon-carbon double bonds

For the initial attack of ozone on carbon-carbon double bonds three possible mechanisms are known. Two of these mechanisms, the 1,3-dipolar cycloaddition (Criegee mechanism) and the electrophilic attack, will be described whereas the nucleophilic mechanism, being of minor relevance, will not be covered.

Criegee mechanism

In 1975, a three-step mechanism for the ozonation of alkenes was proposed, which is illustrated in Figure 1.3 and known as the Criegee mechanism [50]. In the first step, ozone attacks the double bond in the form of a 1,3-cycloaddition forming the so-called primary ozonide. This step is followed by a cyclo-reversion leading to the respective carbonyl oxide and a carbonyl compound. The final step, again a 1,3-cycloaddition, where the carbonyl oxide reacts with the carbonyl compound, results in the formation of the ozonide also known as 1,2,3-trioxolane [50].

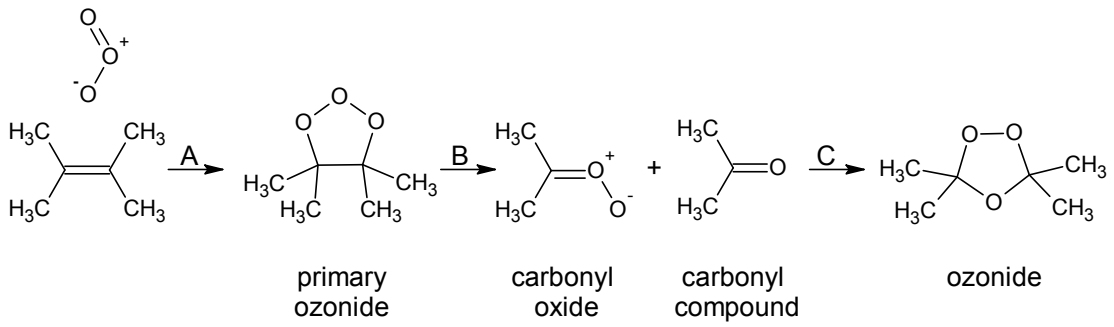

Figure 1.3: Criegee mechanism for the oxidation of a carbon-carbon double bond by ozone [modified from 50].

Five structures were proposed for the olefine-ozone-adduct which are illustrated in Figure 1.4 [50]. In reactions where, instead of the cleavage of the double bond, epoxides or their secondary OPs are formed, the σ-complexes or peroxy-epoxides must be assumed as reaction intermediates. These findings have been demonstrated for sterically strongly hindered olefins [50]. It is assumed that an oxygen molecule is immediately eliminated from the intermediates, forming the epoxides.

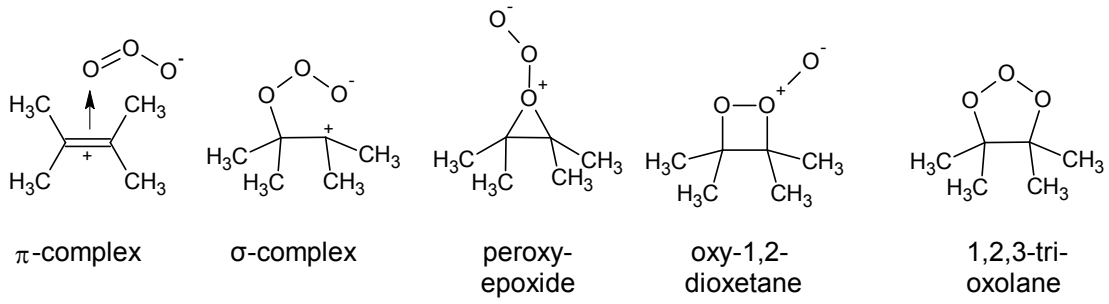

Figure 1.4: Structures proposed for the olefine-ozone-adduct [50].

Electrophilic attack

The ozonation of phenol has been studied in detail by several research groups [53-55]. The reaction of ozone with protic organic molecules like phenol is influenced by their dissociation state and hence is dependent on the pH value. As a rule, ozone favors an electrophilic attack with non-dissociated compounds [38,39]. Based on activation energy calculations for the cycloaddition and the electrophilic attack, it can be assumed that the latter is energetically favored. A mechanism for the electrophilic attack of ozone on phenol was proposed and resulted in the elimination of oxygen and formation of a catechol (Figure 1.5) [35,54,55].

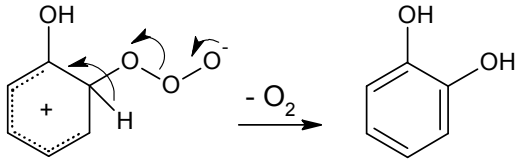

Figure 1.5: Proposed mechanism of the oxidation of an aromatic carbon-carbon double bond via electrophilic ozone attack [modified from 35].

Oxidation products and pathways

The initial attack of ozone on molecules is crucial for the amount of ozone needed for complete elimination of aromaticity. The reactivity of aromatic compounds towards ozone is highly dependent on the functional groups attached to the aromatic ring. Generally, aromatics can be differentiated in two groups depending on the substituents. The substituents can have either an activating or a deactivating influence on the reactivity of ozone towards the ring. Ortho-para groups, basically electron-donating moieties such as hydroxyls or primary amines, have an activating effect. An example for this are phenols that react with ozone to 1,2-catechols or 1,4-catechols [35,56]. In the second group electron-withdrawing substituents result in a deactivation of the ring through directing the attack of ozone in the unfavored meta position. Substituents in this group are -CHO, $-CONH_2$ and $-COCH_3$ [35]. For compounds containing electron-withdrawing groups, for example benzaldehyde, no hydroxylated oxidation products are detected after ozone treatment. In this case, the initial oxidation takes place on the functional group and, in the example of benzaldehyde, results in the oxidation and formation of benzoic acid [35]. Hence, activating moieties result in a primary reaction of the aromatic ring with ozone and thus require less ozone for the elimination of aromaticity. Deactivating moieties, however, require more ozone because the initial reaction with ozone occurs on the functional group and not on the aromatic ring [35].

Depending on the ozonation mechanisms (see above), the formation of different initial oxidation products (OPs) can be observed. The major difference in OP formation between

the two oxidation mechanisms is that in the primary OPs formed by the Criegee mechanism the ring is opened, whereas in those formed by electrophilic attack ring substitution occurs before ring opening (Figure 1.6). The further oxidation of these primary OPs can end, for both mechanisms, in the formation of the same OPs [57]. In general, the oxidation pathway of aromatics can be divided into three steps. In the first step, the loss of total aromaticity results in the formation of unsaturated aliphatics [35]. In the second step, further oxidation results in their saturation. In the third and final step, the oxidation of saturated oxygenated products leads to the mineralization of these compounds [35,56,58]. Generally, a decrease in reactivity towards ozone from step one to three can be noted [35].

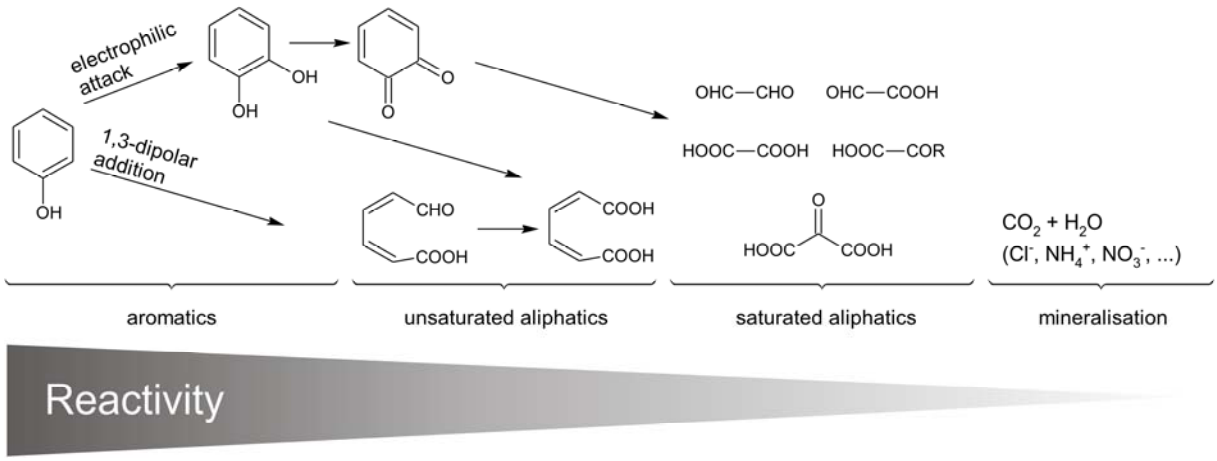

Figure 1.6: Proposed general scheme for the ozonation of simple aromatics [modified from 35,56-58].

1.2.2 Reactions with carbon-nitrogen double bonds

Ozone reacts not only with carbon-carbon double bonds but also with carbon-nitrogen double bonds [34,59]. Four principle ways of how the attack of ozone could occur are conceivable. The first possibility is analog to the Criegee mechanism, leading to four or five-membered rings. The second and third are that an electropilic attack occurs either at the nitrogen atom of the double bond or on the entire double bond. The fourth possibility is a nucleophilic attack on the carbon atom of the double bond. Based on experiments by Riebel et al. [34] and Erickson et al. [59], the ozonation of carbon-nitrogen double bonds can be divided into two principle reaction mechanisms, the nucleophilic and the electrophilic attack of ozone.

Nucleophilic attack

During the nucleophilic attack of ozone, one intermediate is proposed to be formed, which in turn can stabilize in three different reaction ways all having an elimination of oxygen in common (Figure 1.7). In the first, a ring closure results in the formation of an oxazirane; in

the second, an amide is formed by the shift of a proton; and in the third, the carbon-nitrogen double bond is cleaved forming benzaldehyde [34].

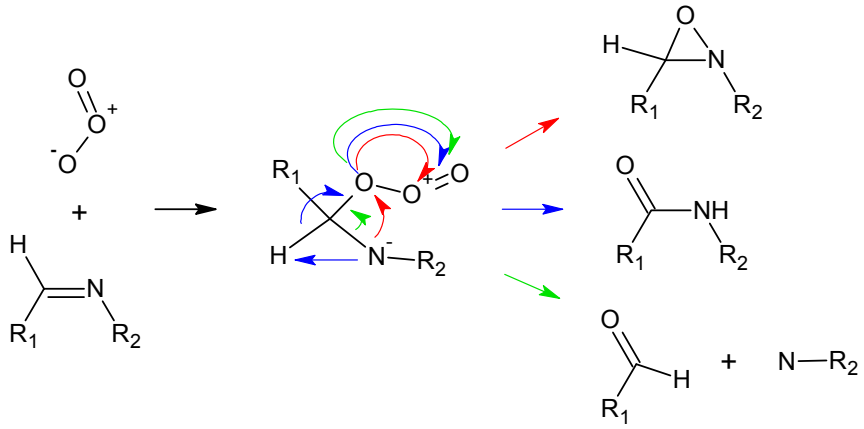

Figure 1.7: Mechanisms proposed for the oxidation of carbon-nitrogen double bonds via nucleophilic attack of ozone [modified from 34].

Electrophilic attack

The mechanism depicted in Figure 1.8 describes the electrophilic attack of ozone on nitrones. A nitrone is a functional group that consists of an N-oxide of an imine and shows zwitterionic properties. The intermediate formed can stabilize under cleavage of the carbon-nitrogen double bond forming one oxidation product with an aldehyde moiety and one with a nitroso moiety [52].

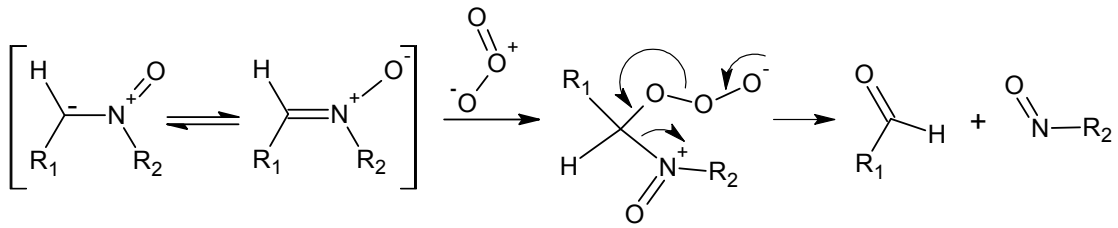

Figure 1.8: Mechanism proposed for the oxidation of a carbon-nitrogen double bond via electrophilic attack of ozone [modified from 52].

Ozonation of nitrones often results in a bluish green coloration of the solution, indicating the formation of nitroso compounds as precursors of nitro compounds [34].

Oxidation products and pathways

Erickson et al. [59] also analyzed the influence of a variety of substituents on the rate of primary ozone attack. Substituents with increasing electron-donating properties attached to the nitrogen atom of the double bond resulted in an increase in reactivity towards ozone. The major difference in OP formation is that in the nucleophilic attack several pathways are known, whereas in the electrophilic attack only one is known (Figure 1.9). Generally, non-cleavage and cleavage products are formed, where the latter are the major products. An

example is the ozonation of N-benzylidene-t-butylamine forming an amide and oxazirane as non-cleavage products and benzaldehyde and benzoic acid as cleavage products [34,59,60].

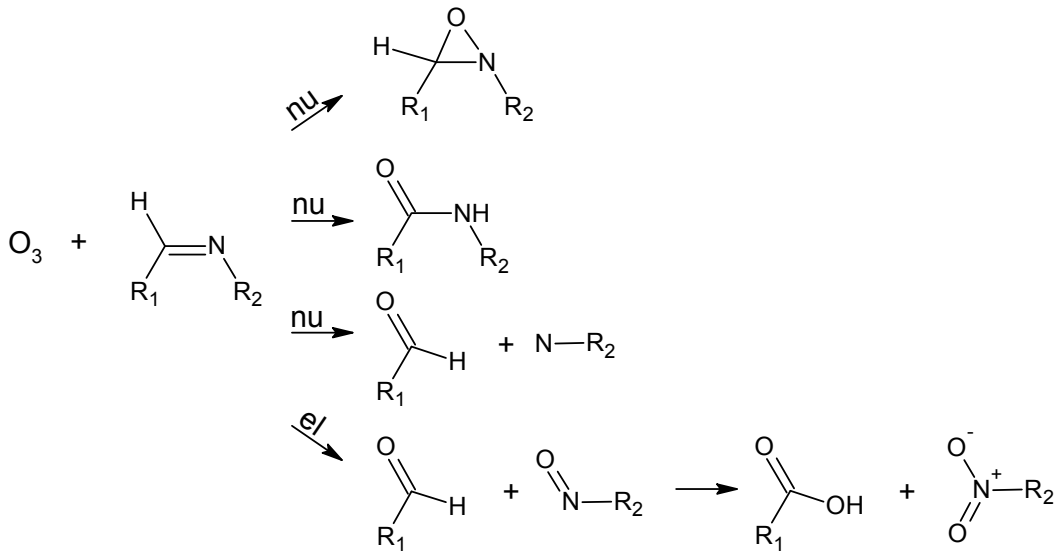

Figure 1.9: Possible oxidation products and basic pathways for the oxidation of carbon-nitrogen double bonds by ozone through nucleophilic (nu) or electrophilic (el) attack of ozone [modified from 34].

1.2.3 Reactions with amines

Ozone reacts not only with unsaturated carbon-carbon or carbon-nitrogen double bonds but also with amines. For the analysis of the reaction of ozone with amines, the fate of primary, secondary and tertiary amines was investigated in several organic solvents [61-67]. The reaction between ozone and amines is generally of electrophilic nature [63]. The mechanisms of amine ozonation are presented in Figure 1.10. Independent of the type of amine, the first step is proposed to form an amine-ozone adduct (Figure 1.10, structure I) [64]. This adduct can in turn react in at least three different ways. The first possibility (a) is the loss of oxygen accompanied by the formation of an amine oxide (II). In the case of tertiary amines, such as *t*-butylamine, the amine oxide (II) stabilizes under re-arrangement to a hydroxylamine (III). Further oxidation occurs via a dihydroxylamine, which under elimination of water results in the formation of a nitroso group (IV). The bluish green color that can often be observed during ozonation of amines is characteristic for the formation of nitrosoalkenes [61]. Nitrosoalkenes in turn are further oxidized to nitroalkenes (V) [62]. In the second possibility (b), in the presence of anions the amine-ozone adduct (I), which is in equilibrium with a nitrogen cation radical, can dissociate and stabilize under formation of a salt [64]. Two mechanisms (c_1 and c_2) have been proposed for the third reaction possibility. In both cases an intra-molecular side chain oxidation resulting in the formation of an amino alcohol (VII) occurs, which can react further [62-67].

The kind of amine as well as the side chains present in the molecule during the reaction can influence the favored mechanism of by-product formation and hence the ratios of the individual OPs formed. It has been stated that during ozonation of tertiary amines mainly side-chain oxidation and amine oxide formation can be observed. The amine to ozone ratio determines where the reaction ends and hence determines the end products formed [62-67].

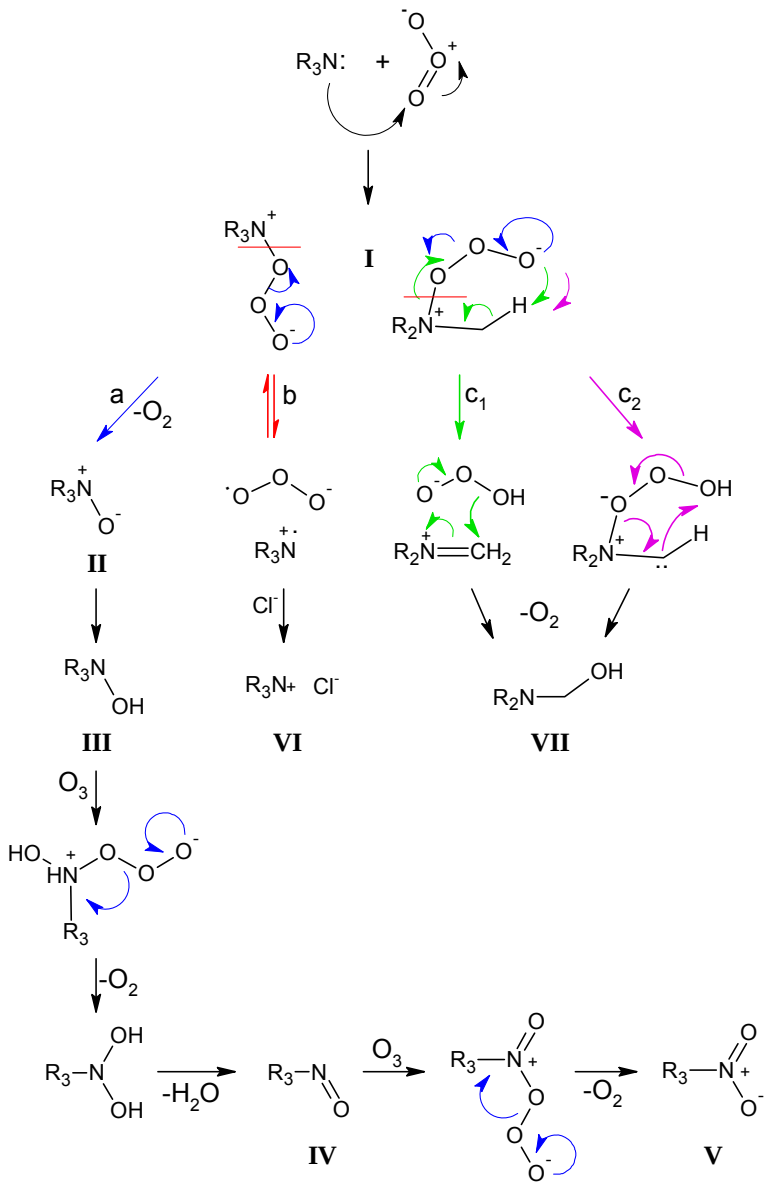

Figure 1.10: Mechanisms proposed for the oxidation of amines by ozone via electrophilic attack. Formed oxidation products and proposed reaction pathways [61-63].

1.2.4 Reactions with aldehydes

Although the reaction of ozone with aldehydes has been studied in several articles, the mechanism still remains uncertain [51,68-70]. Generally, the reaction of aldehydes with ozone is modestly endothermic [70]. The two possible proposed mechanisms for the reaction

of ozone with aldehydes are depicted in Figure 1.11 [51,68]. The initial reaction step can be described either as a concerted hydride ion abstraction or as a 1,3-dipolar insertion reaction where the positively charged end of the ozone molecule abstracts the hydride ion from the aldehyde group and the negatively charged end of the ozone molecule simultaneously attacks the developing acylium ion. The second reaction mechanism results in the formation of an instable intermediate (I) which breaks down to radicals, whereas in the first mechanism radicals are immediately formed. The decomposition of (I) follows at least four different routes (to benzoylperoxy radicals (a), benzoyl radicals (b), benzoyloxy radicals (c) and directly to benzoic acid (d)), of which the formation of the benzoylperoxy radical is considered to be the predominant route [51]. Recent computational investigations on the reaction of ozone with formaldehydes support the existence of the two competitive mechanisms [70].

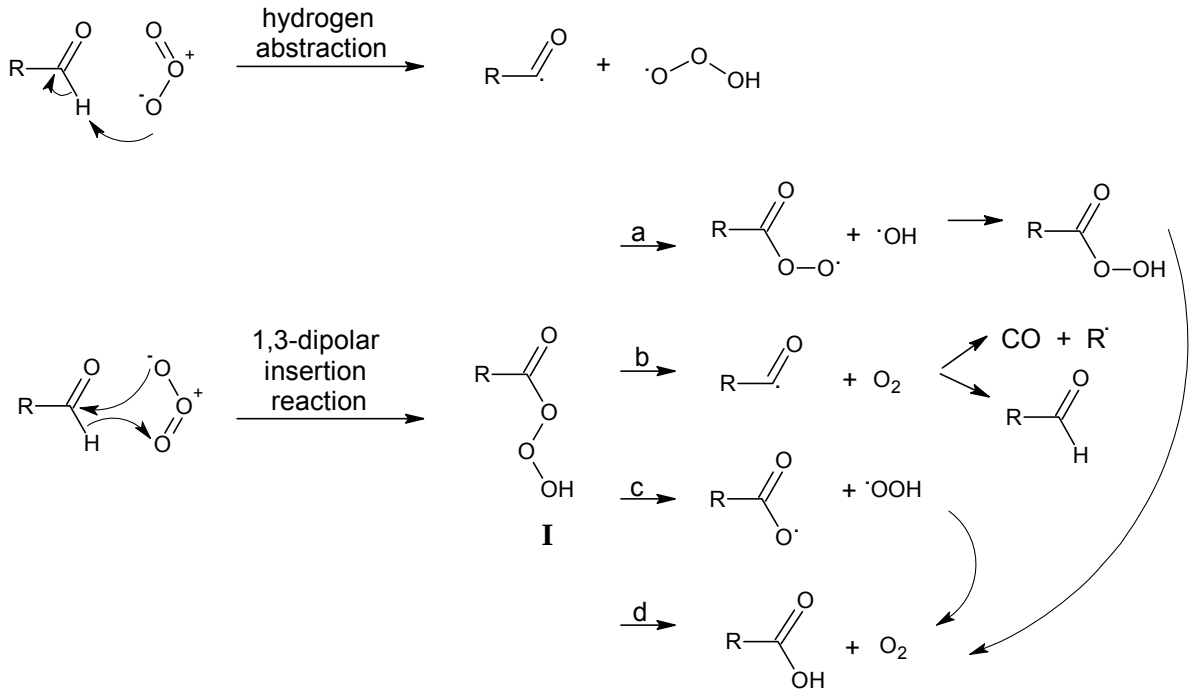

Figure 1.11: Mechanisms proposed for the oxidation of aldehydes by ozone [modified from 51,52].

1.2.5 Reactions with carbon-hydrogen bonds

Mechanistic investigations regarding the reaction of ozone with carbon-hydrogen bonds have been described in literature and four different mechanisms for the formation of a hydrotrioxide (Figure 1.12, structure I) through the reaction of ozone with carbon-hydrogen bonds have been discussed [71-73]. One possibility involves a 1,3-dipolar insertion (Figure 1.12, a), which has been proposed as a mechanism for the reaction of ozone with amines (see section 1.2.3) or aldehydes (see section 1.2.4). Furthermore, a mechanism via hydride abstraction through ozone has been proposed (Figure 1.12, b). The two other possibilities are a mechanism involving radicals formed through hydrogen atom abstraction or, again similar to

the the reaction of amines or aldehydes with ozone, a mechanism involving an initial attack at the heteroatom. Of these four mechanisms (a) and (b) agree best with the experimental results [73,74].

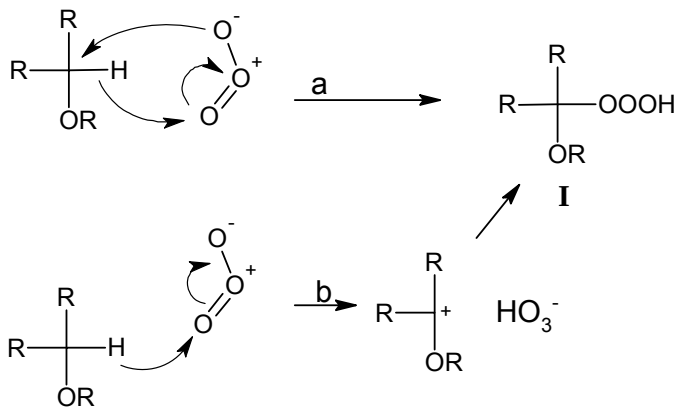

Figure 1.12: Two possible mechanisms for the oxidation of carbon-hydrogen bonds by ozone [modified from 72].

1.3 Pesticides

Over the past years an increase in research on pesticides and biocides regarding their environmental occurrence and fate could be observed. Different definitions exist for the terms pesticide and biocide. In this thesis the terms will be used as follows: Biocide as an umbrella term which covers also pesticides; pesticide as a compound used to control or destroy any pest. Pesticides can be subdivided either by their mode of action and hence by the target they attack or by their chemical configuration. Chemically, pesticides can be divided into chlorinated hydrocarbons, phosphoric acid esters, carbamates, urea derivatives, heterocyclic compounds and chlorinated phenoxyacetic acids. Differentiated by their target of attack, pesticides can be classified as acaricides, algicides, bactericides, fungicides, herbicides, insecticides, molluscicides, nematicides, ovicides, repellents, rodenticides and viricides [72,75-77].

Pesticides strongly differ in their persistency and, when released into the environment, can undergo biotic or abiotic transformation processes resulting in their transformation to so-called metabolites [78,79]. Generally, these transformations result in a loss of (or at least decrease in) the pesticide`s properties, reducing their threat to the environment. However, there are cases where the metabolites show an increased toxicity compared to the mother compound [80,81]. A known example is the transformation of the biocide triclosan, which is chemically situated in the group of polychlorinated phenoxyphenols and is commonly used in personal care products such as toothpastes, deodorants and soaps [82]. In the environment, it is not stable and is microbiologically modified resulting in the formation of its metabolite

methyl-triclosan which shows higher persistency and bioaccumulation potential than the mother compound [81,83,84]. Triclosan, therefore, is an example where environmental transformation leads to an increased risk for the environment.

Due to the new physico-chemical properties of the metabolites, such as an increase in persistency and polarity, they can in turn pose new risks regarding groundwater pollution. In 2007/2008 the Federal Office for Consumer Protection and Food Safety (BVL) in Germany published a list of 43 pesticide metabolites which may be found in groundwaters [85]. How these metabolites can pose a risk when they are present in waters during drinking water preparation will be demonstrated in the following example.

1.3.1 Tolylfluanid

The fungicide tolylfluanid was mainly used in fruit and plant cultivation, for example in strawberry plantations and wine-growing, and was also found in wood protecting agents [86]. Its fungicidal properties derive from the dichlorofluoromethylthiol moiety (Figure 1.13). In the environment, tolylfluanid undergoes degradation through cleavage of the active group and forms the metabolite N,N-dimethyl-N'-(4-methylphenyl)-sulfamide (DMST) with no fungicidal acitvity [86]. This metabolite in turn is not very stable and is further transformed to N,N-dimethylsulfamide (DMS), which is persistent in the environment (Figure 1.13). Its increased polarity enables it to percolate through the soil and contaminate waters. In Germany, DMS was detected not only in surface waters but also in groundwaters in concentrations ranging between 50-90 ng/L and 100-1000 ng/L, respectively [78]. Hence DMS can be present in waters used for drinking water preparation and thus can be exposed to ozone. The proposed transformation mechanism of DMS through ozone involves a re-arrangement of functional groups resulting in the elimination of sulfur dioxide and formation of N-nitrosodimethylamin (NDMA) [78,87]. These findings explained the elevated concentrations of NDMA found after ozonation in some waterworks [78]. Because most nitrosamines show high toxicity and carcinogenic effects in the low ng/L level, these results [88,89] led to the withdrawal of the approval for tolylfluanid by the Federal Office of Consumer Protection and Food Safety in Germany in 2010 [90].

This example demonstrates that natural transformation processes can reduce pesticidal activity. However, it also demonstrates the risks emanating from water treatment techniques such as ozonation when unknown contaminants are present in the waters used.

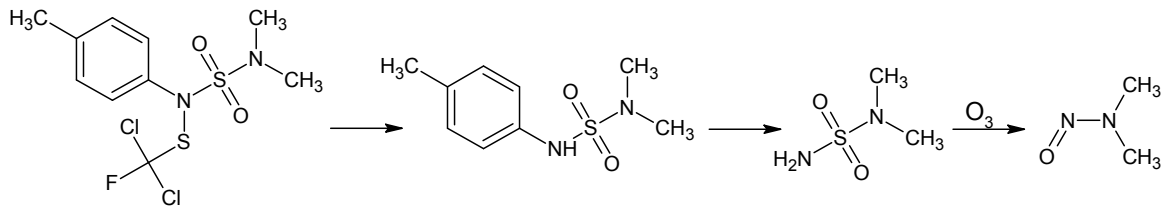

Figure 1.13: Structures of the fungicide tolylfluanid, its metabolites N,N-dimethyl-N'-(4-methyl-phenyl)-sulfamide (DMST) and N,N-dimethylsulfamide (DMS) formed through biological degradation processes as well as the ozonation product of DMS, N-nitroso-dimethylamin (NDMA) [modified from 78].

1.3.2 Chloridazon

Chloridazon has been used as a herbicide for over 40 years. Between 2003 and 2009 the amount of chloridazon annually sold in Germany ranged between 25-100 t [91]. It is used for pre-plant, pre-emergence, and early post-emergence to control annual broad-leaved weeds on sugar beets and red table beets [92]. Chloridazon is rapidly absorbed by roots and translocated to the leaves in the transpirational stream. Although chloridazon is foliar-absorbed, it is not translocated to other parts of the plant. The herbicidal effect of chloridazon is due to the inhibition of photosynthesis by blocking electron transport through photosystem II and by the Hill reaction [93,94].

Chemically, chloridazon belongs to the family of pyridazines, which were widely investigated in the 1960s because of their pesticidal activity and hence several ways to synthesize various derivates have been described [95]. Figure 1.14 illustrates the chemical structure of chloridazon, in which position 2 carries a benzene moiety, position 3 a keto group, position 4 a chlorine atom and position 5 an amino moiety. These modifications result in a change in chemical reactivity of the pyridazine ring. The presence of the amino moiety in position 5, an electron-releasing group, enables the molecule to be attacked by electrophiles (such as ozone, see section 1.2.1). The carbonyl group in position 3 additionally activates the pyridazine ring and enhances the liability of halogens, such as chlorine, to be substituted electrophilically [96].

In the environment microorganisms debenzylate chloridazon in position 2 of the pyridazine ring (Figure 1.14), resulting in the formation of its primary metabolite desphenyl-chloridazon (DPC) [79]. With the loss of the apolar benzene ring, the herbicidal properties are significantly reduced in the metabolite, whereas it shows an increased persistency and polarity. In soil, microorganisms can methylate DPC in position 2 and generate the secondary metabolite methyl-desphenyl-chloridazon (M-DPC) [79].

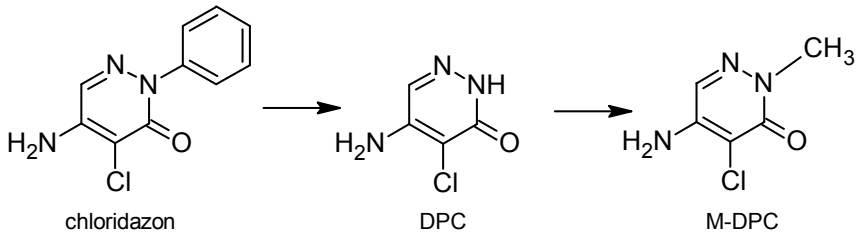

Figure 1.14: Structures of the herbicide chloridazon and its metabolites desphenyl-chloridazon (DPC) and methyl-desphenyl-chloridazon (M-DPC), which are formed in soil [modified from 79].

Because of its biodegradability, chloridazon could only rarely be found in surface and groundwaters [97]. However in 2007 the metabolites DPC and M-DPC were detected in groundwaters for the first time [79]. In 2007 and 2008 groundwaters in the south of Germany (Baden-Württemberg and Bavaria) revealed contaminations with DPC [98,99]. 42 % of the analyzed samples showed concentrations above 1 µg/L and 44 % showed concentrations between 0.11 and 1 µg/L [98]. The maximum concentration for DPC was 8.1 µg/L. M-DPC was present in concentrations over 1 µg/L in 8 % of the locations sampled and in concentrations ranging from 0.11 to 1 µg/L in 45 % of the waters [98]. Since then DPC as well as M-DPC were detected in various waters, such as creaks and rivers, especially in agriculturally stressed regions. These waters showed concentrations of DPC throughout the year in the lower µg/L range [100]. Generally, M-DPC is found almost as frequently as DPC in waters, but in lower concentrations [97].

1.3.3 Legal situation

There are several legislative regulations that have to be taken into account when dealing with pesticides, their metabolites as well as their concentration thresholds in drinking water. On the one hand there are the legislative regulations concerning authorization of pesticides [101,102] and on the other hand those concerning the safety of drinking water [103,104]. The Directive 91/414/ European Economic Community, replaced by the Regulation (EC) No 1107/2009, describes the placing of plant protecting agents on the market. In Germany, this Directive was transferred to national law by the Plant Protection Product Directive. The authority for the approval of pesticides in Germany is the Federal Office of Consumer Protection and Food Safety. In general, the following areas are assessed when considering the approval of a pesticide: the chemical composition of the agent, its physical and chemical properties; effectivity and application; analysis; health (toxicology, application safety, residual behavior); environmental behavior, groundwater; effects on non-target organisms. The environmental fate of radioactively labelled pesticides and their metabolites must be evaluated either if their concentrations in soil degradation studies exceed 5 % of the total radioactivity in tests carried out on two consecutive days, or if they exceed at least once the

concentration of 10 % [105]. In tests performed in lysimeters, their infiltration behavior can be simulated, and degradation products can be identified and quantified in soil and leachate. Concentrations in the leachate must not exceed the limit of 0.1 µg/L with respect to the pesticide and its relevant metabolites [105]. The Plant Protection Product Directive defines relevant metabolites as compounds with similar acitvity compared to the pesticide and defines a threshold of 0.1 µg/L in drinking water. Metabolites that show no, or far lower, activity compared to the pesticide are termed non-relevant and concentration levels of up to 10 µg/L in groundwaters are acceptable according to the Plant Protection Product Directive. For non-relevant metabolites, no analytical methods must be established. The approval for pesticides is granted for ten years and after this period the agent must be re-evaluated [106]. The Drinking Water Ordinance on the other hand gives no clear definition for the classification in “relevant” and “non-relevant” pesticide metabolites. It only defines a threshold for pesticides and relevant metabolites of 0.1 µg/L for individual substances and of 0.5 µg/L for the sum of the selected compounds. However, the understanding of the term ”non-relevant” in the Drinking Water Ordinance does not agree with the definition of the Plant Protection Product Directive. The principle “as low as reasonably achievable” (ALARA) takes effect for non-relevant metabolites. The German Federal Environment Agency has recommended health-based values for non-relevant metabolites between 1-3 µg/L [106,107].

According to the Plant Protection Product Directive, the concentrations of DPC and M-DPC found in waters do not exceed the limit for non-relevant metabolites (see section 1.3.3) but after the identification of a carcinogenic OP formed during ozonation of DMS (see section 1.3.1), an increased interest in the identification of ozonation products can be noted.

2 Objective

The identification of transformation products formed during drinking water treatment is a topic of current research, especially since findings in 2007 revealed that a non-relevant pesticide metabolite (N,N-dimethylsulfamide) frequently present in groundwaters was transformed to a carcinogenic compound (N-nitrosodimethylamine) during drinking water ozonation.

In this work the oxidation of two pesticide metabolites should be investigated in detail. Chloridazon, a herbicide mainly used for weed control on sugar beet fields, is biologically degraded to its two metabolites desphenyl-chloridazon (DPC) and methyl-desphenyl-chloridazon (M-DPC). Due to their increased polarity and persistency the two metabolites are frequently found in German groundwaters. In literature, investigations on the elimination of DPC and M-DPC during ozonation in drinking water preparation are described. Although it was shown that the metabolites can be removed through ozonation, there is currently no information available on the oxidation products (OPs) formed during ozonation of these metabolites.

The primary aim of this work was to identify oxidation products formed during ozonation of DPC and M-DPC. OPs should be identified by applying known ozonation mechanisms to the chemical structures of the metabolites. This theoretical approach should be combined with lab-scale ozonation experiments and with the application of state-of-the-art analytical systems such as HPLC-DAD-Q-ToF-MS, GC-MS and IC-CD.

Formation mechanisms should be proposed for the identified oxidation products. Based on this information, oxidation pathways for both metabolites should be elaborated providing a general overview on the OPs formed. Furthermore, degradation and formation kinetics for selected oxidation products should be investigated, allowing the determination of the temporal evolution of OP formation and the maximum concentrations formed. Finally, the transferability of the lab-scale experiments to environmentally relevant concentrations of the metabolites and ozonation doses used in waterworks should be investigated, enabling an estimation of potential risks for the environment and human health arising from the OPs identified.

3 Materials and Methods

This section lists the different standards and materials used and describes the principles of the experimental methods and the exact parameters and boundary conditions applied in the experiments.

3.1 Materials

3.1.1 Chemicals

Standards:	Desphenylchloridazon 99.8 % (BASF)
	Methyldesphenylchloridazon 99.8 % (BASF)
	Parabanic acid 99 % (Sigma-Aldrich)
	Oxamic acid 98 % (ABCR)
	Oxamide 98 % (Alfa Aesar)
	6-Azauracil 99 % (TCI)
	5-Hydroxyhydantoin 98 % (Chemos)
	Oxalic acid dihydrate 100 % (Merck)
	Formic acid 100 % (Merck)
	Glyoxylic acid 100 % (Merck)
	Acetic acid 96 % (Merck)
Synthesis:	4,5-Dichloropyridazine-3(2H)-one 98 % (Alfa Aesar)
	Ethanol absolute (Merck)
	4,5-Dichloro-2-methyl-pyridazine-3(2H)-one 97 % (Sigma-Aldrich)
	Ammonia (Merck)
GC:	Methyl-tert-butylalkohol Roti solv (Carl Roth)
	Dichlormethan Roti solv (Carl Roth)
	Aceton supra solv (Merck)
Ozonation:	Phosphoric acid (Merck)
	Potassium hydrogen phosphate (Merck)
	Sodium hydroxid (Merck)
	Hydrochloric acid (Merck)
	Tert-butyl alcohol (Fluka)
	Sodium thiosulfate (Sigma-Aldrich)
	Sodium sulfite (Sigma-Aldrich)
	Potassium indigo trisulfonate (Sigma-Aldrich)
Solvents:	Methanol (Roth)

Mobile phase:	Methanol (Roth)
	Acetonitrile (Scharlau)
	MilliQ water (Satorius)
	Ammonia acetate (Fluka)
	Isopropanol (Emsure)
Gases:	Nitrogen (Air liquide)
	Oxygen (Air liquide)
	Helium (Air liquide)
TOC:	Synthetic air (Air Liquide)
	CO_2 absorber (Shimadzu)
	Potassium hydrogen phthalate (Merck)
	Halogen scrubber (Shimadzu)
	Phosphoric acid (Merck)
IC-CD:	Sodium hydrogen carbonate (Fluka)
	Sodium carbonate (Merck)
	Sodium chloride (Fluka)
	Sodium sulfite (Fluka)
	Sodium nitrate (Fluka)
	Sodium fluoride (Fluka)

3.1.2 Consumables

Ozonation:	Polycarbonate filter: poresize 0.45 µm, diameter 25 mm (Machery-Nagel)
	Graduated cylinder (Hirschmann)
	Filters Chromafil-CA-45/25 (Macherey-Nagel)
	Pipette tips (Brand)
	50 mL Tubes (Corning)
	15 mL Tubes (VWR)
	Quarz glas cuvettes 10 mm and 50 mm (Hellma)
	10 µL, 100 µL, 1000 µL and 10 mL pipettes (Brand)
	Volumetric flasks (Brand)
	Polystyrol flasks (Greiner)
	Funnel (Brand)
	HPLC vials with inserts (WICOM)
	1.5 mL vials with poly propylene screw cap (A-Z Analysenzubehör)

SPE:	Strata-X 33 µm polymeric phase 30 mg / 1 mL (Phenomenex) Bond Elut PPL 3 mL, 200 mg (Varian) Strata-X 6 mL 200 mg (Phenomenex) Bakerbond SDB 1 6 mL 200 mg and 500 mg (self-filled cartridges) (Baker) Isolute C18 (EC) 6 mL; 1.5 g self-filled cartridges (Biotage) Strata-X-A; 6 mL 200 mg (Phenomenex) LiChrolut EN 6 mL 200 mg and 500 mg self-filled cartridges (Merck)

3.1.3 Equipment

Ultra pure water generator:	MilliQ, 18.2 Ω (Sartorius)
Ozone generator:	Ozomat GM-6000-OEM (Anseros)
Supersonic bath:	Sonorex (Bandelin)
pH-electrode:	N1051A (Schott)
Magnetic stirrer:	RCT classic (IKA)
Photometer:	CADAS 200 (Dr Lange) Ozomat GM (Anseros)
Pipettes:	1 µL-10 µL, 10 µL-100 µL, 100 µL-1000 µL, 1 mL-10 mL (Brand)
Refrigerator:	Premium (Liebherr)
Scales:	High-precision scales AE136 (Mettler)
SPE-Enrichment:	VacMaster (IST)
Centrifuges:	Table centrifuge CR422 (Jouan)
$SAC_{254\ nm}$ and $SAC_{436\ nm}$:	UV/VIS spectrometer Lambda 2 (Perkin Elmer)
TOC-system:	TOC analyzer (Shimadzu), Automated sample changer, ASI-V, Computer software, TOC control (Shimadzu)

3.2 Methods

3.2.1 Ozonation

Oxygen gas was used to generate ozone by dielectric barrier discharge where oxygen molecules are dissociated and recombine forming ozone (details about the ozone generator see section 3.1.3). For the ozonation experiments, the ozone-containing oxygen gas was added to the samples in two different ways. One was by passing ozone-containing oxygen gas directly through the sample (direct ozonation), the other one was by preparing an ozone stock solution and adding aliquots of this stock solution to the samples (indirect ozonation).

An advantage of the direct method is that higher ozone concentrations can be inserted into samples whereas an advantage of the indirect method is the more precise addition of ozone to the sample and the possibility of generating data for degradation and formation kinetics.

Direct ozonation

Determination of the ozone concentration:

Ozone-containing oxygen gas was bubbled through the samples. The inserted amount of ozone was calculated based on the gas flow rate of the ozone/oxygen mixture and by the difference in ozone concentration in the influent and effluent which was measured by gas photometric detection (254 nm). To determine the flow rate, a 500 mL volumetric flask was filled to the mark and held into a basin filled with water. The oxygen releasing hose was inserted in this flask. The time required to replace the water by air was determined and the gas flow was calculated with Equation 3.1.

$$\text{Gas flow (L/min)} = \frac{\text{Volume of volumetric flask (L)}}{\text{Time (sec)}} * 60 \text{ (sec/min)}$$

Equation 3.1: Determination of the gas flow (L/min).

The calculated gas flow rate (L/min) was then multiplied by the ozone concentration (mg/L) in the gas stream which led to the ozone mass flow rate (mg/min) (Equation 3.2, a). The ozone rate multiplied by the duration of ozone treatment corresponds to the total amount of applied ozone inserted in the sample (Equation 3.2, b).

$$\text{a) Ozone rate (mg/min)} = \text{Ozone gas concentration (mg/L)} * \text{Gas flow (L/min)}$$

$$\text{b) Ozone amount (mg)} = \text{Ozone rate (mg/min)} * \text{Time of ozonation (min)}$$

Equation 3.2: (a) Determination of the ozone rate (mg/L) and (b) determination of the total ozone amount (mg).

Samples:

Experiments for the structural elucidation of OPs were performed by bubbling ozone-containing oxygen gas through aqueous solutions containing DPC or M-DPC. These experiments were performed in demineralized water and the initial concentrations of the compounds were 1 mM (145 mg/L DPC and 160 mg/L M-DPC, respectively). The production rate of ozone was set to 12 % and the flow rate of the gas stream was determined as 0.67 L/min. With the ozone concentration in the gas stream (18.2 mg/L) the amount of ozone bubbled through the samples was determined and adjusted to 12.2 mg/min (0.25 mmol/min).

Samples were taken at regular time intervals (2, 4, 6 and 8 min) and immediately analyzed without quenching the residual ozone in the samples.

Blanks:

To ensure that the OPs identified were not caused by compounds other than DPC or M-DPC three different kinds of blanks were analyzed. The first blank consisted of the water used for the experiments without addition of ozone. For the second blank the water used was treated with the corresponding amount of ozone from the experiments, but without spiking of any compound. The third blank contained the analyte in the water matrix but was not treated with ozone. Through the analysis of these blanks it could be ensured that the detected OPs were only formed through ozonation of DPC or M-DPC.

Indirect ozonation

For the indirect ozonation an ozone-containing aqueous stock solution was prepared as well as an indigo trisulfonate reagent for the determination of the ozone concentration in the stock solution.

Preparation of the ozone stock solution:

For the generation of the ozone stock solution, ozone-containing oxygen gas was bubbled through 5 °C cooled MilliQ water. By measuring the influent concentration of ozone in the water and the efluent concentration photometrically (λ = 254 nm), it was possible to determine when the solution was saturated. This was the case, when the ozone influent and effluent concentrations reached a balance which was usually after 2 hours. After reaching the balance the ozone concentration in the stock solution was determined based on the indigo method (see the following paragraph). The ozone concentrations in the stock solutions usually ranged between 20 mg/L and 28 mg/L.

Determination of the ozone concentration by the indigo method:

The ozone concentration was determined by the indigo method on the basis of the German standard method DIN 38408-G 3-3; 2011-04 [108]. The princliple of this method is that the blue coloration of indigo trisulfonate is removed by ozone in a stoichiometric reaction and enables the quantification of ozone present in a sample (Figure 3.1).

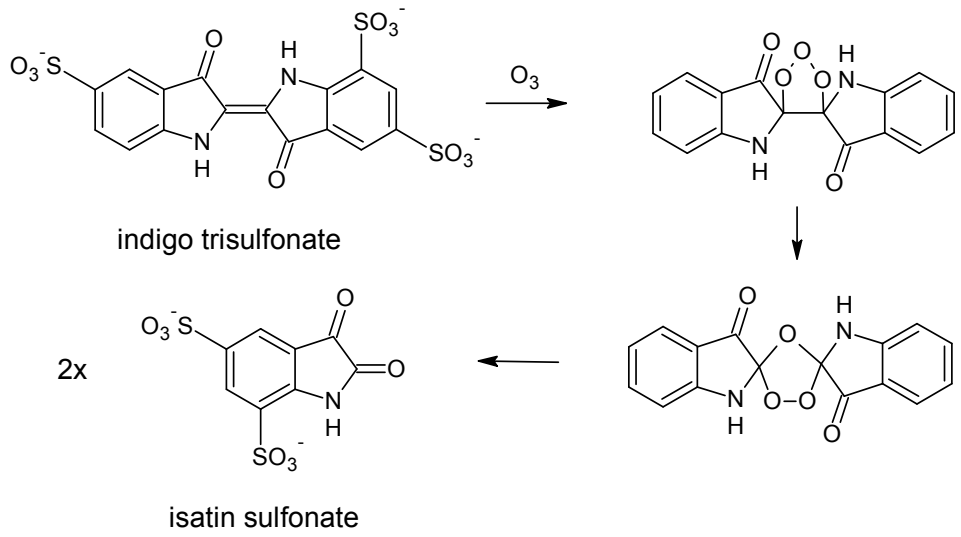

Figure 3.1: Reaction mechanism between indigo trisulfonate and ozone resulting in a loss of blue color [109].

Preparation of the indigo stock solution and working solution:

0.25 mL concentrated phosphoric acid (ρ = 1.70 g/mL) were mixed with 100 mL demineralized water in a 250 mL volumetric flask. After adding and dissolving 193 mg potassium indigo trisulfonate the flask was filled to the mark. The solution was stable for approximately four months when stored at 4 °C. To check if the concentration was correct, the extinction at 600 nm was measured each time the stock solution was used. For this the stock solution was diluted (1:100) and had to show an extinction of 1.00 ± 0.05 in a 5 cm cuvette. If the extinction was below 0.95 a new solution was prepared.

To produce the working solution the indigo stock solution was diluted 1:10 with demineralized water in a volumetric flask. The working solution was prepared fresh before analysis. For the determination of the ozone concentration 10 mL aliquots of the working solution were pipetted into 100 mL volumetric flasks. The zero value was gained by filling the flask with demineralized water. The volume of the sample containing ozone added to the working solution depended on the ozone concentration in the sample and ranged between 10 mL and 80 mL. Photometric determination was performed at 600 nm in a 5 cm cuvette directly after filling and mixing in the flasks. Measurements were performed within four hours after preparation and ozone concentrations were determined by Equation 3.3.

$$\beta_{ozone}\,(mg/L) = \frac{(Ext_{Ref} - Ext_{sample}) * f * V_{max}}{s * V_p}$$

Equation 3.3: Determination of the ozone concentration in aqueous solutions. β, concentration of ozone (mg/L); Ext_{Ref}, extinction of the reference sample; Ext_{sample}, extinction of the sample; f, calibration factor = M*(1000 mg/g)/ε_{600nm} = 2.4 mg*cm/L with M, molar mass of ozone = 48 g/mol; ε_{600nm} = 20000 L/(mol*cm);·V_{max}, volume of the volumetric flask (mL); s, path length of the cuvette (cm); V_p, volume of the sample (mL).

3.2.2 Stock solutions

All standards were prepared in MilliQ water as methanol quenches ozone and therefore must be avoided for ozonation experiments. For the preparation of 1 mM stock solutions 7.3 mg of DPC, 8.0 mg of M-DPC, 5.7 mg of 6-azauracil and 5.8 mg of 5-hydroxyhydantoin were dissolved in 50 mL of MilliQ water. The DPC standard was stirred over night because of the low solubility of DPC in water. Parabanic acid (6.6 mg/50 mL) was prepared freshly for all experiments because of its instability. All standards were stored at 4°C. From these stock solutions, dilutions containing 100 µM of the required analytes were prepared and further diluted for the experiments.

3.2.3 Determination of TOC

Principle of the method:

Total organic carbon (TOC) is a parameter used in water analysis to describe the content of organic compounds in a water sample. The method is based on the oxidation of carbon-containing compounds through pyrolytic combustion of the aqueous sample and subsequent determination of the formed carbon dioxide by infrared spectrometry. With this method, carbon-containing compounds are detected independently of their oxidation state. The method is based on the German standard method DIN EN 1484 [110]. As drinking water has no particles that can be removed by filtration, the parameters TOC and dissolved organic carbon (DOC), which is determined after filtration of samples, show the same values.

Procedure:

20 mL of sample were acidified with 200 µL of 2 M hydrochloric acid and the inorganic carbon was stripped from the sample through insertion of nitrogen gas. After this, the organic carbon was transformed to inorganic carbon by thermal combustion, stripped from the sample and detected by infrared spectrometry. The limit of detection for this method is 0.2 mg/L.

3.2.4 Determination of $SAC_{254\ nm}$ and $SAC_{436\ nm}$

Principle of the method:

With this method the spectral absorption coefficient (SAC) is determined by measuring the spectrometric UV absorption at 254 nm [111] and at 436 nm [112]. These sum parameters describe the content of waters with organic compounds which, in the case of the absorption measured at 436 nm, can lead to coloration of waters. The method is based on the German standard methods DIN 38404-3 und DIN EN ISO 7887, respectively.

Procedure:

The water sample was filtered through single-use syringes and cellulose acetate filters (0.45 µm pore width). The first 3 mL of the filtrate were discarded. In general, measurements were performed with 5 cm cuvettes where the zero point was set using demineralized water prior to analysis of the samples. The spectral absorption coefficients $SAC_{254\ nm}$ and $SAC_{436\ nm}$ were determined by Equation 3.4. The limit of detection for both parameters is 0.1 m^{-1}.

$$SAC\,(m^{-1}) = \frac{AU}{d}$$

Equation 3.4: Determination of the spectral absorption coefficient (SAC) at either 254 nm or at 436 nm. Absorption at the corresponding wavelength (AU), path length (d).

3.2.5 HPLC-DAD-Q-ToF-MS

The following HPLC-DAD-Q-ToF-MS-system and conditions were used to analyze samples treated with ozone for structural identification of oxidation products. The ToF system was used in scan mode as well as in MS/MS mode.

HPLC-DAD-Q-ToF-system: HPLC: Analytical high pressure gradient system 1290, binary pump G4220A, degaser G1330B, auto sampler G4226A, oven heating G1316C, DAD-Detector G4212A (Agilent Technologies)
ToF: 6540 Q-ToF G6540A, ESI ionization chamber G3251B (Agilent Technologies)

Column: Hypercarb, 150 mm x 2.1 mm, 5 µm inner diameter (Thermo-Fisher Scientific)

Pre-column: Fusion C18 – RP 4 mm x 3.0 mm (Phenomenex)

Mobile Phase: A = 10 mM ammonium acetate in methanol
B = 10 mM ammonium acetate in MilliQ water

Gradient:

Time (min)	A (%)	B (%)
0.1	90	10
7	90	0
12	0	100
24.5	0	100
25	90	10

Flow rate: 0.35 mL/min

Injection volume: 5 µL- 20 µL

Column temp.: 40 °C

DAD: Set at wavelengths: 220 nm, 250 nm and 280 nm and entire spectrum from 190 nm to 640 nm

ToF conditions:

Parameter	MS	MS/MS
Mode	Pos/neg	Pos/neg
Scan range (*m/z)*	50-1000	40-200
Desolvation gas flow (L/min)	8	8
Desolvation temperature (°C)	300	300
Nebulizer pressure (psi)	35	35
Capillary voltage (V)	3500	3500
Fragmentor voltage (V)	100-175	100-175
Skimmer (V)	65	65
Oct 1 RF Vpp* (V)	750	750
Collision gas (V)	5-25	5-25

*Oct 1 RF Vpp (octopole 1 radio frequency peak-to-peak voltage)

Software: Mass hunter data acquisition and mass hunter qualitative analysis, B.03.01 Build 3.1.346.0 (Agilent Technologies)
ACD/ChemSketch and ACD/MS Fragmentor, Version 12.5 Build 47844 (ACD/Labs)

For continuous internal mass calibration, a minimum of two references (in positive mode: fragment ions at *m/z* 121.0509 and *m/z* 922.0098; in negative mode: fragment ions at *m/z* 68.9958, *m/z* 112.9856 and *m/z* 119.0363) were used during all measurements. The high mass accuracy of HPLC-Q-ToF-MS measurements allowed the molecular weights of OPs, and therefore of elemental compositions, to be determined with a high degree of confidence.

3.2.6 HPLC-MS/MS

The following HPLC-MS/MS-system and conditions were used to quantify both degradation curves of DPC and M-DPC and formation curves of oxidation products identified.

HPLC-MS/MS-system: HPLC: Analytical high pressure gradient system 1290 G422A, binary pump (with integrated degaser) G4220A, auto sampler G4226A, oven heating G226A (Agilent Technologies)
MS: 5500 QTrap, ESI ionization chamber (AB Sciex)

Column: Hypercarb, 150 mm x 2.1 mm, 5 µm inner diameter (Thermo-Fisher Scientific)

Pre-column: Fusion C18 – RP 4 mm x 3.0 mm (Phenomenex)

Mobile phase: A = 10 mM ammonium acetate in methanol
B = 10 mM ammonium acetate in MilliQ water

Flow rate: 0.3 mL/min

Gradient:

Time (min)	A (%)	B (%)
0.01	95	5
7	95	5
12	0	100
24	0	100
25	95	5

Injection volume: 40 µL

Column temp.: 40°C

MS conditions:

Ion chamber temp.:	500 °C
Curtain gas:	40 psi
Spray gas (GS 1):	60 psi
Spray gas (GS 2):	75 psi
Collision gas:	Medium
Ion spray potential:	-4500 V or +5500 V
Entrance potential:	-10 V or +10 V

MS parameter settings for individual analytes: Declustering potential (DP); collision energy (CE) and collision exit potential (CXP).

Compound	Mode	Precursor ion (*m/z*)	Product ion (P1/P2) (*m/z*)	DP (V)	CE (P1/P2) (eV)	CXP (P1/P2) (V)
M-DPC	+	159.9	117.0, 88.0	106	33, 41	12, 10
DPC	+	145.9	117.0, 100.9	41	31, 33	12, 12
6-Azauracil	-	112.0	42.0	-60	-28	-7
5-Hydroxy-hydantoin	-	114.9	71.9, 42.0	-80	-18, -24	-11, -7
Parabanic acid	-	112.9	85.0, 42.0	-35	-12, -24	-9, -7
Oxaluric acid	-	130.9	59.0, 42.0	-50	-16, -34	-9, -19

Software: Analyst 1.5.1 (AB Sciex)
SQS 2000, version 2.01 (Dr. Joachim Kleiner)

3.2.7 GC-MS

GC-MS-system:	GC: Agilent 6890N (Agilent Technologies) auto sampler 7683B tower, auto sampler 7683B plate, diffusion pump MSD 5975, ionization gauge 59864B MS: Agilent 5973
Column:	RTX 502.2 (30 m x 0.25 mm ID x 1.4 µm df) crossbond 50% diphenyl/ 50% dimethyl polysiloxane (Restek)
Gas:	Helium
Flow rate:	1.0 mL/min
Temp. programm:	Initial temp.: 45 °C Isotherme 1: 2 min Temp. Increase: 25 °C/min Temp. 2: 260 °C Isotherme 2: 8 min
Injection volume:	1 µL pulsed splitless (80 kPa; 0.5 min)
Sample matrix:	Acetone
Temp injector:	230 °C
MS temp.:	Quadrupole: 150 °C Source: 200 °C Solvent delay: 8 min
Scan range:	33-380 *m/z*
Ionization mode:	Electron impact (EI) 70 eV
Software:	MSD Chem Station D.02.00 (Agilent Technologies) NIST Mass spectral library 2002 Version 2.0 (National Institute of Standards and Technology)

3.2.8 IC-CD

IC-CD:	ICS 3000 Ion chromatograph, auto sampler (Dionex)
Column:	IonPac AS10, 4 mm x 250 mm (Dionex)
Pre-column:	IonPac AG10, 4 mm x 50 mm (Dionex)
Cleaning-column:	ATC3 Ion Pac Anion Trap Column (Dionex)
Mobile Phase:	A: MilliQ water B: 200 mmol/L sodium hydroxide solution C: 10 mmol/L sodium hydroxide solution

Gradient:

Time (min)	A (%)	B (%)	C (%)	Comment
-11	37	63	-	Purging with 126 mmol/L NaOH
-10	20	-	80	Equilibration with 8 mmol/L NaOH
0	20	-	80	Sample injection
10	20	-	80	Isocratic with 8 mmol/L NaOH
23	37	63	-	Gradient to 126 mmol/L NaOH
35	37	63	-	Isocratic with 126 mmol/L NaOH

Flow rate: 1 mL/min

Injection volume: 500 µL

Suppressor: Anion self-regenerating suppressor ASRS 300, 4-mmm, Auto-Suppression® External Water Mode (Dionex)

Software: Chromeleon 6.80 (Dionex)

3.2.9 Fraction collection

For the fraction collection the following HPLC system was coupled to a fraction collector. For this, a column with a larger internal diameter was used. The increase in internal diameter (from 2.1 mm to 4.6 mm) led to a 4 times higher capacity of the separation. In order to enable peak retention times to remain constant the change in flow rate was calculated with the help of a scale-up factor. Under the assumption of a constant column length the scale-up factor was determined with Equation 3.5. The scale-up factor was determined as 4.8. The initial flow rate lay by 0.35 mL/min and was increased to 1.7 mL/min.

$$\text{Scale-up factor} = \frac{d_{c2}^2}{d_{c1}^2}$$

Equation 3.5: Determination of the scale-up factor. original internal diameter (d_{c1}, in mm), new internal diameter (d_{c2}, in mm).

The HPLC method used for structural identification of OPs (see section 3.2.5) was slightly modified for fractionation to have more time between the collected peaks and reduce problems due to retention time shifts. Additionally, because of a delay between the DAD detector and fraction collector 0.3 min delay time had to be set in the collection configuration.

HPLC/DAD-system: HPLC: Analytical high pressure gradient system 1100, binary pump G1312A, degaser G1379A, auto sampler G1313A, oven heating G1316A, DAD detector G1315B (Agilent Technologies)

Column: Hypercarb, 150 mm x 4.6 mm, 5 µm inner diameter (Thermo-Fisher Scientific)

Pre-column: Fusion C18 – RP 4 mm x 3.0 mm (Phenomenex)

Mobile phase: A = 10 mM ammonium acetate in methanol

B = 10 mM ammonium acetate in MilliQ water

Flow rate: 1.7 mL/min

Injection volume: 40 µL

Column temp.: 40 °C

Fraction collector: FC 204 (Gilson)

Gradient:

Time (min)	A (%)	B (%)
0.01	95	5
0.5	95	5
4	60	40
5	0	100
10	0	100
11	95	5
15	95	5

Collection windows:

Peak	Retention (min)
1	1.8-2.0
2	2.1-2.4
3	2.6-3.1
m/z 115	3.2-3.8
5	3.9-4.5
m/z 128	5.5-6.1

Software: Agilent Chem Station Rev. B.04.02 SP1 (Agilent Technologies)

Sample preparation for fraction collection experiments:

500 mg of 6-azauracil were dissolved in 200 mL demineralized water in a volumetric flask. The ozone generator was set to 25 %. Ozone-containing oxygen gas was bubbled through the sample for 20 min. After analyzing the sample for OPs to estimate the yield of the reaction further ozone was added in 20 min intervals. Maximum oxidation product formation (*m/z* 115 and *m/z* 128) was observed after 80 min. The ozone was quenched through the addition of sodium sulfite and the solution was then chromatographically separated and fracitonated. The collected fractions were concentrated to dryness under nitrogen at 40 °C reconstituted in MilliQ water and analyzed by HPLC-DAD-Q-ToF-MS.

3.2.10 Syntheses

Because not all compounds proposed as OPs were commercially available as standards, compounds with similar or the same structures as the proposed ones were synthesized to verify the structures proposed for the oxidation products.

3.2.10.1 (2-Methyl)-4,5-dihydroxy-pyridazine-3-one

For the synthesis of 4,5-dihydroxy-pyridazine-3-one, 200 mg of 4,5-dichloro-pyridazine-3-one were heated in ethanolic (20 mL) sodium hydroxide (one pellet) under reflux for 40 h. The temperature remained at 78 °C throughout the synthesis. Chlorine atoms, as good leaving group, were substituted by hydroxyl groups (Figure 3.2). The solution was dried under nitrogen and a small amount of the residue was dissolved in MilliQ water and analyzed by HPLC-DAD-Q-ToF-MS to confirm the identity of the reaction product.

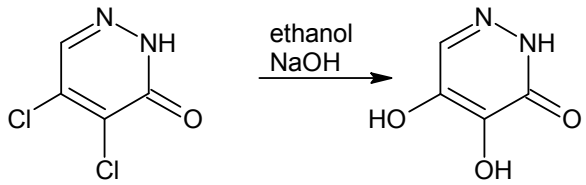

Figure 3.2: Schematic reaction of 4,5-dichloro-pyridazine-3-one with sodium hydroxide for the synthesis of 4,5-dihydroxy-pyridazine-3-one.

For the synthesis of 2-methyl-4,5-dihydroxy-pyridazine-3-one, 200 mg of 2-methyl-4,5-dichloro-pyridazine-3-one were treated in the same way as described for the non-methylated compound (Figure 3.3).

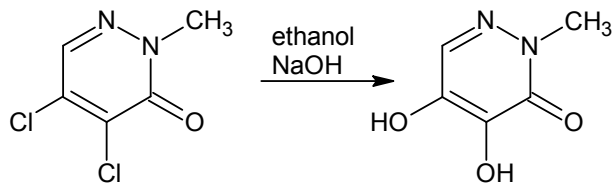

Figure 3.3: Schematic reaction for the synthesis of 2-methyl-4,5-dihydroxy-pyridazine-3-one.

3.2.10.2 5-Amino-4-hydroxy-pyridazine-3-one

For the synthesis of 4-hydroxy-5-amino-pyridazine-3-one 200 mg of desphenyl-chloridazon (DPC) were dissolved in ethanolic (20 mL) sodium hydroxide (one pellet) solution and heated at 78°C throughout the synthesis for 40 h under reflux. After 24 h the initially colorless and clear solution showed a light yellow color but remained clear. Chlorine as a better leaving group than the amino moiety was substituted by a hydroxyl group (Figure 3.4). The solution was dried under nitrogen and a small amount of the residue was dissolved in water and used for verification of the oxidation product by HPLC-DAD-Q-ToF-MS.

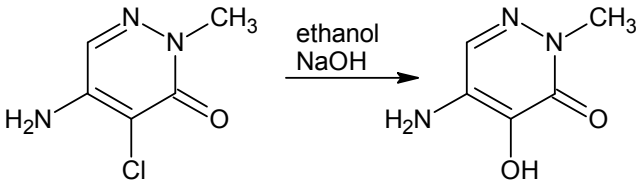

Figure 3.4: Schematic reaction of desphenyl-chloridazon with sodium hydroxide for the synthesis of 5-amino-4-hydroxy-pyridazine-3-one.

4 Results and discussion

A combination of various analytical instruments such as HPLC-DAD-ESI-Q-ToF-MS, GC-MS and ion chromatography (IC) coupled with a conductivity detector (CD) were used to gain information about the oxidation products (OPs) formed. Based on this information structures were proposed and where possible verified by standards.

4.1 Identified oxidation products of DPC in MilliQ water

A chromatographic separation of DPC from its OPs measured with HPLC-DAD is depicted in Figure 4.1 A. t_0 represents a chromatogram of the initial concentration of DPC (1 mM) prior to ozonation. The oxidation of DPC through ozone, which follows a pseudo first order reaction, resulted in the formation of more than 6 UV absorbing OPs (λ = 250 nm), labelled with numbers in Figure 4.1 A. The concentration of each OP formed depends on the ozonation time and therefore on the applied ozone dose (0.25 mmol/min). Figure 4.1 B illustrates the formation of OPs as a function of ozonation time. For this, UV signals were integrated and the resulting peak areas were plotted against the time of ozonation. Intensities of all OPs rose during the first 6 min of ozone exposure. It can be noted that the intensities of OP 2 and OP 4 showed a faster increase than those of the other OPs. After 6 min, DPC was almost fully transformed and primary OPs started to undergo further reactions with ozone. Especially OP 2 and OP 4 showed a fast decline in intensity, while at the same time the intensity of OP 5 rose more rapidly (Figure 4.1 B). These results suggest that OP 2 or OP 4 might be precursors of OP 5.

In the following the identification of OP 2 to OP 5 formed through ozonation of DPC will be described in detail, mechanisms explaining the formation of these OPs will be proposed and both will be discussed. OP 1 eluting after 2.2 min showed two UV maxima (λ = 205 nm and λ = 265 nm) and OP 6 eluting after 7.4 min showed two UV maxima (λ = 222 nm and λ = 265 nm). However, the mass spectra at the retention times of these two OPs showed no noticeable fragment ions on which an empirical formula could have been proposed. Hence, OP 1 and OP 6 could not be identified and will therefore not be discussed in the following.

Generally, all the analyzed OPs showed lower molecular masses than the parent compound indicating a loss of atoms. At the end of the section, information on all analyzed OPs regarding retention time, UV maxima, ionization mode, MS and MS/MS detection, is summarized in Table 4.1. Mass error differences between the measured *m/z* and the calculated exact *m/z* were less than 1 ppm in all cases and are also included in the summary.

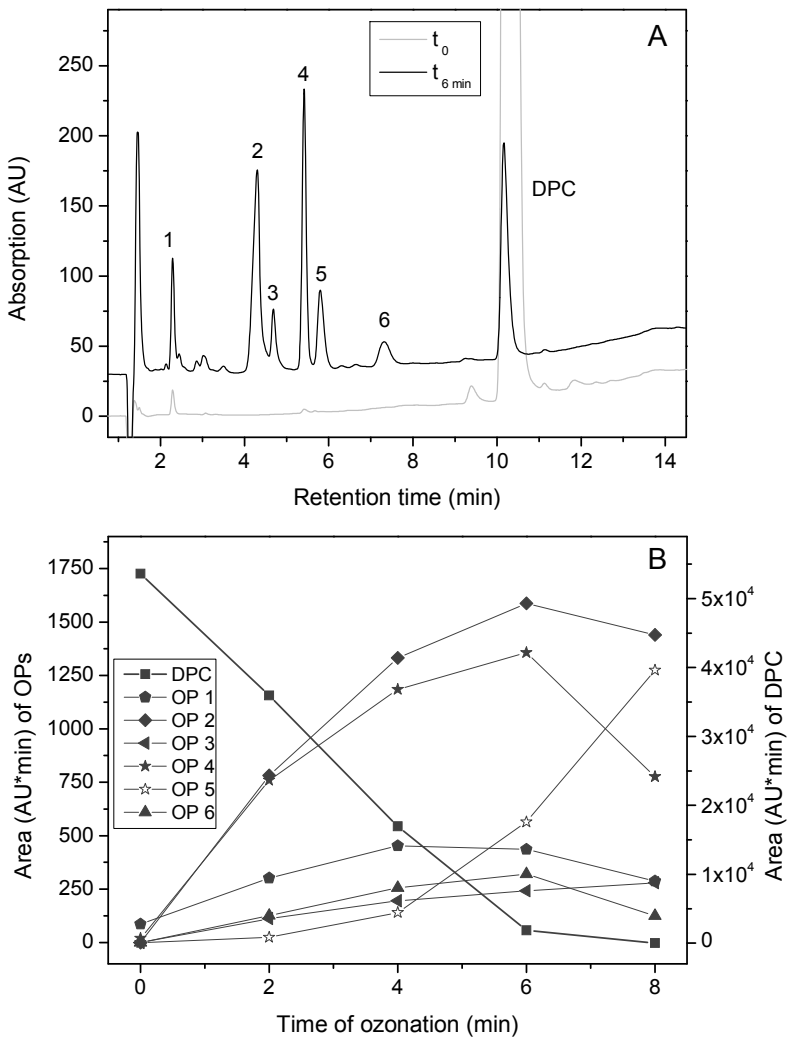

Figure 4.1: (A) UV chromatograms (λ = 250 nm) of DPC and the OPs formed through ozonation and (B) OP formation as a function of the applied ozone dose.

4.1.1 Pyridazine-3,4,5-trione (OP 2)

Ozonation of DPC led to the formation of a UV-absorbing OP (maxima at 226 nm and at 252 nm) which eluted after 4.3 min. Based on exact mass, intensity of the isotopes and their calculated abundance, the neutral empirical formula for the fragment ion at *m/z* 127.0138 was proposed as C4H2N2O4. The calculated double bond equivalents (DBEs) in this OP were determined as five DBEs. Because there was no standard commercially available, a reference compound with a similar structure to the proposed was synthesized (see section 3.2.10.1). Comparison of results from MS/MS experiments for the synthesized product 4,5-dihydroxy-pyridazine-3-one and the OP (Figure 4.2, A and B) revealed great similarities in fragmentation pattern. The two major product ions (*m/z* 56.0499 and *m/z* 70.0655) were present in both compounds. For the compound 4,5-dihydroxy-pyridazine-3-one it was possible to link the product ions to parts of the structure. These parts must also be present in OP 2. The product ion (*m/z* 99.0194), only present in the spectra of the OP, must be caused

by a structural variation compared with 4,5-dihydroxy-pyridazine-3-one. Also the finding that OP 2 consists of five DBEs, and 4,5-dihydroxy-pyridazine-3-one of four, agrees with the proposed structure, namely pyridazine-3,4,5-trione.

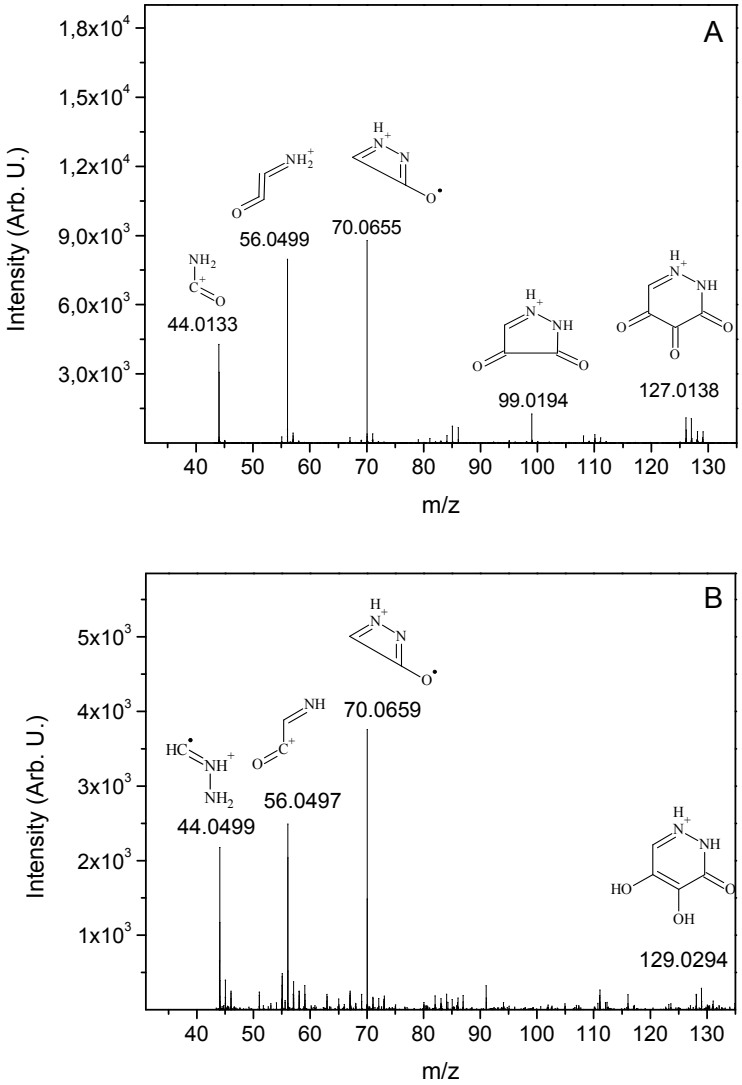

Figure 4.2: (A) MS/MS spectra of OP 2 (*m/z* 127.0138) and (B) for the synthesis product 4,5-dihydroxy-pyridazine-3-one (*m/z* 129.0295).

A mechanism explaining the formation of OP 2 is depicted in Figure 4.3. In its initial steps the reaction follows the Criegee mechanism (see section 1.2.1). The primary attack of ozone at the double bond situated between C4 and C5 in DPC results in the formation of the primary ozonide (Figure 4.3, structure 1). Through the loss of oxygen this intermediate forms an epoxide (Figure 4.3, structure 2). Attack of water in position 5 not only opens the epoxide by formation of a keto group in position 4 and subsequent elimination of the chlorine atom but also leads to the formation of a hemi-aminal group in position 5 of the ring. In the final step of the reaction, the alcohol moiety of the hemi-aminal is oxidized to a keto group eliminating the primary amine and forming OP 2, pyridazine-3,4,5-trione.

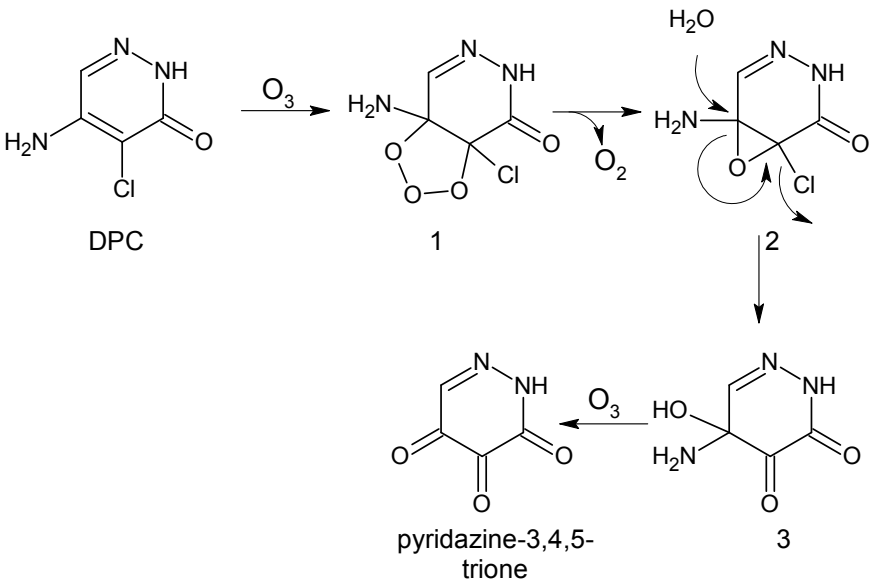

Figure 4.3: Proposed oxidation mechanism for the formation of OP 2 (pyridazine-3,4,5-trione) from DPC.

The principle substitution of primary amines or chlorine atoms by ketone groups during ozonation have been described for carbon-nitrogen double bonds [44]. Mechanistic investigations regarding the fate of bromacil during ozonation also describe OP formation via a peroxide intermediate which is similar to the here proposed mechanism [113]. However the ring closure and simultaneous ring reduction to a 5-membered ring in bromacil differ from the here proposed mechanism due to the fact, that bromacil has a vicinal nitrogen atom whereas DPC does not.

4.1.2 6-Azauracil (OP 4)

OP 4 eluted after 5.2 min retention time and the UV spectrum showed two maxima at 205 nm and at 258 nm (Figure 4.4, A and B). The UV spectrum of this OP indicated the presence of an aromatic ring. Total ion chromatograms (TIC) of HPLC-ToF data measured in negative ionization mode showed a fragment ion at *m/z* 112.0152 (Figure 4.4, A). The extracted ion chromatogram (EIC) of this fragment ion resulted in two peaks, one after 4.7 min and one after 5.2 min (Figure 4.4, A). Therefore ozonation of DPC results in the formation of two isomers. Based on high mass accuracy measurements, the empirical formula for the uncharged OP was proposed as C3H2N3O2 and the DBEs were determined as four. Analyses in positive ionization mode showed that OP 4 could not be detected in this mode, whereas its isomer could be detected in positive ionization mode and will be further discussed in section 4.1.4. The MS/MS spectrum of OP 4 showed one product ion at *m/z* 68.9961 (Figure 4.4, C). Further information regarding the structure of this OP was gained by GC-MS experiments. Under the chosen GC-MS conditions (see section 3.2.7), DPC was separated from its OPs (Figure 8.2 in the appendix). Based on a hit in the NIST

data base a structure for this OP could be proposed as 6-azauracil and was confirmed by a commercial standard (Figure 8.2).

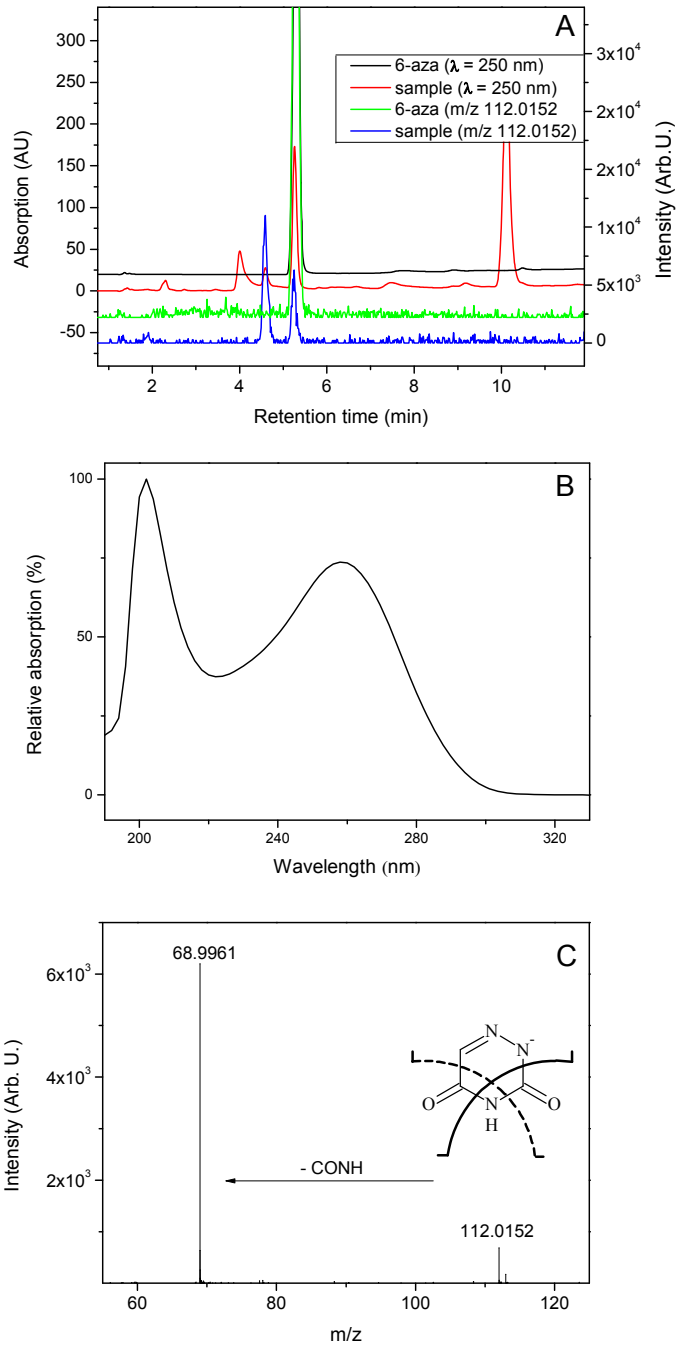

Figure 4.4: (A) UV chromatograms (λ = 250 nm) and EIC (*m/z* 112.0152) of 6-azauracil and the ozone-treated DPC sample, (B) UV spectrum of 6-azauracil (OP 4) and (C) MS/MS spectrum of the product ion at *m/z* 112.0152 (6-azauracil) and its proposed fragmentation.

One explanation for the formation of 6-azauracil is that DPC is directly attacked by ozone via the so-called Criegee mechanism (Figure 4.5). The carbon-carbon double bond between position C4 and C5 of the pyridazine ring is attacked by ozone forming the primary ozonide through 1, 3-dipolar cycloaddition (Figure 4.5, A), followed by a cycloreversion (Figure 4.5, B)

and further cycloaddition (Figure 4.5, C) forming the ozonide (Figure 4.5, 3). The reaction with water results in an opening of the ring. The free primary amine in position 5 subsequently attacks the carbonyl group in position 3 and under elimination of formyl chloride the intermediate stabilizes forming a 1,2,4-triazine ring. The formation of formyl chloride has been reported as a product of ozonation [114]. Formyl chloride, as an instable OP, undergoes further decomposition resulting in the formation of carbon monoxide and hydrochloric acid.

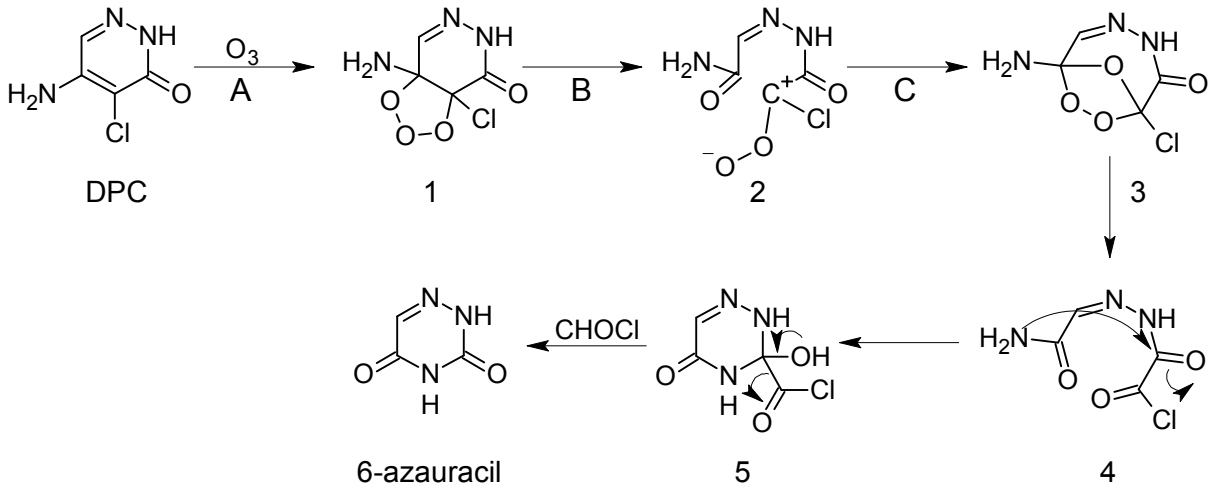

Figure 4.5: Proposed mechanism for the formation of 6-azauracil (OP 4). (A) 1,3-dipolar-cycloaddition; (B) cycloreversion; (C) 1,3-dipolar-cycloaddition.

This finding demonstrates the complexity of mechanisms involved in oxidation product formation by ozonation and in oxidation product prediction. Furthermore, these results show the importance of nitrogen atoms in a molecule when considering oxidation products formed by ozonation. It is not necessarily the case that primary amines are immediately oxidized to nitrate via nitrones [60] but they can lead to new ring systems through the formation of a peptide bond with keto groups present in the molecule. As an example the oxidation products formed through ozonation of the anti-epileptic pharmaceutical carbamazepine should be noted. The proposed mechanism for oxidation product formation shows similarities to the mechanism proposed here and hence a broad variety in strucures of OPs [33].

Further research focused on the degradation pathway of 6-azauracil when treated with ozone because of its maximum formation of 20 % (compare Figure 4.1, B, OP 4).

4.1.3 OPs derived from 6-azauracil

To differentiate between OPs directly formed from DPC or via 6-azauracil, the OPs formed from 6-azauracil will be numbered with Roman numbers (those of DPC with Arabic numbers).

4.1.3.1 N-(Nitrosocarbamoyl)-2-oxoacetamide (OP IV)

In tests with 6-azauracil dissolved in MilliQ water and directly treated with ozone gas the chromatographic separation was optimized for the new OPs and gave an overview over the number of OPs formed (Figure 4.6, A). The first and most eye-catching result was the generation of a yellowish color after ozone exposure and its disappearance after 24 hours. In following tests, MilliQ water was spiked with 0.1 mM 6-azauracil and 0.2 mM ozone. The ratio of 6-azauracil to ozone was 1:2. The samples were analyzed directly after ozone addition and then at one hour intervals for the next eight hours. Analyses of these samples with HPLC-DAD showed the formation of four OPs immediatly after ozone addition (Figure 4.6, A). After 24 h OPs III and IV were no longer present in the samples. Experiments performed in drinking water at pH 6 and pH 8 showed that the influence of the water matrix on OP formation was neglectable (compare Figure 8.3 in the appendix). Due to its UV spectrum, the coloration could be attributed to OP IV (Figure 4.6, A).The decomposition of OP IV seems to follow first order kinetics, independent of the water matrix which means that the reaction rate only depends on the concentration of the degrading compound (see Figure 4.6, B and Figure 8.4 in the appendix). Due to the relatively fast decline in concentration of OP IV, measurements concerning this OP should be finished within 2 h of preparing the solution. For this OP, it was possible to identify the fragment ion at *m/z* 144.0051 in negative ionization mode, of which the decline in area corresponds to the decline in UV area (Figure 4.6, B). Based on high resolution mass spectrometric measurements the uncharged empirical formula for this compound was proposed as C3H3N3O4.

As the formation of the instable OP IV can be observed during ozonation of 6-azauracil (Figure 4.6, OP IV) and ozonation of DPC (Figure 4.1 via OP 4 to OP 5), further experiments concerning the elucidation of this instable OP can be performed using 6-azauracil.

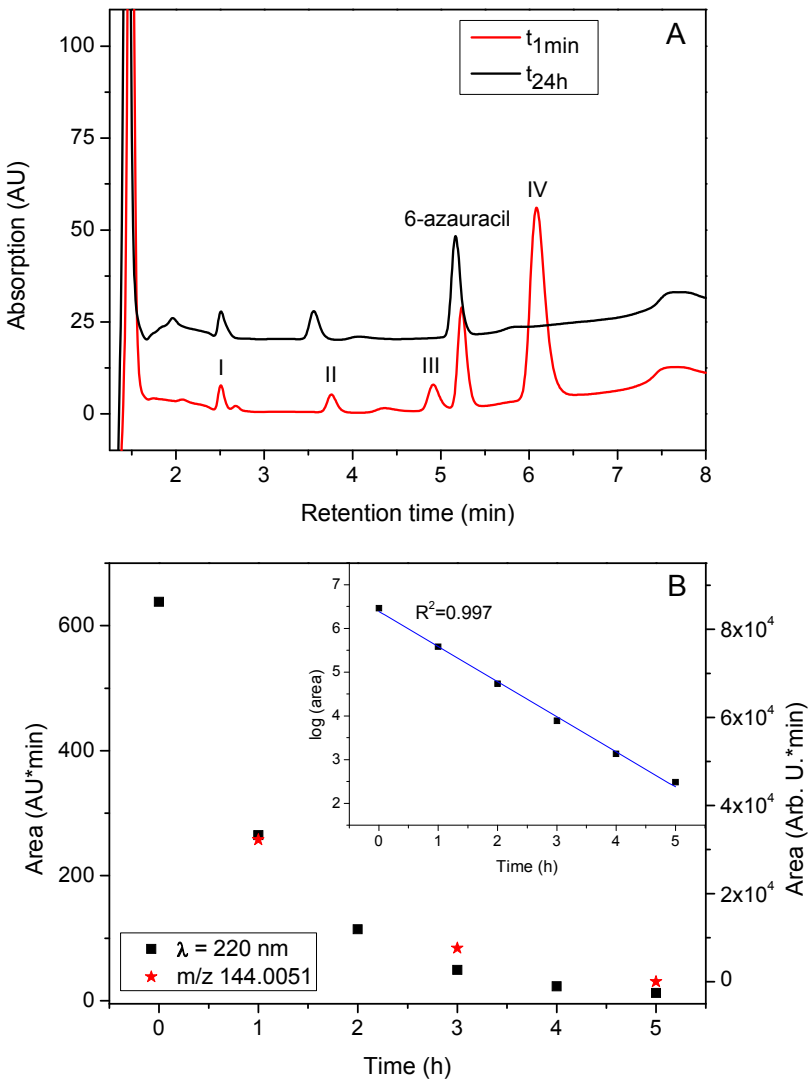

Figure 4.6: (A) UV chromatograms (λ = 220 nm) of an ozone-treated 6-azauracil sample directly after ozonation and after 24 h. (B) Decomposition of OP IV over time (decrease in area of the UV signal at 220 nm and decrease in area of the fragment ion at *m/z* 144.0051) and plotted on a logarithmic scale.

With MS/MS experiments exact masses for the product ions at *m/z* 45.0101, *m/z* 72.9938 and *m/z* 98.9955 were gained. Based on these measurements, the elemental composition for the negatively charged product ions (Figure 4.7, A) were HN2O (*m/z* 45.0101), CHN2O2 (*m/z* 72.9938) and C3HNO3 (*m/z* 98.9965). Since no structure for OP IV could be proposed based on this information, the Criegee mechanism was applied to the 6-azauracil molecule. This, in a first step, would result in the formation of the primary ozonide followed by the ozonide and would form an intermediate (N-(nitrosocarbamoyl)-2-oxoacetamide) depicted in Figure 4.7, structure 4. The elemental composition of this intermediate agrees with the proposed empirical composition gained from high resolution MS data. All the product ions could be explained by the proposed structure (Figure 4.7, A). The structure consists of a nitroso moiety which is a known group formed during ozonation of amines [61]. Furthermore, ozonaton of amines is known to go along with coloration of the reaction solution varying in

intensity and shade depending on the nature of the amine. Tertiary amines are strongest in color and bluest, whereas primary alkylamines are the weakest in color and greenest [61]. These findings agree with the light coloration during ozonation of 6-azauracil.

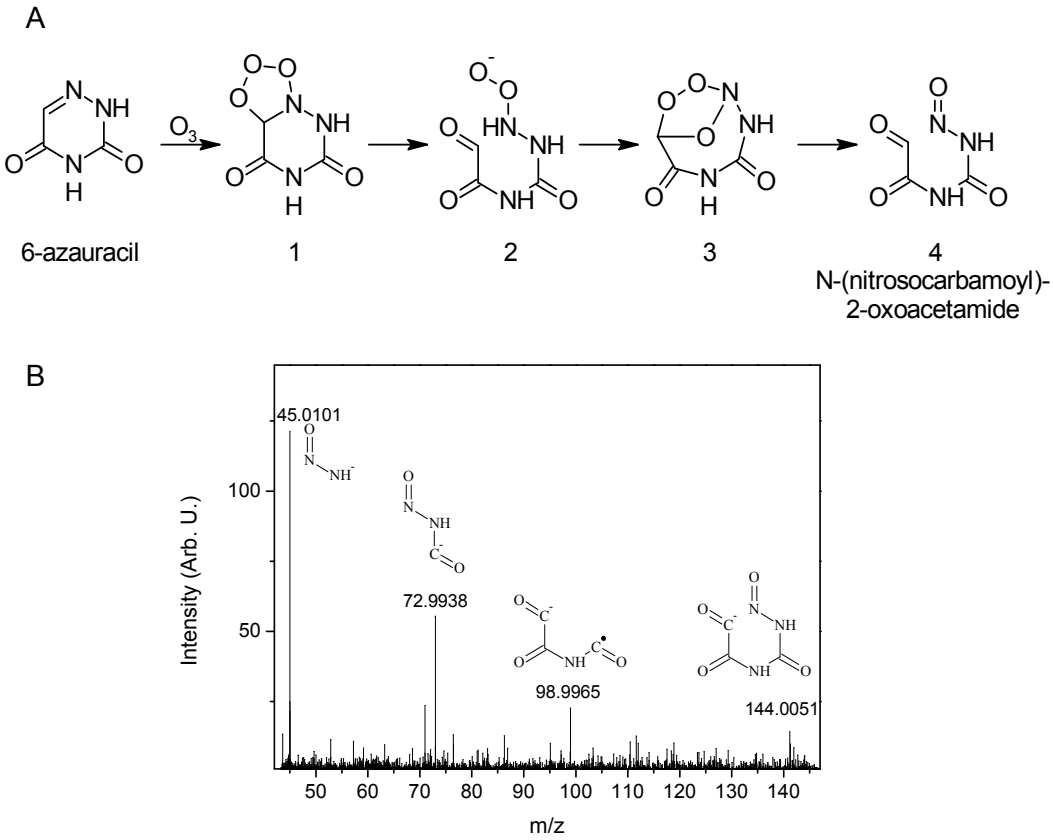

Figure 4.7: (A) Proposed reaction mechanism of ozone with 6-azauracil and formation of N-(nitrosocarbamoyl)-2-oxoacetamide (OP IV). (B) MS/MS spectrum of the fragmentat ion at *m/z* 144.0051 and structures proposed for the major product ions.

Further information regarding this OP was gained by collecting it as a fraction during HPLC analysis. For this, the ozone-treated sample was spiked with sodium sulfite eliminating ozone still present in the sample and thus ensuring no further reactions with ozone could take place. The collected fraction was dried under nitrogen, re-analyzed after reconstition in MilliQ water, and showed a peak eluting after 2.5 min. Because the retention time agreed with that of OP I, which was formed during ozonation of 6-azauracil, it was assumed that OP IV stabilizes under formation of OP I. Hence, the focus then lay on the identification of OP I (see section 4.1.3.2).

4.1.3.2 5-Hydroxyhydantoin (OP I)

Considering the fact that OP IV was unstable as well as its proposed structure, the stabilization was predicted to occur through the elimination of nitrogen monoxide and subsequent ring formation resulting in an OP known as 5-hydroxyhydantoin. When re-analyzing the data, the fragment ions *m/z* 115.0150 and *m/z* 97.0046 were detected in

negative ionization after 2.5 min retention time. Both fragment ions could be attributed to a compound with the uncharged empirical formula C3H4N2O3, which would agree with the structure of 5-hydroxyhydantoin. In-source fragmentation of the *m/z* 115.0150 resulting in the loss of water explains the presence of *m/z* 97.0046. Based on the results from MS/MS experiments (Figure 4.8, A), the suggested structure of the molecule was strengthened and agreed with the proposed mechanism (Figure 4.8, B). OP I could finally be confirmed by a commercial standard as 5-hydroxyhydantoin.

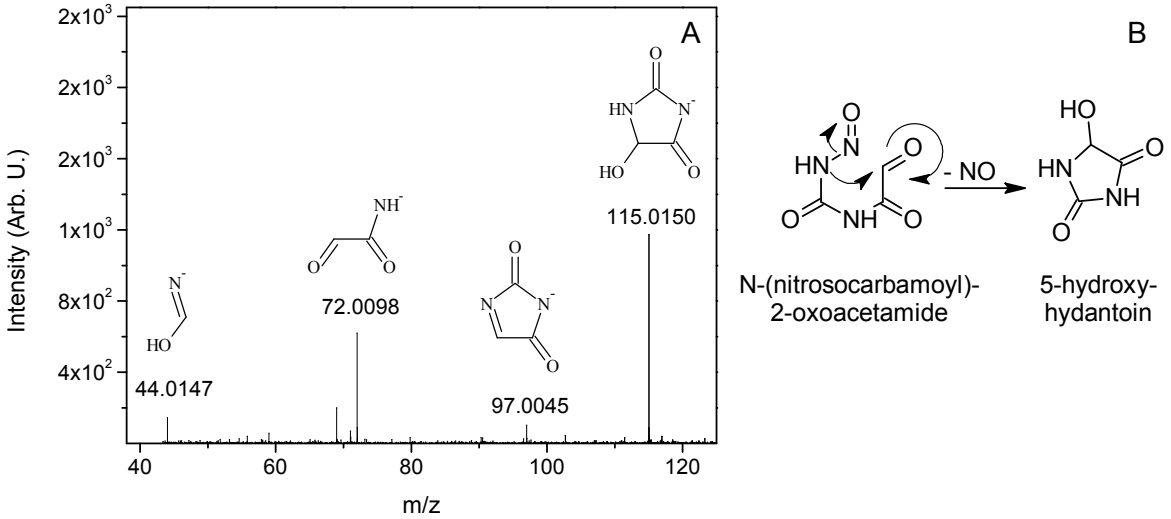

Figure 4.8: (A) MS/MS spectrum of OP I with the fragment ion at *m/z* 115.0150 and structures proposed for the product ions. (B) Proposed formation mechanism of 5-hydroxyhydantoin (OP I) from N-(nitrosocarbamoyl)-2-oxoacetamide (OP IV).

4.1.3.3 Parabanic acid (OP III)

OP III eluted after 4.8 min retention time and showed a fragment ion at *m/z* 112.9993 measured in negative ionization mode. The empirical composition for this OP was C3H2N2O3 and the DBEs were calculated as four.

When regarding elemental compositions of the OPs, 5-hydroxyhydantoin (see section 4.1.3.3) and OP III showed high similarities. The only differences were the additional DBE and the reduction of two hydrogen atoms in OP III. Based on these observations the oxidation of 5-hydroxyhydantoin was investigated and confirmed that OP III was formed through ozonation of 5-hydroxyhydantoin. The OP formed is known as parabanic acid and was verified by a commercial standard (retention time, UV spectrum, exact mass and MS/MS, see Figure 4.9, A). An explanation for the formation of parabanic acid during ozonation is that the hydroxyl group of 5-hydroxyhydantoin is further oxidized and forms a keto group (Figure 4.9, B).

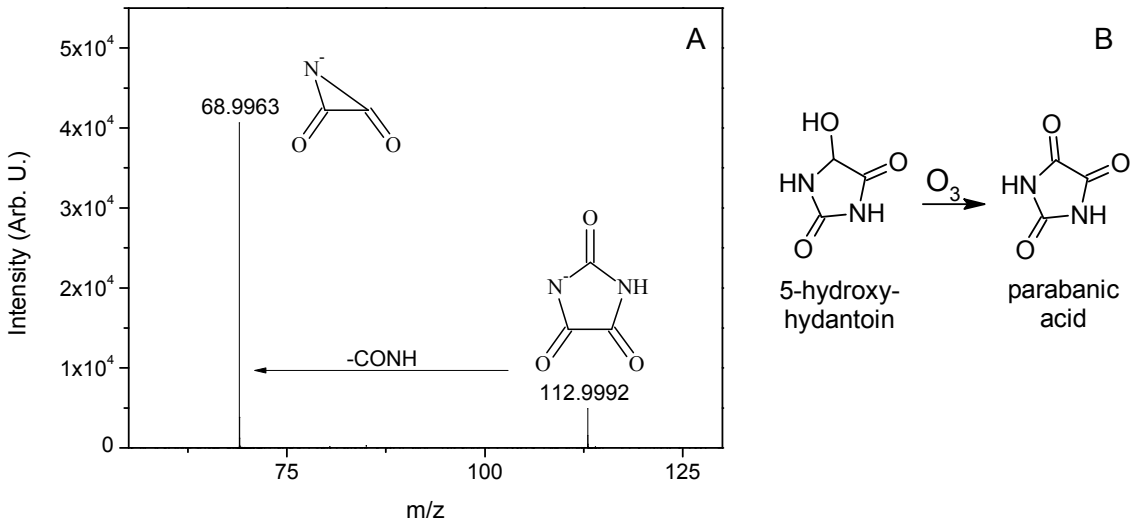

Figure 4.9: (A) MS/MS spectrum of parabanic acid (*m/z* 112.9993) in negative ionization mode. (B) Proposed formation of parabanic acid (OP III) via oxidation of 5-hydroxyhydantoin (OP I).

4.1.3.4 Oxaluric acid (OP II) and small organic compounds

A parabanic acid standard showed two UV signals (parabanic acid after 4.8 min and a new product after 4.3 min) in the chromatogram when re-analyzed the day after preparation (Figure 4.10, A). After one week stored at room temperature, parabanic acid was no longer detectable in the standard. The new product showed the same retention time as OP II. The change in UV spectrum from parabanic acid to the new product resulted in a loss of absorbance at 280 nm (Figure 4.10, A). This supports the theory that a hydrolysis with a ring opening occurs. Furthermore, for the fragment ion at *m/z* 131.0098 measured in negative ionization mode the neutral empirical formula (C3H4N2O4) revealed the addition of water. Furthermore, OP II has three double bond equivalents, one less than parabanic acid. Hydrolysis of parabanic acid could occur in two different positions (either the isolated keto group or the adjacent keto groups). Based on MS/MS experiments on the fragment ion at *m/z* 131.0098 and the only product ion (*m/z* 59.0255), a structure for the hydrolyzed product could be proposed (Figure 4.10, B). It is known as oxaluric acid and is formed through hydrolysis at the adjacent keto groups of parabanic acid (Figure 4.11, A).

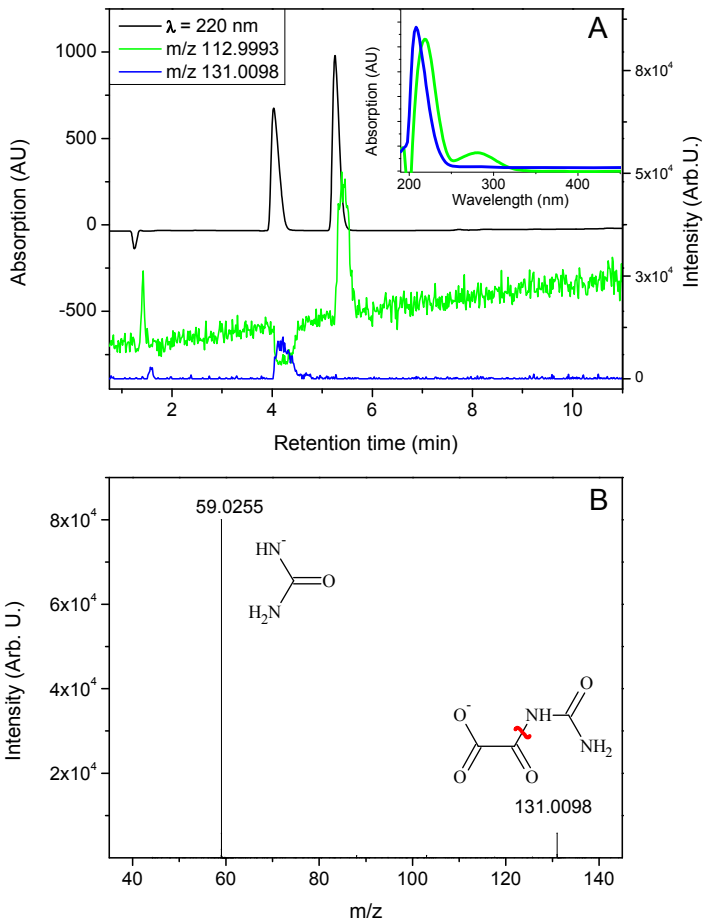

Figure 4.10: (A) UV chromatograms (λ = 220 nm) and EIC of parabanic acid (*m/z* 112.9993) and the hydrolysis product oxaluric acid (*m/z* 131.0098). (B) MS/MS spectrum of oxaluric acid (OP II) and the structure proposed for the product ion.

The identification of the hydrolysis product of parabanic acid as oxaluric acid has been reported in literature [115]. Oxaluric acid in turn is instable and can react in two different ways (Figure 4.11, A). The first way results in the formation of oxalic acid (confirmation see Figure 4.11, B) and urea. These again hydrolyze to ammonia and carbon dioxide [115]. The second pathway proposed is based on results from treating paraquat, a pesticide, with ozone. Here, an OP was identified as N-formyl oxamide acid which further reacted to oxamic acid [116]. Based on the structural similarity of oxaluric acid (contains a primary amine) and N-formyl oxamide acid (instead of the amine there is a hydrogen atom), the second reaction pathway seems plausible and hence would result in the formation of oxamic acid and carbamic acid, of which only the first could be confirmed by IC-CD analysis (Figure 4.11, B). In agreement with these results, it has been reported that hydrolysis of an acetamide moiety leads to the formation of the dealkylated degradation product and acetic acid [117]. However, the formation of oxamide could not be explained with these reaction pathways.

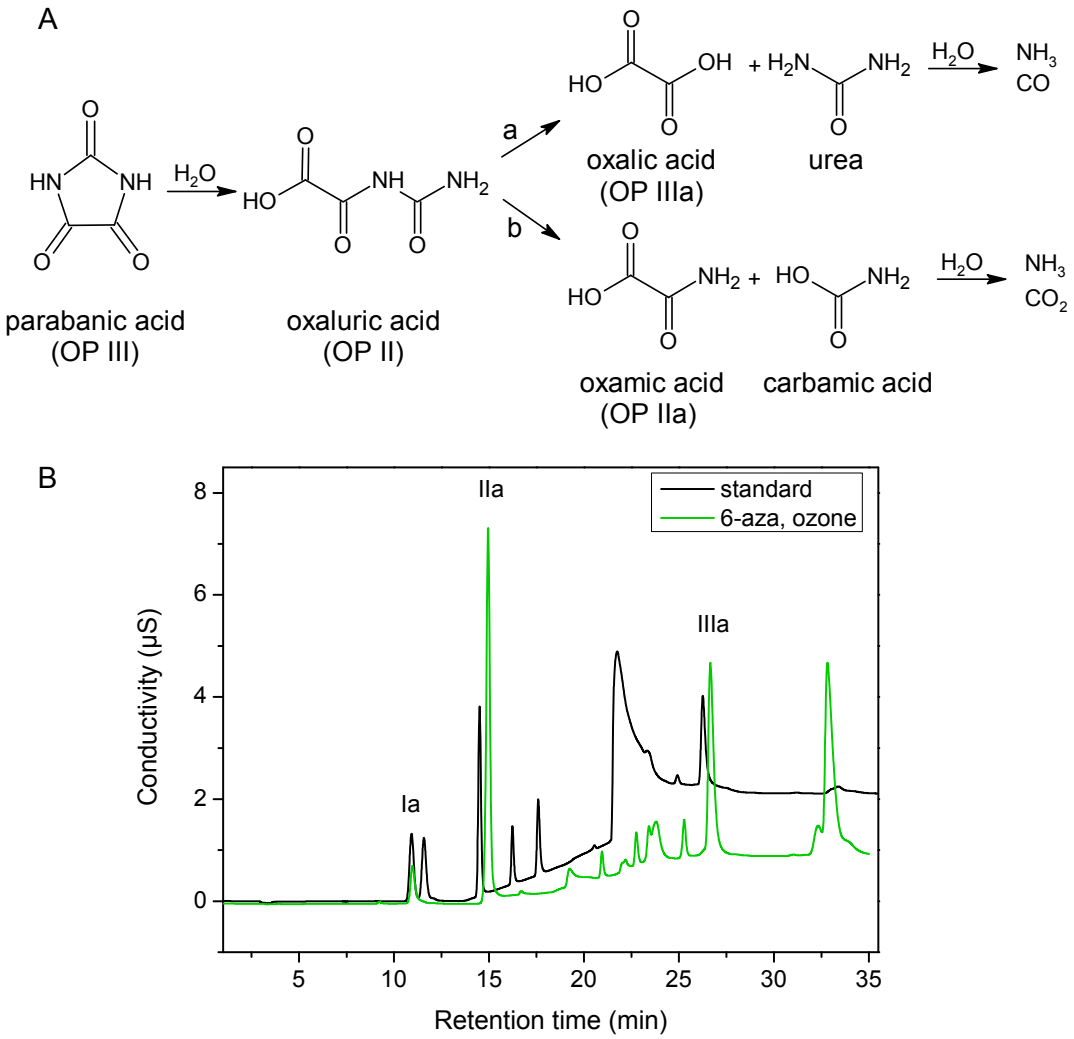

Figure 4.11: (A) Degradation of parabanic acid forming oxaluric acid which can decompose in two ways. Pathway (a) results in the formation of oxalic acid and urea. These in turn hydrolyze to ammonia and carbon dioxide [115]. Pathway (b) results in the formation of oxamic acid and carbamic acid (not detected), which further decompose to ammonia and carbon dioxide. (B) IC chromatogram of a standard solution containing oxamide (Ia), oxamic acid (IIa) and oxalic acid (IIIa) and an ozone-treated 6-azauracil (6-aza) sample.

To determine whether oxaluric acid undergoes further reactions with ozone, an oxaluric acid-containing solution was treated with ozone. The treatment with ozone resulted in no decrease in concentration. Therefore a decrease in concentration over time can only be attributed to other reactions occurring than ozonation, such as hydrolysis.

4.1.3.5 1,2,4-Triazinane-3,5,6-trione (OP V)

Based on high resolution MS data, the uncharged empirical formula C3H3N3O3 was proposed for the fragment ion at *m/z* 128.0102 of a minor OP eluting after 4.3 min. Because this OP was formed from 6-azauracil, the only change in elemental composition was the addition of one oxygen molecule. The formation of this OP can be explained by the known nucleophilic attack of ozone to carbon-nitrogen double bonds and results in the oxidation of

the carbon atom [34]. The proposed structure for OP V (1,2,4-triazinane-3,5,6-trione) is able to account for the major product ions from MS/MS experiments (Figure 4.12, A and B).

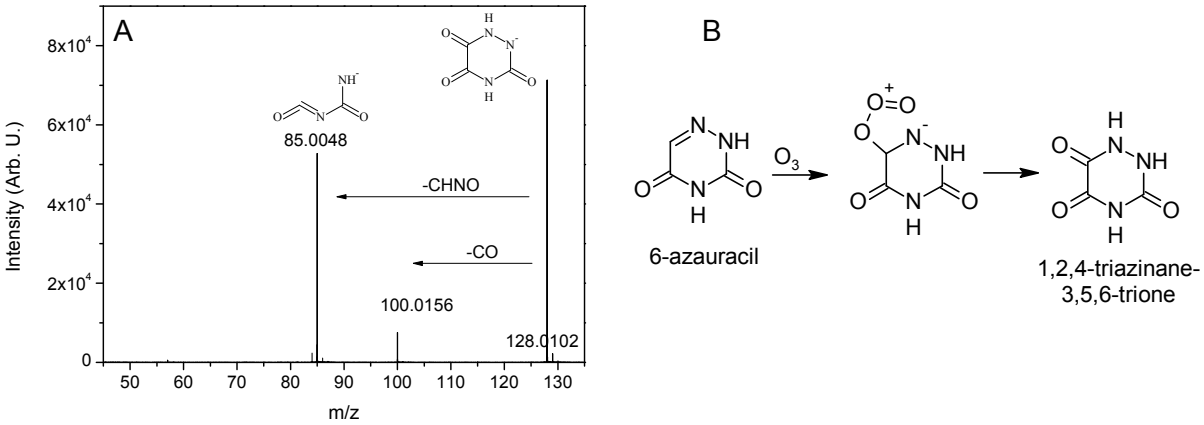

Figure 4.12: (A) MS/MS spectrum of the fragment ion at *m/z* 128.0102. (B) Proposed formation mechanism via a nucleophilic attack of ozone on the carbon-nitrogen double bond of 6-azauracil resulting in the formation of 1,2,4-triazinane-3,5,6-trione (OP V).

4.1.4 1,2-Dihydro-1,2,4-triazine-3,6-dione (OP 3)

The structural isomer of 6-azauracil eluted after 4.7 min retention time. Due to structural differences, this OP could be detected in both positive (*m/z* 114.0298) and negative (*m/z* 112.0152) ionization mode, whereas 6-azauracil could only be detected in negative mode. The UV maximum at 272 nm for OP 3 indicated that this compound still consisted of conjugated π-electrons and therefore preservation of a ring structure was likely. Furthermore, the slight bathochrome shifts observed from 6-azauracil (205 nm and 258 nm, section 4.1.2 Figure 4.4, B) to OP 3 (232 nm and 272 nm, Figure 8.5) could be explained by an increase in the conjugated π-electron system.

A comparison of the product ions of 6-azauracil (see section 4.1.2, Figure 4.4, C) with the product ions of OP 3 (Figure 4.13, A) showed that the major fragment ion at *m/z* 68.9961 was identical and thus both OPs must have structural similarities. Furthermore, a comparison of MS/MS experiments on OP 3 in both ionization modes revealed the formation of two product ions (Figure 4.13, A and B). The exact masses of the product ions in positive ionization mode corresponded to those in negative mode and hence the neutral fragments were of identical elemental composition. The second product ion was formed through the elimination of carbon monoxide. Based on these results the structure depicted in Figure 4.13 was proposed and is called 1,2-dihydro-1,2,4-triazine-3,6-dione. However, it was not possible to propose a plausible mechanism for the transformation of DPC to this OP.

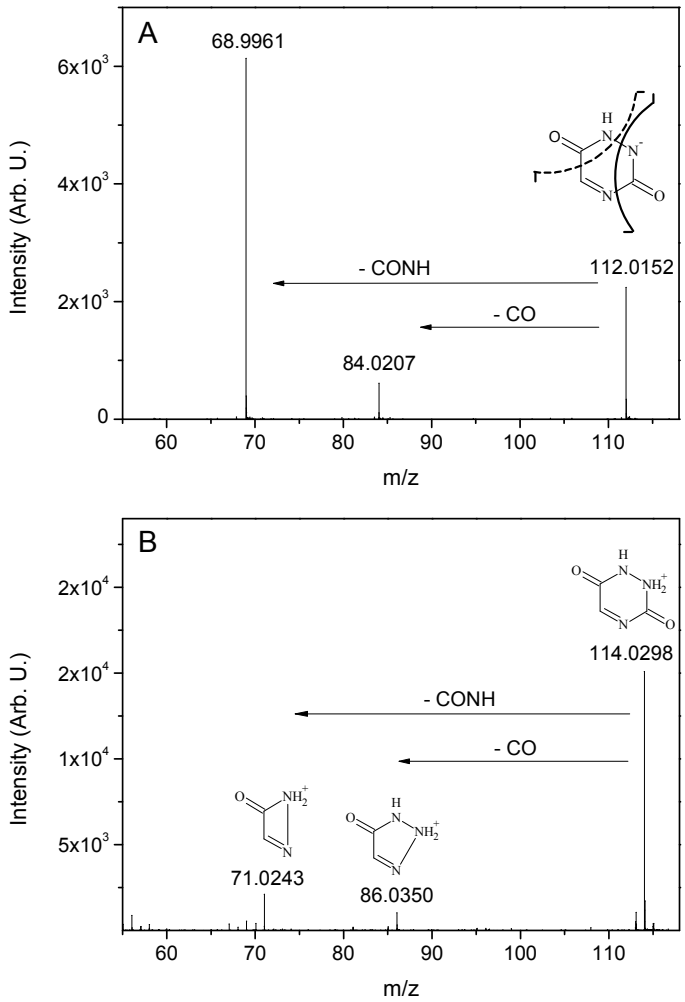

Figure 4.13: (A) MS/MS spectra of iso-6-azauracil measured in negative and (B) positive ionization mode. Based on the product ions the structure for OP 3 is proposed as 1,2-dihydro-1,2,4-triazine-3,6-dione.

Table 4.1: Retention times, UV maxima, MS and MS/MS ions gained from desphenyl-chloridazon, its primary OPs (A), OPs from 6-azauracil (B) and the synthesized reference compound (C). Numbering of OPs formed from DPC depicted in Figure 4.1 and numbering of OPs formed from 6-azauracil depicted in Figure 4.6. Mass error differences were calculated as the deviation of the measured *m/z* from the calculated exact *m/z* and were smaller than 1 ppm in all cases.

Peak No./OP No.	Proposed products	Reference standard	Retention time	UV maxima	Ionization mode	Observed fragment ions MS	MS/MS	Calculated mass to charge ratio	Mass error
A			min	nm	+/-	*m/z*	*m/z*	*m/z*	ppm
DPC	-	Yes	10.4	198, 224, 278	+	146.0116	116.9980, 100.9901, 87.9949, 73.9911, 66.0218, 54.0345	146.0116	0.06
OP 1	Not identified	No	2.2	205, 265					
OP 2	Pyridazine-3,4,5-trione	No	4.3	226, 252	+	127.0138	99.0194, 70.0655, 56.0499, 44.0133	127.0138	0.38
OP 3	1,2-Dihydro-1,2,4-triazine-3,6-dione	No	4.7	232, 272	+	114.0298	86.0350, 71.0243, 44.0129	114.0298	0.39
OP 4	6-Azauracil	Yes	6.0	205, 258	-	112.0152	68.9962	112.0152	0.18
OP 5 or OP IV	N-(Nitrosocarbamoyl)-2-oxoaceamide	No	6.5	225, 250	-	144.0051	98.9965, 72.9938, 45.0101	144.0051	0.07
OP 6	Not identified	No	7.4	222, 265					
B			min	nm	+/-	*m/z*	*m/z*	*m/z*	ppm
OP I	5-Hydroxyhydantoin	Yes	3.0	220	-	115.0150	97.0048, 72.0092	115.0149	0.44
OP II	Oxaluric acid	No	4.3	208	-	131.0098	59.0255	131.0098	0.61
OP III	Parabanic acid	Yes	5.6	220, 280	-	112.9992	86.9963	112.9993	0.32
OP V	1,2,4,-Triazine-3,5,6-trione	No	4.3	Not detectable	-	128.0102	100.0156, 85.0048	128.0102	0.37
C			min	nm	+/-	*m/z*	*m/z*	*m/z*	ppm
Synthesis product	4,5-Dihydroxy-pyridazine-3-one	No	13.4	216, 288	+	129.0297	70.0659, 56.0501, 44.0500	129.0295	0.50

4.1.5 Summary and discussion of the oxidation pathway of DPC

Although several mechanisms for the reaction of ozone with carbon-nitrogen double bonds have been described (see introduction, section 1.2) they were not detected during ozonation of DPC [34,59]. However the reaction of ozone with the carbon-carbon double bond of DPC via 1,3-dipolar cycloaddition could be observed. The chronological formation of the identified OPs from DPC during ozonation is proposed in the oxidation pathway depicted in Figure Figure 4.14. In a first step, the double bond situated between C4 and C5 of the pyridazine ring in DPC is attacked by ozone. It is oxidized either to pyridazine-3,4,5-trione (OP 2) or to 6-azauracil (OP 4).

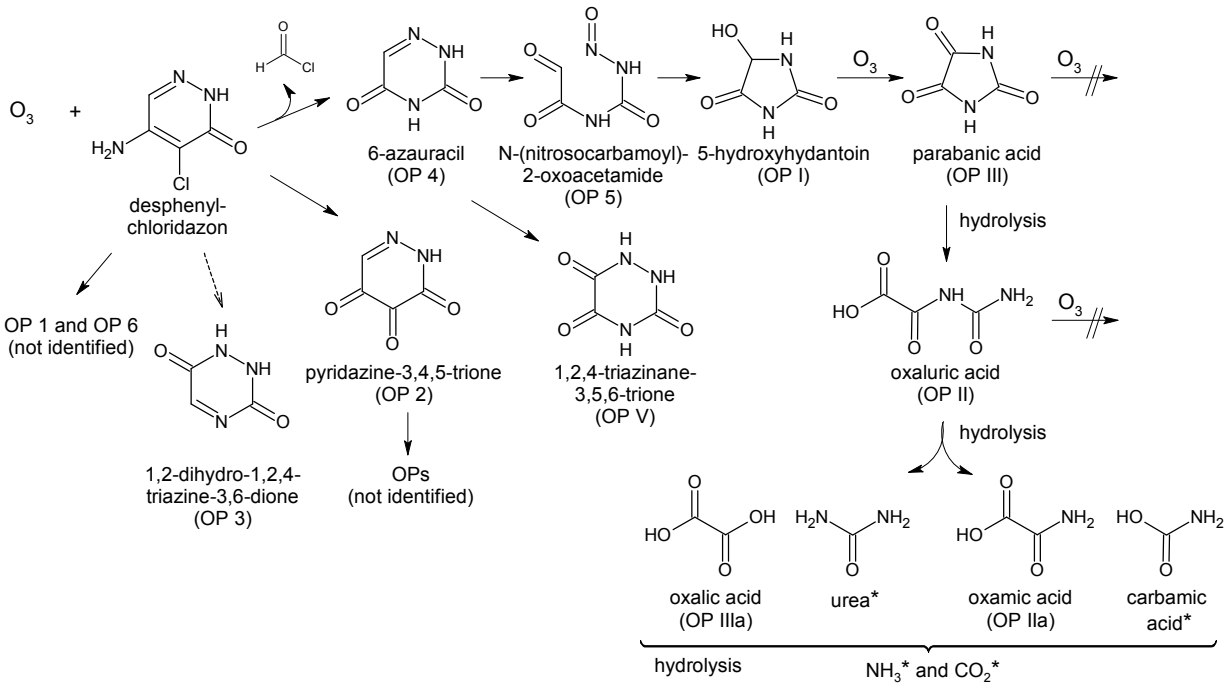

Figure 4.14: Proposed oxidation pathway for DPC. A reaction mechanism for the formation of OP 3 could not be proposed. OPs not detected are marked with (*).

OPs arising through further oxidation of pyridazine-3,4,5-trione could not be identified due to the lack of a commercial standard. A possibility for the elucidation of these OPs is to apply the described HPLC method (section 3.2.9) to ozone-treated DPC samples and collect OP 2 as a fraction. After purification, it could be treated with ozone and the missing pathway could be investigated with a focus on the formation of small organic acids. Fractionation could also help to gain further information on the formation mechanism of OP 3 and on the structures of the two unknown oxidation products OP 1 and OP 6. For example, the presence of functional groups such as aldehydes and primary or secondary amines in the OP could be confirmed through specific tests. Furthermore, derivatization and analyses by GC-MS, or nuclear

magnetic resonance (NMR) measurements could help to elucidate the structures of these OPs.

In contrast to OP 2 the further oxidation of 6-azauracil (OP 4) could be elucidated. 6-Azauracil undergoes further reactions with ozone forming 5-hydroxyhydantoin via the instable intermediate N-(nitrosocarbamoyl)-2-oxoacetamide. Under further oxidative conditions, the hydroxyl group of 5-hydroxyhydantoin is oxidized to a keto group forming parabanic acid. This compound shows no reactivity towards ozone, but is hydrolyzed to oxaluric acid. Oxaluric acid decomposes either to oxalic acid and urea or to oxamic acid and carbamic acid. It is known that, in both cases, further decomposition results in the formation of ammonia and carbon dioxide.

When considering possible adverse effects from the identified OPs, no data is available for pyridazine-3,4,5-trione, however 6-azauracil is a well described chemical because it has been investigated as a chemotherapeutic agent [118,119]. Hence, several effects caused through 6-azauracil have been reported in literature [120,121]. 6-Azauracil is structurally closely related to the RNA-base uracil. It has been shown that effects of 6-azauracil strongly vary between different species and especially children and younger animals show higher sensitivity towards treatment with 6-azauracil [119,121]. Not only does 6-azauracil show adverse effects towards animals and humans, it is also absorbed by plants, such as the cocklebur [122]. When absorbed, it is converted to azauridine, to azauridine-5´-phosphate and then incorporated into RNA. The observed inhibition of flowering induction after treatment with 6-azauracil could be due to these “inactive” RNA molecules, as there is evidence that normal RNA synthesis is essential for the induction of flowering in plants [123]. Furthermore, 6-azauracil has been classified as highly hazardous to water [124,125].

Because of the known effects of 6-azauracil which have been described in literature the formation of this OP from DPC in environmentally relevant concentrations is of particular interest. Hence, an enrichment method was established for further investigations. The following section describes the development and validation of a solid-phase extraction (SPE) method as well as the results from its application to natural waters [118,120,122].

4.2 Development and application of an SPE enrichment method

To enable the detection of 6-azauracil formation in samples with low initial concentrations of DPC an enrichment step is required because of the relatively high detection limit of 6-azauracil (~1 µg/L) when using direct injections. Hence, an enrichment via SPE was established. As 5-hydroxyhydantoin is the primary OP formed through oxidation of 6-azauracil this OP was also included in the method. For the development of the method several SPE materials, pH values, sample volumes and sample concentrations were tested. Furthermore, the method was validated by determining compound stabilities, recoveries, limits of detection (LOD) and limits of quantification (LOQ) as well as matrix effects. The results are presented in this sections.

4.2.1 Sample preparation

25 mL of 1 mM stock solutions of each analyte were prepared in MilliQ water. Because of the low solubility of the analytes the solutions were stirred over night. Solutions were first diluted to a 100 µM stock solution mixture and then further diluted with MilliQ water to 1 µM solutions for the experiments. Aliquots of the 100 µM solution were stored at -18°C.

Conditioning of the SPE cartridges was performed with 5 mL of methanol and 10 mL of MilliQ water with the respective pH value of the water sample. After this each SPE cartridge was loaded with 20 mL of drinking water (for details see Table 8.1) with the adjusted pH value which previously had been spiked with 200 µL of the 1 µM standard mixture. Hence, the concentration of the analytes in the water samples was set to 0.01 µM. The cartridges were dried under nitrogen (45 min) and in a first step the analytes were eluted with 6 mL methanol followed by a second elution step performed with 6 mL iso-propanol. The solutions were dried under a gentle nitrogen stream and re-constituted in 200 µL of MilliQ water. Thus, the theoretical enrichment factor for these experiments is 100.

4.2.2 Method development

4.2.2.1 Selection of SPE material

The following six SPE materials were tested for the enrichment of 0.01 µM solutions of the analytes DPC, 6-azauracil and 5-hydroxyhydantoin: Bakerbond SDB 1, LiChrolut EN, Isolute C18, Bond Elut PPL (PPL), Strata-X and Strata-XA (for details see section 3.1.2). Strata-XA is a strong anion-exchange material with a functionalized polymeric sorbent which shows good retention for acidic compounds. Bond Elut PPL is a styrene-divinylbenzene polymer with a non-polar surface which is used for the enrichment of highly polar analytes. Bakerbond

SDB 1 (SDB 1) and Strata-X materials are based on divinylbenzene polymers. SDB 1 is a non-funtionalized phase and Strata-X is surface modified to increase selectivity towards polar compunds. Isolute C18 is a non-endcaped octadecyl functionalized silica-based phase and LiChrolut EN is a hypercrosslinked polystyrene material with high sorption capacity towards both polar and non-polar organic compounds. The enrichment experiments were performed in drinking water at pH 3 and pH 7 for all materials, except for Strata-XA where drinking water with a pH value of 10 was used. All experiments were performed in a minimum of duplicates and average values are reported.

The results for the enrichment after methanol elution are summarized in Table 4.2. For all SPE materials tested the recoveries at pH 7 (Table 4.2, A) for 6-azauracil and 5-hydroxyhydantoin were lower than 22 %. Best recoveries for DPC were achieved at pH 7 with the LiChrolut EN material (63 %). Comparison of the enrichment at the different pH values showed that the enrichment at pH 3 was generally more efficient than at pH 7. The best enrichment at pH 3 for DPC (83 %) and 6-azauracil (53 %) could be achieved with the SPE materials SDB 1 and LiChrolut EN. The enrichment at pH 10 with Strata-XA showed low recoveries for 6-azauracil (23 %) and DPC (20 %), however it showed the best recovery for 5-hydroxyhydantoin (42 %). As no further elution occurred when using iso-propanol in addition to methanol, this step was discarded in future experiments.

Table 4.2: Recoveries for 20 mL of 0.01 µM concentrations of the three analytes DPC, 6-azauracil and 5-hydroxyhydantoin (5-OH) with different SPE materials. (A) shows the results at pH 7 and (B) the results at pH 3 (Strata-XA at pH 10); n = 2.

A

Analyte	C18	PPL	SDB 1	Strata-X	LiChrolut EN
6-Azauracil (%)	4 ± 0	5 ± 0	8 ± 1	7 ± 0	22 ± 6
5-OH (%)	15 ± 9	< 1	6 ± 0	3 ± 0	5 ± 2
DPC (%)	22 ± 0	51 ± 0	51 ± 5	35 ± 0	64 ± 23

B

Analyte	C18	PPL	SDB 1	Strata-X	LiChrolut EN	Strata-XA
6-Azauracil (%)	8 ± 0	14 ± 0	53 ± 3	12 ± 0	56 ± 1	23 ± 6
5-OH (%)	9 ± 4	5 ± 1	13 ± 2	9 ± 0	12 ± 0	42 ± 2
DPC (%)	21 ± 1	48 ± 0	84 ± 2	32 ± 0	83 ± 1	20 ± 1

4.2.2.2 Optimization of enrichment parameters

Based on the material selection experiments (section 4.2.2.1) SDB 1 and LiChrolut EN were chosen for further optimization. To determine if an increase in SPE bed material volume

results in an increase in recovery the bed volume was changed from 200 mg to 500 mg. The other parameters were as described in section 4.2.1.

The results presented in Table 4.3 demonstrate that increasing the volume of the bed-material from 200 mg to 500 mg resulted in an increase of recovery for 5-OH from 13 % to 32 % and for 6-azauracil from 53 % to 70 %. The recovery for DPC remained unchanged (~85 %).

Table 4.3: Recoveries of the analytes using 200 mg and 500 mg of SDB 1 and LiChrolut EN material; n = 3.

Analyte	SDB 1 (mg)		LiChrolut EN (mg)	
	200	500	200	500
6-Azauracil (%)	53 ± 3	69 ± 3	56 ± 1	71 ± 4
5-Hydroxyhydantoin (%)	13 ± 2	32 ± 2	12 ± 0	32 ± 2
DPC (%)	84 ± 2	85 ± 1	83 ± 1	85 ± 2

In summary the enrichment of DPC, 6-azauracil and 5-hydroxyhydantoin can be performed with either SDB 1 or LiChrolut EN SPE cartridges, if 500 mg material is used. As 500 mg SDB 1 columns are not commercially available, further experiments were performed with the 500 mg LiChrolut EN cartridges.

4.2.2.3 Influence of sample volume and concentration

To determine whether the sample volume or the concentration of the analyte influences recoveries, experiments using different volumes of drinking water (20 mL, 50 mL, and 100 mL) and increasing concentrations (5 nM, 10 nM, and 20 nM) of analytes were performed in triple determination. Depending on the concentration, samples were reconstituted with either 100 µL, 300 µL or 500 µL of MilliQ water after SPE and this dilution factor was included in the results summarized in Table 4.4.

The results show that the recovery of DPC under the chosen conditions was around 80 % and was independent of the sample volume and concentration. Hence, the enrichment volume could be increased to 100 mL, if required. The results also show that the chosen bed volume of 500 mg SPE material was sufficient for the enrichment even of 100 mL sample volume.

Table 4.4: Influence of sample concentration and enrichment volume on recoveries for DPC, 6-azauracil and 5-hydroxyhydantoin. Percentage of recovery and standard deviation; n = 3.

c (nM)	DPC (%) Enrichment volume (mL)			6-Azauracil (%) Enrichment volume (mL)			5-Hydroxyhydantoin (%) Enrichment volume (mL)		
	20	50	100	20	50	100	20	50	100
5	86 ± 1	78 ± 1	72 ± 3	74 ± 1	43 ± 2	22 ± 0	20 ± 0	8 ± 1	4 ±1
10	77 ± 7	75 ± 1	81 ± 0	71 ± 4	47 ± 2	24 ± 0	15 ± 3	6 ±	< 2
20	79 ± 2	75 ± 0	83 ± 0	62 ± 2	41 ± 0	25 ± 0	14 ± 1	< 2	< 2

In the case of 6-azauracil, increasing analyte concentrations for the enrichment of 20 mL samples had no effects on recoveries, which were around 70 %. It was observed that doubling the sample volume from 20 mL to 50 mL and from 50 mL to 100 mL resulted in a loss of recovery of 25 % independent of the sample concentration. To determine whether the loss of enrichment was caused by insufficient SPE bed material the comparison of the following samples was of use. The enrichment of 50 mL of a 10 nM solution should result in the same concentration after SPE as when enriching 100 mL of a 5 nM solution. The same should apply for the comparison of concentrations after SPE for 50 mL of a 20 nM solution and 100 mL of a 10 nM solution. Enrichment of 50 mL of a 10 nM solution resulted in a concentration of 1.2 µM 6-azauracil after SPE whereas enrichment of 100 mL of a 0.5 nM solution resulted in a concentration of 0.5 µM 6-azauracil after SPE (compare Table 8.2 in the appendix). Similar results were obtained for the other comparison. Hence, insufficient bed material can be exluded as reason for the lower recoveries. Although a higher loss of 6-azauracil was observed when enriching 50 mL, an increase in sample volume from 20 mL to 50 mL still resulted in a higher concentration in all enriched samples, whereas an increase to 100 mL did not result in any further enrichment (compare Table 8.2). For example, the enrichment of 20 mL of a 5 nM solution resulted in a concentration of 0.3 µM after SPE, whereas 50 mL and 100 mL of the same solution each resulted in a concentration of 0.5 µM after SPE. Hence, the enrichment volume could be increased to 50 mL, if required, but an increase to 100 mL would show no effect on enrichment and thus on the sensitivity of the method.

For 5-hydroxyhydantoin an increase in analyte concentration when enriching 20 mL water samples showed no effect on recoveries which were approximately 20 %. However an increase in sample volume from 20 mL to 50 mL or 100 mL resulted in no further increase in the concentration of 5-hydroxyhydantoin in the extracts and therefore higher sample volumes decrease recoveries for 5-hydroxyhydantoin.

4.2.3 Method validation

4.2.3.1 Compound stability

The influence of the water matrix and the pH value on the stability of the compounds was determined. For this, pH values in MilliQ water and drinking water were set to pH 3, pH 7 and pH 10 and samples were spiked with the analytes (concentration 1 µM). After storage at room temperature for one month the samples were analyzed. Furthermore, the influence of sodium sulfite, which was used to destroy residual ozone in the oxidation experiments, was investigated under the same conditions to ensure that this reagent has no effect on the analytes and can be used for the experiments.

DPC and 6-azauracil were stable independent of water matrix and pH value, showing concentrations ranging between 110 % and 140 % recoveries. This could be caused through variations in the sensitivity of the instrument such as ionization yield. 5-Hydroxyhydantoin was only stable at pH 3. At pH 7 5-hydroxyhydantoin showed a faster decrease in concentration in drinking water compared to MilliQ water. At pH 10 only traces of 5-hydroxyhydantoin were present in both matrices after one month (Table 8.3 in the appendix). Despite the overall statement that DPC and 6-azauracil are stable under the chosen conditions, the test was repeated under slightly modified conditions. Double determinations of DPC and 6-azauracil containing solutions at pH 3 and pH 7 were re-analyzed after storage for two weeks at 4 °C and the results are presented in Table 4.5. The results confirm that the stability of DPC and 6-azauracil is independent of the pH value and the water matrix.

Table 4.5: Analyte stability depending on water matrix and pH value. Drinking water (DW), MilliQ water (MQ); n = 2.

	pH 3		pH 7	
Analyte	MQ	DW	MQ	DW
DPC (%)	100 ± 2	98 ± 0	101 ± 1	98 ± 0
6-Azauracil (%)	95 ± 1	103 ± 1	100 ± 4	102 ± 1

To determine the influence of sulfite on the analytes, samples were spiked with sulfite and compared to control samples in double determinations. The recoveries for DPC (97 % ± 1 %) and 6-azauracil (99 % ± 0 %) show that the presence of sulfite in the samples has no influence on the analytes (see Table 8.4 in the appendix).

4.2.3.2 Recovery, RSD, LOD and LOQ

The enrichment of a calibration should clarify if the recovery of different concentrations of the analytes is linear. For this, eight drinking water samples with concentrations between 0.05 nM and 5 nM of the analytes were subjected to the entire enrichment procedure. The absolute recoveries over the whole sample preparation procedure were calculated for the calibration curves by comparing the slope of the direct calibration with the slope after SPE enrichment. Furthermore, nine identical samples of drinking water containing the analytes in a concentration of 5 nM were subjected to the entire analytical procedure to determine relative standard deviations (RSD) of the method. The limits of detection (LOD) and the limits of quantification (LOQ) were calculated with the SQS software according to the German standard DIN 32645 [126]. Slopes of the direct calibration curves (0.05 nM to 20 nM) and of the curves after SPE enrichment are compared in Table 4.6. Recoveries for the analytes were calculated by the following equation:

$$\text{Recovery (\%)} = \frac{\text{slope}_{\text{SPE}}}{\text{slope}_{\text{direct}}} * 100$$

Equation 4.1: Determination of the recovery of the SPE enrichment of DPC, 6-azauracil and 5-hydroxyhydantoin.

The recoveries varied for each analyte. DPC (80 %) showed the best recovery and was followed by 6-azauracil (68 %). 5-Hydroxyhydantoin (25 %) showed the lowest recovery. Although varying recoveries were observed for the individual analytes, DPC and 6-azauracil showed high linearity in enrichment which is represented through high values of correlation coefficients (R^2 > 0.999), but 5-hydroxyhydantoin showed a slightly larger deviation (R^2 > 0.977). However, the total recovery does not distinguish between the losses during sample preparation and ion suppression or enhancement in the interface of the mass spectrometer. The origin of the reduced recoveries will be further investigated in section 4.2.3.3.

Table 4.6: Slopes of the direct and enriched calibration curves for the individual analytes and the calculated recoveries in %.

	DPC	6-Azauracil	5-Hydroxyhydantoin
$\text{Slope}_{\text{SPE}}$	0.8028	0.6779	0.2453
$\text{Slope}_{\text{direct}}$	1.0004	1.0006	1.0005
Recovery (%)	80.2	67.7	24.5

For each analyte the RSD over the entire method was calculated as the ratio of the standard deviation to the mean value and ranged between 2 % and 8 % (Table 4.7). Furthermore, a standard solution with a concentration of 0.5 µM was re-injected and analyzed (without SPE enrichment) six times to determine the RSD caused through injections into the HPLC system

(Table 4.8). The RSD values showed low differences for DPC (0.4 %) and 6-azauracil (1.3 %) and a slightly higher value for 5-hydroxyhydantoin (4.0 %).

Table 4.7: Reproducibility over the entire SPE method with a 5 nM solution. Mean values (MV), standard deviations (SD) and relative standard deviations (RSD); n = 9.

Analyte	DPC	6-Azauracil	5-Hydroxyhydantoin
MV (µM)	0.868	0.674	0.128
SD (µM)	0.020	0.045	0.010
RSD (%)	2.3	6.7	8.1

Table 4.8: Reproducibility of injections with a 0.5 µM solution. Mean values (MV), standard deviations (SD) and relative standard deviations (RSD); n = 6.

Analyte	DPC	6-Azauracil	5-Hydroxyhydantoin
MV (µM)	0.531	0.483	0.558
SD (µM)	0.002	0.006	0.022
RSD (%)	0.40	1.33	4.00

The limits of detection and limits of quantification calculated with the SQS software are summarized in Table 4.9. For DPC the LOQ according to the German DIN standard was calculated as 0.17 nM (25 ng/L) and for 6-azauracil the LOQ according to the German DIN standard was 0.234 nM (26 ng/L). For 5-hydroxyhydanotin the LOQ was an order of magnitude higher and was determined as 1.37 nM (159 ng/L). Thus, the quantification levels for DPC and 6-azauracil are sufficient for the planned experiments.

Table 4.9: Determination of the limit of detection (LOD) and limit of quantification (LOQ) for the analytes DPC, 6-azauracil and 5-hydroxyhydantoin.

Analyte	DPC	6-Azauracil	5-Hydroxyhydantoin
LOD (nM)	0.05	0.06	0.39
LOQ (nM)	0.17	0.23	1.37
LOQ (ng/L)	25	26	159

4.2.3.3 Determination of matrix effects

Since no internal standards were used for quantification it was important to estimate matrix effects. To determine the origin of reduced recoveries of the analytes, triple determinations of drinking water (DW) samples spiked with 200 µL of a 1 µM stock solution (Std) at different steps of the enrichment procedure were performed. The final concentration in the samples (assuming a 100 % recovery) was 1 µM for all analytes. The following procedure gives an overview of where the standard was added to the sample:

I) DW sample + Std → SPE → dry → reconstitute

II) DW sample → SPE → + Std → dry → reconstitute

III) DW sample → SPE → dry → + Std → reconstitute

In the first set of samples the standard with the analytes was added directly to the drinking water (I). In the second set drinking water was enriched via SPE and after elution with methanol the standard was added. In the third set of samples the standard was used to reconstitute the dried sample.

Results gained from samples spiked prior to SPE (I) and after SPE elution (II) enable the determination of losses caused by SPE enrichment. The decrease in concentration by SPE was 14 % for DPC, 3 % for 6-azauracil and 82 % for 5-hydroxyhydantoin (Table 4.10). Furthermore, comparison of samples which were spiked after SPE (II) and samples spiked after evaporation to dryness (III) enabled the determination of the effects caused through evaporation. Losses attributed to evaporation were determined as 6 % for DPC, 24 % for 6-azauracil and 0 % for 5-hydroxyhydantoin. Finally, to estimate matrix effects on ionization in the interface of the mass spectrometer, a sample was spiked after its evaporation (III) and compared to the direct injection at the same concentration. Samples derived from (III) showed the same matrix burden as (I) but did not undergo changes in analyte concentration during SPE enrichment. Thus, reduced recoveries for (III) can be attributed to either signal suppression or enhancement in the interface and were smaller than 9 % for all analytes (Table 4.10).

Table 4.10: Determination of the influence of matrix effects due to SPE, evaporation or MS on recoveries in % for DPC, 6-azauracil and 5-hydroxyhydantoin (5-OH); n = 3.

Analyte	Prior SPE (I)	After SPE elution (II)	After reconstitution (III)
DPC (%)	73 ± 2	86 ± 3	91 ± 1
6-Azauracil (%)	69 ± 4	72 ± 1	95 ± 1
5-OH (%)	19 ± 5	107 ± 0	107 ± 8

Some experiments were also performed in river water (river Rhine, for details see Table 8.1 in the appendix) and thus the influence of this matrix on recoveries could also be determined. For this, drinking water and river water samples were spiked with 200 µL of a 0.5 µM stock solution of the analytes resulting in a concentration of 5 nM prior to SPE. The results from these samples were then compared to determine differences in recovery caused through the river water matrix. The results shown in Table 4.11 demonstrate that applying the SPE method to river water samples showed no significant effects on the enrichment behavior of the analytes. Hence this method can also be used for the enrichment of river water samples.

Table 4.11: Determination of losses caused by SPE in drinking water (DW) and water from the river Rhine (RDK) for the analytes DPC, 6-azauracil and 5-hydroxyhydantoin (5-OH); n = 3.

Analyte	DW	RDK
DPC (%)	80 ± 2	88 ± 3
6-Azauracil (%)	69 ± 4	75 ± 2
5-OH (%)	38 ± 5	44 ± 6

4.2.4 Validated SPE method

The principle procedure for the SPE enrichment is summarized in Table 4.12 and the main results for the validation are listed in Table 4.13. It was possible to develop a method for the quantitative trace level analysis of DPC and 6-azauracil in different matrices. A representative chromatogram of the analytes and an extracted ion chromatogram of a drinking water blank after SPE enrichment are shown in Figure 8.9 in the appendix.

Table 4.12: SPE procedure for the enrichment of 6-azauracil and DPC.

Preparation steps	Procedure
SPE material	LiChrolut EN 6 mL; 500 mg
Conditioning	a) 10 mL methanol b) 10 mL MilliQ water (pH 3)
Load	20 ml DW sample
Dry	45 min
Elute	6 mL methanol
Dry	Under nitrogen
Reconstitute	100 µL MilliQ water

Table 4.13: Results of the validation: sample preparation recoveries, correlation coefficients, relative standard deviations (RSD) and limits of quantification (LOQ) for the chosen analytes DPC, 6-azauracil and 5-hydroxyhydantoin (5-OH).

Analyte	Recovery (%)	Correlation coefficient	RSD (n=9) (%)	LOQ (nM)	LOQ (ng/L)
DPC	80.2	0.9992	2.3	0.17	25
6-Azauracil	67.7	0.9997	6.7	0.23	26
5-OH	24.5	0.9774	8.1	1.37	159

4.2.5 Application and determination of 6-azauracil formation

Because of the adverse effects of 6-azauracil which have been described in literature the formation of this OP in natural waters is of interest and was therefore further investigated. To estimate the formation of 6-azauracil in drinking water from Karlsruhe and water from the river Rhine (for details of both waters see Table 8.1 in the appendix) during ozonation of DPC, these waters were spiked with 100 µg/L of DPC and analyzed at regular time intervals after treatment with 0.5 mg/L and 2 mg/L ozone, respecitively.

4.2.5.1 Formation in drinking water

Under the chosen conditions the transformation of DPC followed pseudo first order kinetics (Figure 8.6 in the appendix). The increase of the ozone dose applied, resulted in a faster oxidation of DPC which was already fully removed after 6 min when 2 mg/L ozone were added or after 30 min when 0.5 mg/L ozone were added (Figure 4.15, A and B).

In both experiments the concentration of 6-azauracil steadily increased and reached its formation maximum when DPC was almost fully removed. Depending on the applied ozone dose 6-azauracil was either at its formation maximum (0.5 mg/L ozone) or further oxidized (2 mg/L) to other oxidation products at the end of the experiments (after 30 min). Under both conditions the formation maximum for 6-azauracil was determined as 1.7 mol percent (1.2 µg/L) of the initial DPC concentration (100 µg/L). When DPC was fully oxidized, the excessive ozone further reacted with 6-azauracil resulting in a constant decrease in its concentration (Figure 4.15, B).

Comparison of the formation and decomposition of 6-azauracil in drinking water with the formation in MilliQ water demonstrates, that although 6-azauracil is formed in both waters, the extent varies (compare Figure 4.1 with Figure 4.15). The formation of 6-azauracil in MilliQ water with 20 % is an order of magnitued higher than the formation in drinking water of 1.7 %.

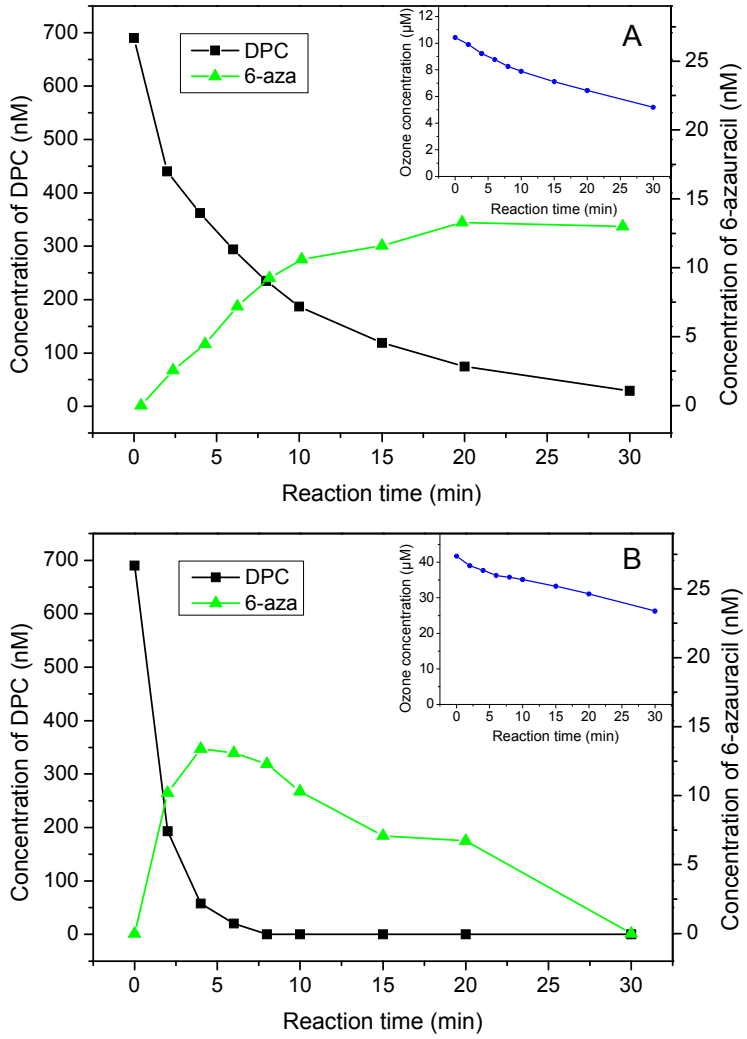

Figure 4.15: Oxidation kinetics of 100 µg/L DPC treated with (A) 0.5 mg/L ozone and (B) 2 mg/L ozone and the corresponding formation of 6-azauracil in drinking water and the respective ozone decomposition during the reaction.

4.2.5.2 Formation in river water

To compare the formation of 6-azauracil in different matrices water from the river Rhine (for details see Table 8.1 in the appendix) was used as a second natural water. The river water was also spiked with 100 µg/L of DPC and analyzed after treatment with 0.5 mg/L and 2 mg/L ozone, respectively.

Because of the higher ozone demand of river water (due to the presence of more reaction components) compared to drinking water, the lower ozone dose (0.5 mg/L) only removed DPC to 42.8 % (295 nM) (Figure 4.16 A). After 2 min of reaction time no residual ozone was present in the sample. The residual 57.2 % of DPC (395 nM) remained constant for the rest of the monitoring period. This reduced transformation in turn resulted in a lower formation of 6-azauracil (4.4 nM). When considering the molar 6-azauracil formation (based on 295 nM DPC oxidation and 4.4 nM 6-azauracil formation) 1.5 mol % transformation occurred. Hence,

the molar transformation results correlate very well with the findings in drinking water (1.7 %), although there a complete removal of DPC during the experiments was observed (compare section 4.2.5.1).

The higher ozone dose (2 mg/L) on the other hand was able to fully remove DPC already after 6 min of ozonation (Figure 4.16 B). The maximum of 6-azauracil formation (12 nM or 1.2 µg/L) was reached after 2 min of ozonation followed by a decline in 6-azauracil concentration. In principle the decline of DPC, the formation and decline of 6-azauracil both resemble the results in drinking water (compare section 4.2.5.1). Here too the maximum molar formation of 6-azauracil was determined as 1.7 % based on the initial DPC concentration.

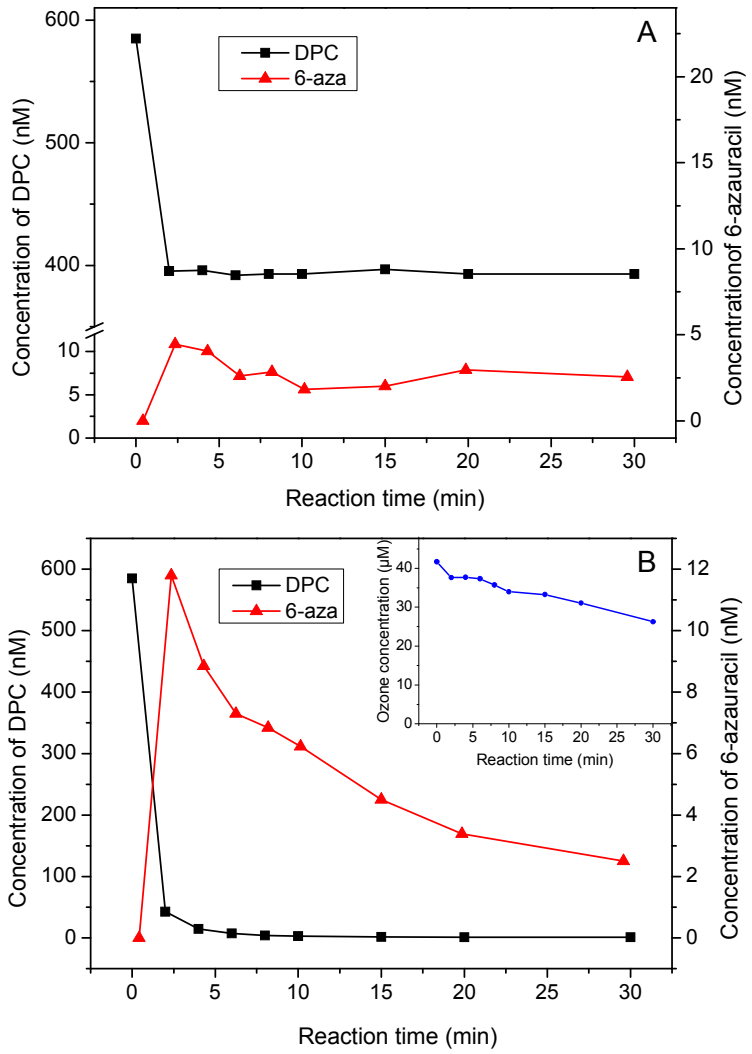

Figure 4.16: Oxidation kinetics of 100 µg/L DPC treated with (A) 0.5 mg/L ozone and (B) 2 mg/L ozone and the corresponding formation of 6-azauracil in river water and the respective ozone decomposition during the reaction.

The results both in drinking water and river water demonstrate that 6-azauracil is also formed in natural water matrices. Thus, the formation of 6-azauracil at environmentally relevant DPC concentrations was further investigated.

4.2.5.3 Formation in environmentally relevant concentrations

To assess the transferability of the experiments in natural matrices (drinking and river water) but with higher concentrations of DPC (100 µg/L) to environmentally more relevant conditions further experiments were performed in drinking water spiked with 10 µg/L DPC and treated with 0.5 mg/L ozone.

The results for low DPC concentrations which are depicted in Figure 4.17 show an analog removal behavior of DPC compared to drinking water results at higher DPC concentrations (Figure 4.15, A). Furthermore, the formation of 6-azauracil could also be observed under environmentally relevant conditions. The formation of 6-azauracil reached its maximum after 15 min and was relatively stable for the remaining monitoring period. The maximum concentration of 6-azauracil found in the samples was determined as 2.5 nM (0.3 µg/L). Based on the initial concentration of DPC (69 nM) this represents a maximum molar formation of 3.6 % 6-azauracil.

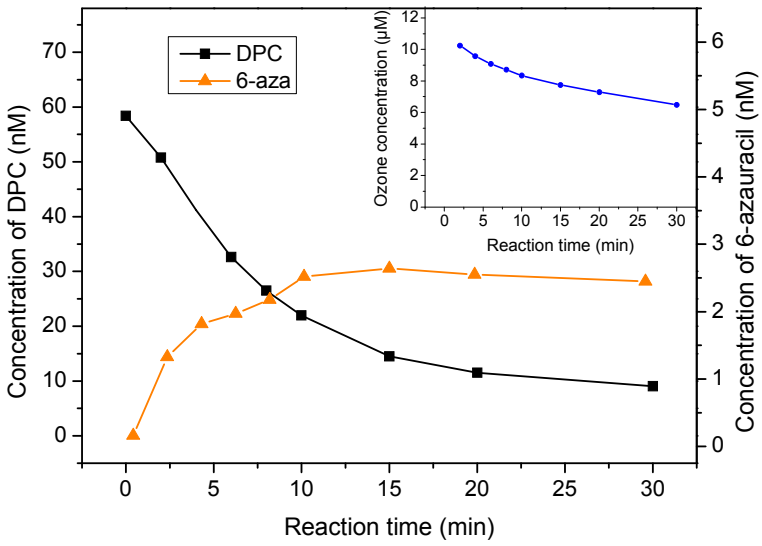

Figure 4.17: Oxidation kinetics of 10 µg/L DPC treated with 0.5 mg/L ozone, the corresponding formation of 6-azauracil and the ozone demand in drinking water.

Hence, the following conclusions from these results can be made: firstly, the maximum concentration of 6-azauracil is always reached when DPC is almost fully transformed and secondly, a decrease of initial DPC concentration in the water (from 100 µg/L to 10 µg/L) resulted in an increase in molar transformation to 6-azauracil (from 1.5 % to 3.6 %).

4.2.6 Summary and discussion of the SPE method and application

Although the analytes DPC and 6-azauracil are highly polar, which makes their enrichment more difficult, a method enabling the quantitative trace level analysis in different matrices could be developed and validated. For DPC the recovery was determined as 80 % and the LOQ as 25 ng/L (0.17 nM). For 6-azauracil the recovery was 68 % and the LOQ was 26 ng/L (0.23 nM).

The results in drinking water and in river water demonstrate that 6-azauracil is also formed in natural water matrices. In all the experiments the maximum formation of 6-azauracil is always reached when DPC is almost fully transformed, and is independent of the water matrix. However, a decrease of initial DPC concentration in the water from 100 µg/L to 10 µg/L resulted in an increase in molar transformation to 6-azauracil from 1.5 % to 3.6 %. A possible explanation for this could be a change in the ratio of ozone/radical reactions. Hence, further research should focus on the causes of varying extents of 6-azauracil formation. In particular, the effects of different initial DPC concentrations under varying pH values influencing the ozone/radical ratio, and the effect of the presence of radical scavengers inhibiting radical reactions should be determined.

In the experiment with 10 µg/L DPC, the maximum concentration of 6-azauracil found in the samples was determined as 2.5 nM (0.3 µg/L). With regard to environmental impact, lower initial DPC concentrations, for example 0.1 µg/L, can be expected to result in 6-azauracil concentrations in the lower ng/L range. Based on the toxicological data available, no threat to human health can be expected from these low concentration levels of 6-azauracil [119].

4.3 Identified oxidation products of M-DPC in MilliQ water

A chromatographic separation measured with HPLC-UV (λ = 250 nm) of M-DPC from its OPs after ozonation is depicted in Figure 4.18 A. The initial concentration of M-DPC prior to ozonation is presented by t_0. The oxidation of M-DPC through ozone follows a multistep degradation mechanism, involving the formation of several UV absorbing OPs. The concentration of each OP formed is illustrated as a function of ozonation time in Figure 4.18 B. For this, UV signals were integrated and plotted against ozonation time. This enables the identification of OP 3 as a major oxidation product, whereas the other OPs show similar concentrations in formation.

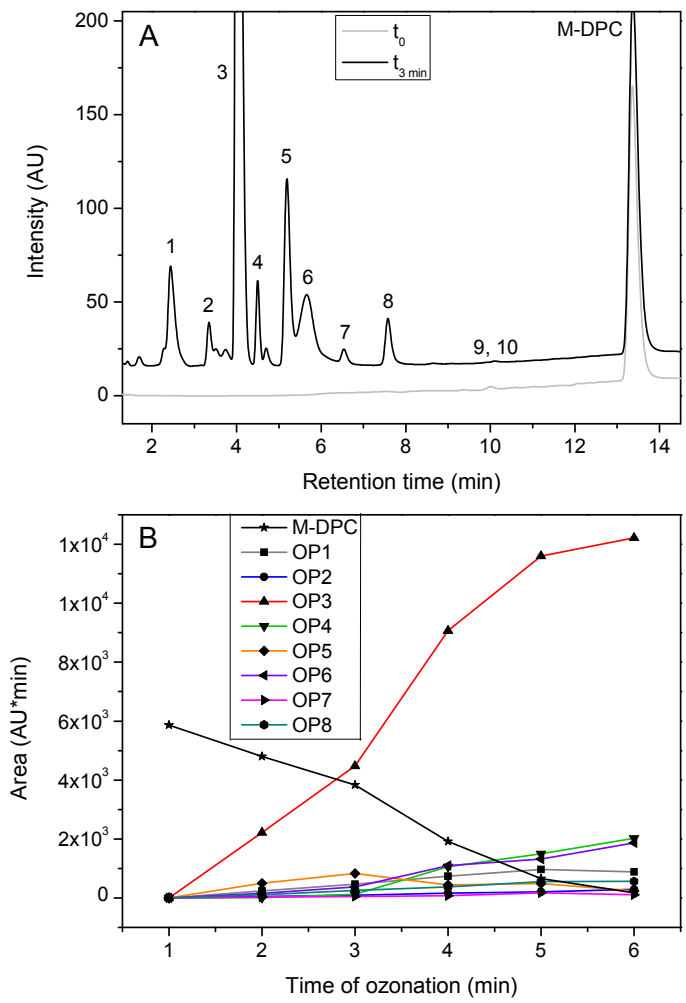

Figure 4.18: (A) Chromatographic separation (λ = 250 nm) M-DPC and its OPs formed during ozonation (B) Oxidation product formation and decline of M-DPC as a function of the applied ozonation time.

In the following sections the details of the structural elucidation of the oxidation products OP 1, OP 3 and OP 5 to OP 10 are discussed and either confirmed by authentic standards or proposed on the basis of similarity in their fragmentation pattern when compared to compounds with similar structures. Neither OP 2 nor OP 4 showed any characteristic fragment ion in the mass spectrum and could not be identified. Hence, they will not be included in the discussion. At the end of the section information on the analyzed OPs regarding retention time, UV maxima, ionization mode, MS and MS/MS detection, is summarized in Table 4.14. Mass error differences between the measured *m/z* and the calculated exact *m/z* were less than 1 ppm for all OPs with one exception and are also included in the summary.

4.3.1 M-OA-HEA (OP 3)

OP 3 eluting after 3.9 min showed a UV maximum at 260 nm. In positive ionization mode the two fragment ions at *m/z* 157.0244 and at *m/z* 174.0509 were detected. The neutral elemental compositions proposed were C5H4N2O4 and C5H7N3O4. Due to the presence of ammonia in the buffer the fragment ion *m/z* 174.0509 could either be an ammonia adduct or the molecular ion peak $[M+H]^+$ itself. Due to the fact that the corresponding negatively charged fragment ion to *m/z* 174.0509, namely *m/z* 172.0364, was detectable, the calculated empirical formula for the uncharged molecule was proposed as C5H7N3O4 (fragment ions *m/z* 172.0364 in negative ionization mode and *m/z* 174.0509 in positive ionization mode). The DBEs present in OP 3 were calculated as four. Regarding the fact that the chlorine atom situated in position 4 of the pyridazine ring was eliminated from the molecule through oxidation, the proposed position of ozone attack was the double bond between C4 and C5 in M-DPC. Further structural information was gained through MS/MS experiments performed in both ionization modes (Figure 4.19 and Figure 4.20).

MS/MS experiments performed in negative ionization mode showed a product ion at *m/z* 100.0524 which could be explained through the elimination of carbon dioxide and carbon monoxide as neutral losses (Figure 4.19, A and B). Through in-source fragmentation of the fragment ion at *m/z* 172.0364 and fragmentation of the fragment ion at *m/z* 100.0524 in the collision cell the product ion at *m/z* 85.0306 was formed (Figure 8.7, A in the appendix). The formation of this product ion supports the presence of an unchanged methyl group in position two of the pyridazine ring and hence supports the assumption that the pyridazine ring of M-DPC was opened and that the carbon atom in position C4 of the ring was oxidized to a carbonic acid moiety. Finally the product ion at *m/z* 129.0199 indicates the loss of the C5 atom with the unmodified primary amine and a keto group as CONH.

In addition MS/MS experiments in positive ionization mode showed a product ion at *m/z* 157.0242 indicating a loss of ammonia and supporting the theory that the primary amine was still present and has not been modified in the OP (Figure 4.20, A and B). Further neutral losses such as carbon monoxide and carbon dioxide from MS^3 experiments of the product ion at *m/z* 157.0242, again performed through in-source fragmentation, agreed with the results already described (Figure 4.20 B and Figure 8.7, B in the appendix). Under consideration of all the information gained a structure named (2*Z*)-2-[2-methyl-2-(oxoacetyl)-hydrazinylidene]-ethanamide (M-OA-HEA) can be proposed (Figure 4.19, B).

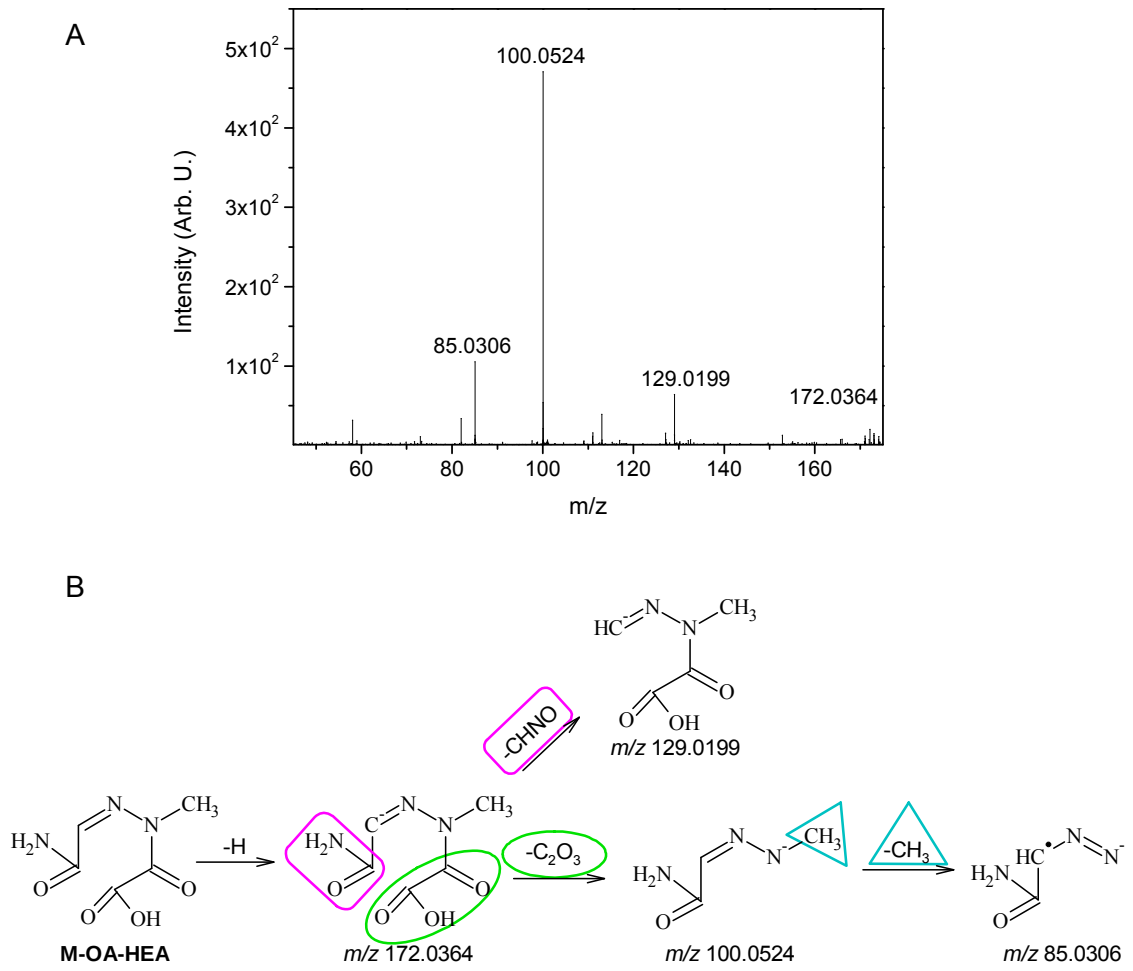

Figure 4.19: (A) MS/MS spectrum of the fragment ion at *m/z* 172.0364 in negative mode. (B) Proposed product ions based on high resolution MS^2 and MS^3 experiments data of OP 3 in negative mode (compare Figure 8.7, A in the appendix).

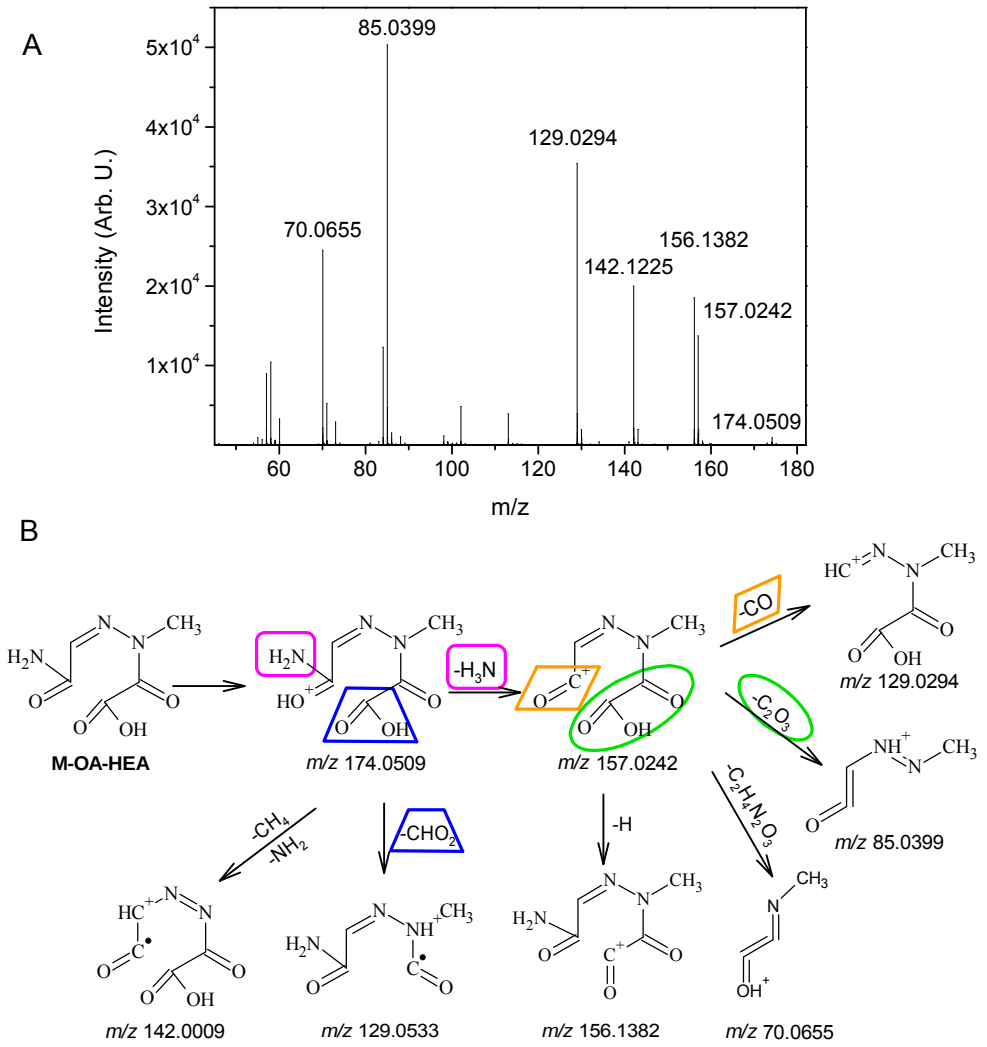

Figure 4.20: (A) MS/MS spectrum of the fragment ion at *m/z* 174.0509 in positive ionization mode. (B) Proposed product ions based on MS^2 and MS^3 experiments (compare Figure 8.7, B in the appendix).

The formation of the structure of OP 3 can be explained by applying the classical Criegee mechanism to the carbon-carbon double bond situated between C4 and C5 of the pyridazine ring of M-DPC (Figure 4.21, structures 1-3). The ozonide could stabilize under opening of the ring and subsequent elimination of the chlorine atom. This would result in the formation of an aldehyde moiety at the C4 and an amide moiety at the C5 (Figure 4.21, structure 4). This reaction is followed by the oxidation of the aldehyde moiety to a carbonic acid moiety forming the OP (2*Z*)-2-[2-methyl-2-(oxoacetyl)-hydrazinylidene]-ethanamide (M-OA-HEA) depicted in Figure 4.21, structure 5.

As a comparable example the ozonation of m-cresol, should be mentioned. The oxidation of the benzene ring resulted in the formation of a catechol and was followed by cleavage of the ring under formation of first aldehydes and then carbonic acids [47].

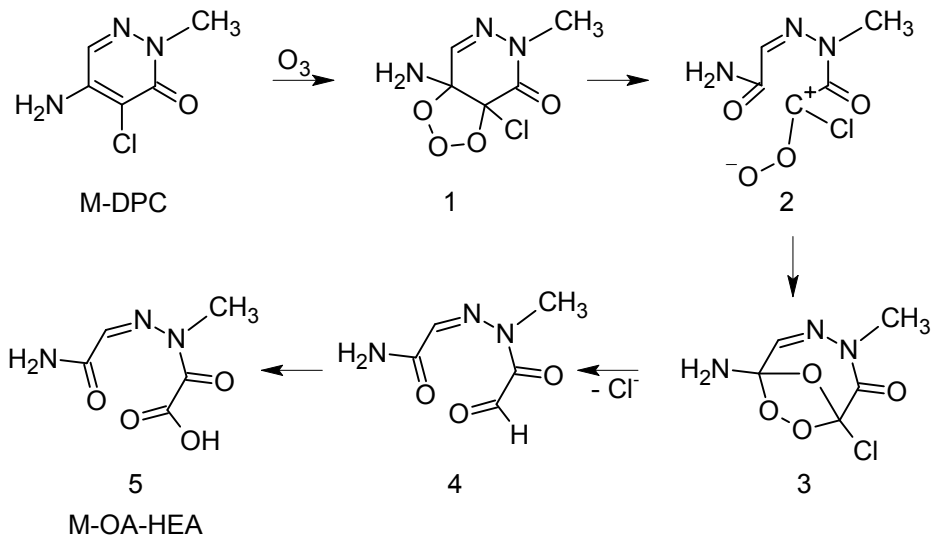

Figure 4.21: Proposed reaction mechanism between M-DPC and ozone resulting in the formation of OP 3, (2*Z*)-2-[2-methyl-2-(oxoacetyl)hydrazinylidene]ethanamide (M-OA-HEA).

4.3.2 CM-MHAA (OP 1)

After 2.3 min retention time the UV absorbing OP 1 which could be measured only in negative ionization mode (m/z 173.0204) eluted. Based on the high mass accuracy of the ToF-MS detector the elemental composition of this OP was assigned as C5H6N2O5. The DBEs present in this OP were calculated as four. Regarding the fact that the chlorine atom situated in position 4 of the ring as well as the primary amine in position 5 of the ring were eliminated from the molecule, the proposed position of ozone attack is the double bond between C4 and C5 in the pyridazine molecule. Based on additional MS/MS experiments functional groups present in the OP could be identified due to the neutral losses of specific leaving groups and the following conclusions regarding the structure of OP 1 could be made.

Firstly, the neutral loss of carbon dioxide and a methyl group (product ion at m/z 112.9863) in the MS/MS spectrum indicated that the methyl group had not been modified and hence the loss of carbon dioxide could only be explained through a ring opening and oxidation of a carbon atom to a carbonic acid moiety (Figure 4.22, A and B). Secondly, the neutral losses of carbon dioxide and carbon monoxide (product ion at m/z 101.0365) and alternatively of carbon dioxide and hydrocyanic acid (product ion at m/z 102.0186) could represent the elimination of neutral losses of different sides of the opened ring. Hence, C4 and C5 were possibly oxidized to carbonic acids. In the case of the C4 oxidation the carbon monoxide elimination represents the unchanged keto group (position 3 in the ring) present in M-DPC. In the case of C5 oxidation the elimination of hydrocyanic acid represents C6 and the nitrogen molecule in position 1 of the pyridazine ring.

Comparison of the empirical formula of OP 3 (C5H7N3O4) with the elemental composition of OP 1 (C5H6N2O5) revealed that OP 3 consists of one nitrogen atom more but lacked one oxygen atom as well as one hydrogen atom. Both OPs consist of the same amount of double bond equivalents (four). The fact that OP 3, in contrary to OP 1, could also be analyzed in positive ionization mode, must be due to structural differences (possibly due to the presence of the nitrogen atom). Not only the elemental composition of both OPs showed great similarity but also the product ions gained from MS/MS experiments in negative ionization mode (compare Figure 4.19, B and Figure 4.22, B). For example, OP 1 and OP 3 showed the same neutral losses of carbon dioxide and carbon monoxide (forming the product ion at *m/z* 101.0365) supporting the assumption that the ring was opened and that the carbon atom is oxidized to a carbonic acid moiety in both OPs. Because of all these similarities certain structural analogies of both OPs can be expected.

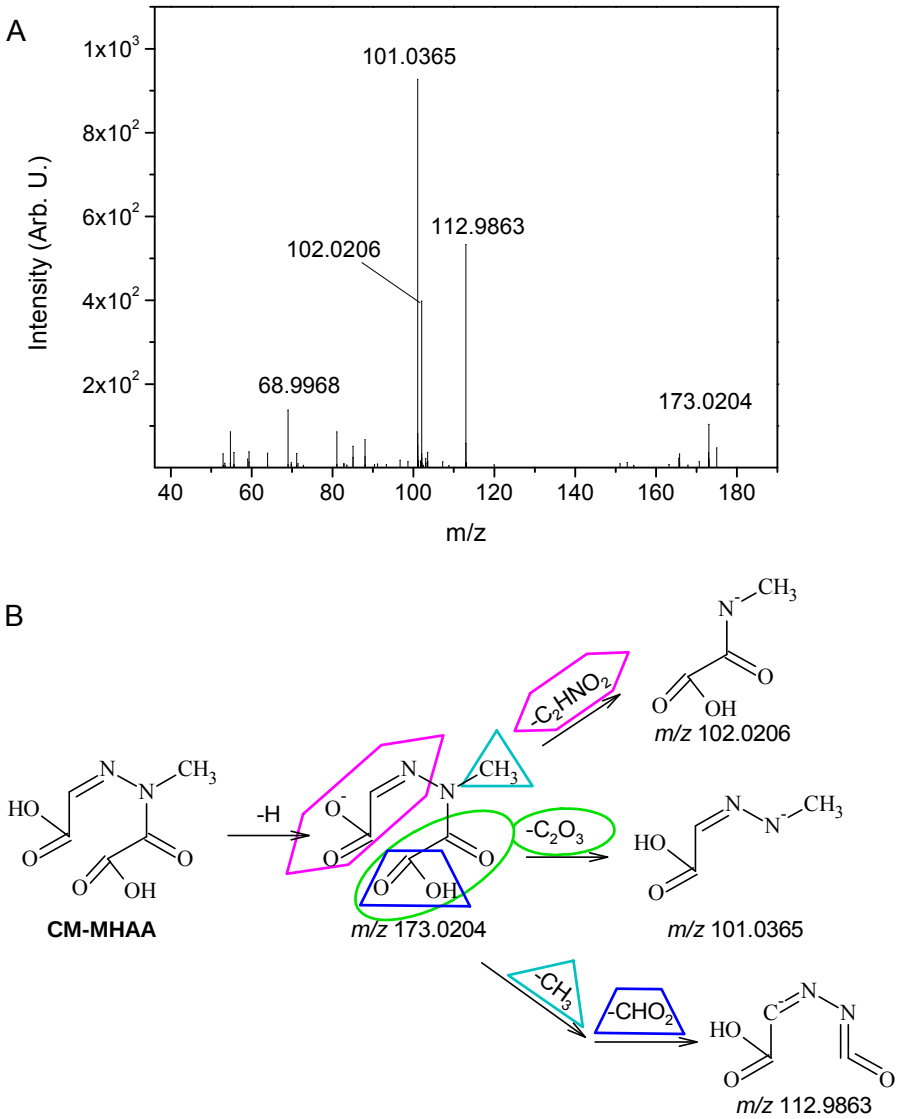

Figure 4.22: (A) MS/MS spectrum of the fragment ion at *m/z* 173.0204 in negative ionization mode. (B) Proposed structures for major product ions based on high resolution MS/MS data.

In accordance with all the information gained, a structure for OP 1 was proposed (Figure 4.22). This structure named [(2Z)-2-(carboxymethylidene)-1-methyl-hydrazinyl]oxoacetic acid (CM-MHAA) is supported by the experimental data: the elemental composition proposed, it contains an unmodified methyl group as well as a carbonic acid moiety and finally its double bond equivalents agree with the amount calculated. Based on these results, it is proposed that OP 3 is a precursor for OP 1 and through continuous oxidative conditions the primary amine is substituted by a hydroxyl group (Figure 4.23).

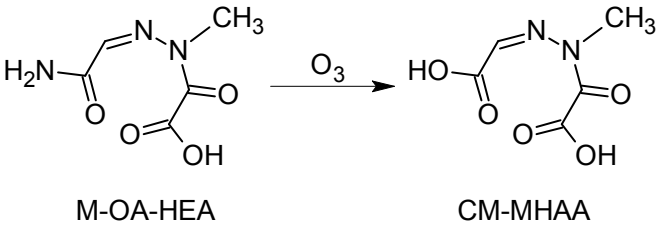

Figure 4.23: Proposed formation mechanism of OP 1 through oxidation of OP 3 during ozonation of M-DPC.

4.3.3 2-Methyl-pyridazine-3,4,5-trione (OP 6)

OP 6 eluted after 6.1 min (Figure 4.18) and its UV maxima were at 222 nm and at 265 nm. Based on its fragment ion at *m/z* 141.0295 measured in positive ionization mode, the empirical formula for the uncharged molecule was assigned as C5H4N2O3. Comparison with the elemental composition of M-DPC (C5H6N3O1Cl1) revealed that the chlorine, one nitrogen and two hydrogen atoms were removed and two oxygen atoms were introduced. The DBEs calculated for this OP were five.

Possible reactions leading to this OP are the substitution of the chlorine atom in position 4 as well as the primary amine in position 5 through hydroxyl groups and their subsequent oxidation to keto groups. Regarding the mechanism of oxidation, the loss of chlorine indicates an attack of ozone at the carbon-carbon double bond situated between position C4 and C5.

Through comparison with the already identified OPs from DPC (section 4.1) the structure for OP 6 could be proposed as 2-methyl-pyridazine-3,4,5-trione. Comparison of its product ions (at *m/z* 113.0344, *m/z* 70.0654, *m/z* 58.0291, *m/z* 57.0448, *m/z* 44.0498) gained from MS/MS experiments with a synthesized reference compound (2-methyl-4,5-dihydroxy-pyridazine-3-one) supports the proposed structure (Figure 4.24). The proposed mechanism for the formation of 2-methyl-pyridazine-3,4,5-trione is analog to the formation of pyridazine-3,4,5-trione previously described (section 4.1.1, Figure 4.3).

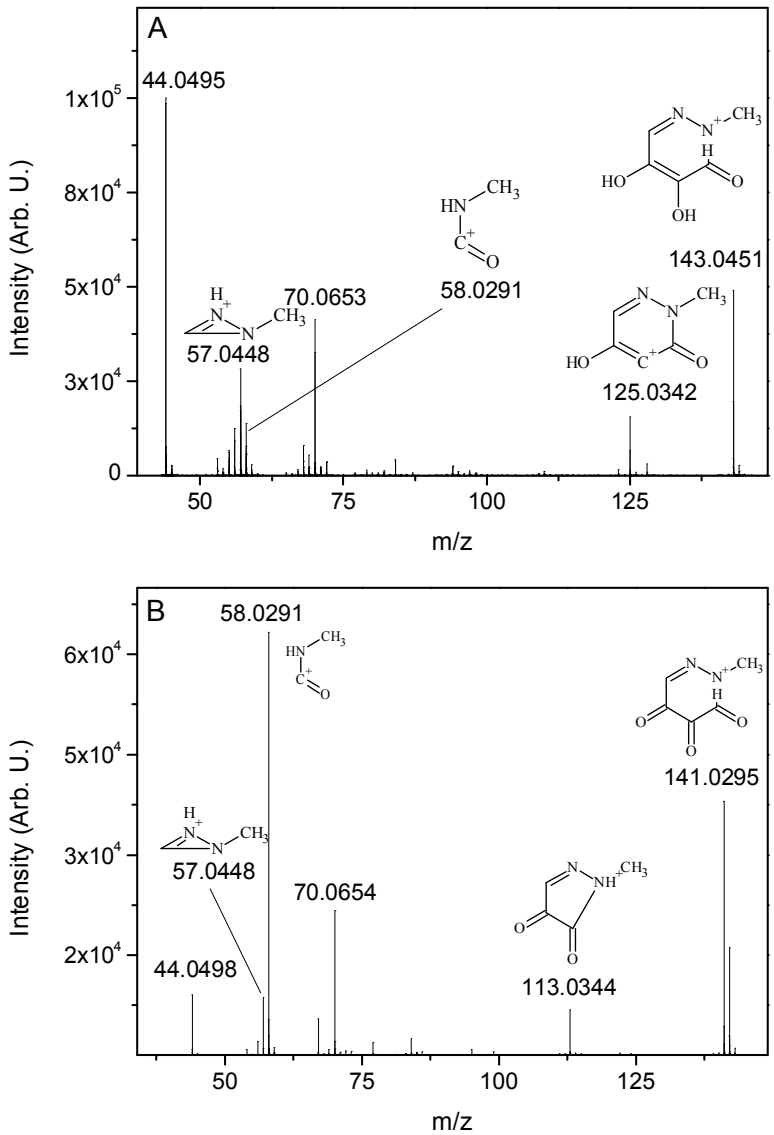

Figure 4.24: (A) MS/MS spectrum for the synthesized reference compound 2-methyl-4,5-dihydroxy-pyridazine-3-one (*m/z* 143.0451) and (B) MS/MS spectrum of OP 6 2-methyl-pyridazine-3,4,5-trione (*m/z* 141.0295).

4.3.4 5-Amino-4-hydroxy-pyridazine-3-one (OP 7)

OP 7 eluted after 6.6 min with UV maxima at 220 nm and at 270 nm (Figure 4.18, OP 7). Based on the fragment ion at *m/z* 128.0455 measured in positive ionization mode the elemental composition for the uncharged OP was proposed as C4H5N3O2. Comparison of the proposed empirical formula with the elemental composition of M-DPC (C5H6N3O1Cl1) revealed that the chlorine, one carbon and one hydrogen atom were removed and an oxygen atom was added. In M-DPC and in the OP, four double bond equivalents are present. These findings suggest that the carbon atom was removed through oxidation of the methyl group to formic acid which is subsequently eliminated from the molecule. The chlorine atom on the other hand was substituted by a hydroxyl group. These reactions would result in a compound named 4-hydroxy-5-amino-pyridazine-3-one, which is depicted in Figure 4.25. MS/MS

experiments lead to various product ions which support the suggested structure (Figure 4.25). The product ion with the highest intensity was at *m/z* 83.0244, formed by a loss of NHCO from *m/z* 128.0454. The other product ions were formed through elimination of known leaving groups such as water, carbon monoxide or hydrogen cyanide. Retention times, UV spectra, exact mass measurements and MS/MS data of the synthesized compound 4-hydroxy-5-amino-pyridazine-3-one (section 3.2.10.2) coincided with the data from OP 7.

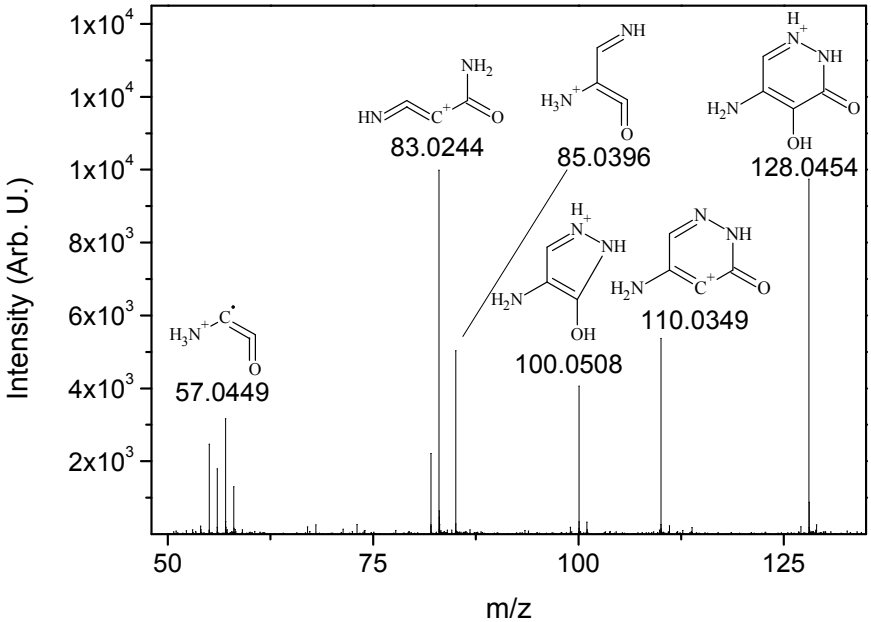

Figure 4.25: MS/MS spectrum of OP 3 with the fragment ion at *m/z* 128.0454 and proposed structure as 5-amino-4-hydroxy-pyridazine-3-one supported by the observed product ions.

4.3.5 1-Methyl-6-azauracil (OP 8)

After 7.7 min retention time, OP 8 eluted (UV maxima at 204 nm and 272 nm) and showed the same number of DBEs (four) in the molecule and the identical fragment ion at *m/z* 126.0309 as OP 7 when measured in negative ionization mode. However, unlike OP 7, this OP-isomer could not be detected in positive ionization mode. This different behavior must be based on structural differences. These findings indicate that both isomers are structural isomers rather than stereoisomer. Under consideration of OPs formed during ozonation of DPC (section 4.1), the formation of the analog OP to 6-azauracil (section 4.1.2), namely 1-methyl-6-azauracil, could be a possible structural explanation. 6-Azauracil too could only be detected in negative ionization mode, caused through the modification of the primary amine. The exact mass and DBEs (four) of OP 8 would also agree with 1-methyl-6-azauracil. The UV spectra of 6-azauracil and OP 8 showed similarities regarding the overall progression (Figure 8.8 in the appendix), though a bathochrom shift for the UV maxima of OP 8 (possibly due to the methyl group) must be noted.

The product ions gained from MS/MS experiments in negative ionization mode for varying collision energies are depicted in Figure 4.26. Independent of the applied collision energy, OP 8 only showed one product ion at *m/z* 41.9 (Figure 4.26, A) which had a chemical composition of CON and agreed with the proposed structure. On the other hand, 5-amino-4-hydroxy-pyridazine-3-one (OP 7) showed three product ions (*m/z* 42.1, *m/z* 83.0, *m/z* 98.2) depending on the applied collision energy (Figure 4.26, B).

Whether 1-methyl-6-azauracil poses similar adverse toxicological effects as 6-azauracil is not known and hence of further interest [121,122].

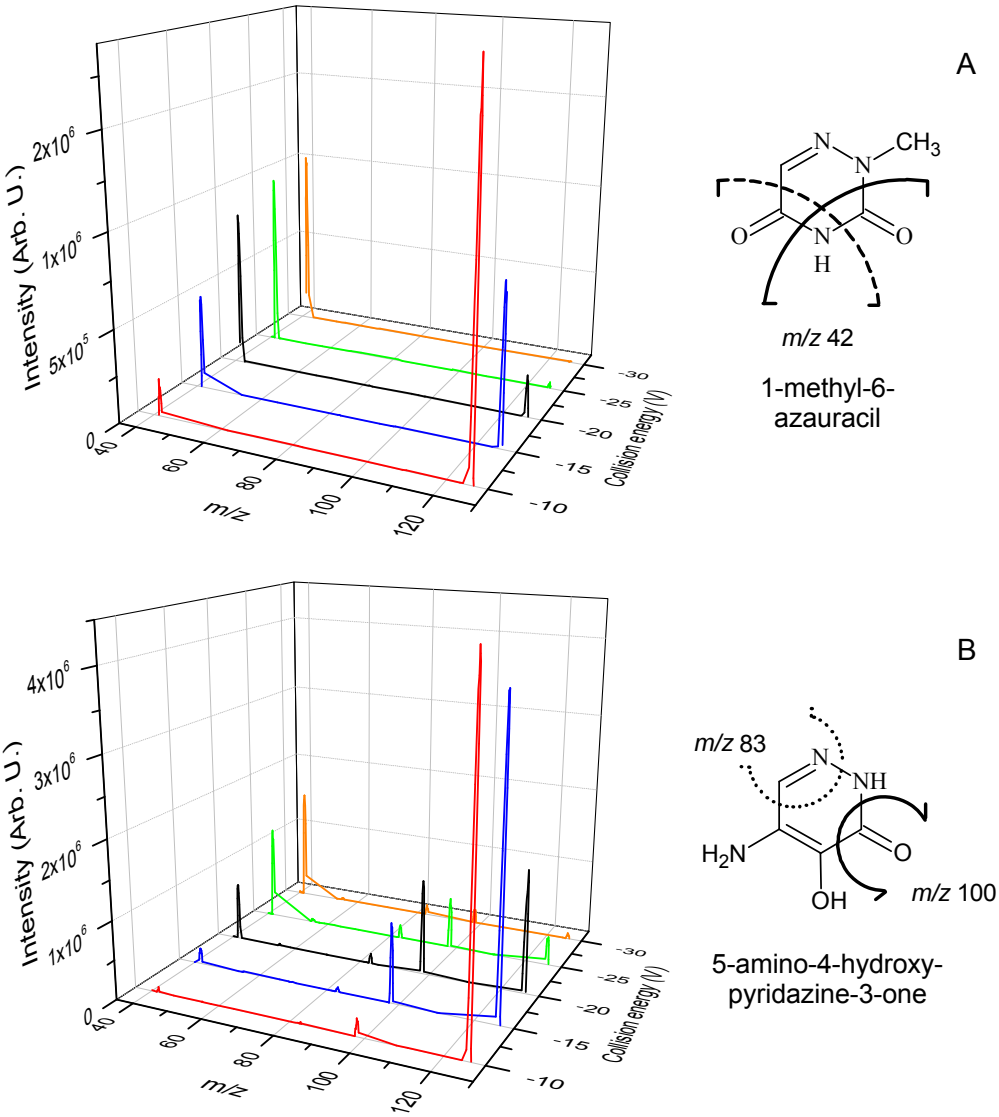

Figure 4.26: (A) MS/MS spectrum of 1-methyl-6-azauracil and (B) MS/MS spectrum of 5-amino-4-hydroxy-pyridazine-3-one (structural isomer, see section 4.3.4) at collision energies ranging from -10 V to -30 V. The product ion of 1-methyl-6-azauracil is *m/z* 41.9 and for 5-amino-4-hydroxy-pyridazine-3-one the product ions are at *m/z* 42.1, *m/z* 83.0, *m/z* 98.2.

4.3.6 2-Methyl-4-chloro-5-amino-pyridazine-3,6-dione (OP 9)

The ozonation of M-DPC also lead to the formation of a fragment ion at *m/z* 176.0223 eluting after 9.8 min retention time. The mass spectrum for this OP showed the typical isotopic pattern for molecules containing one chlorine atom (Figure 4.27, A). The proposed empirical formula for OP 9 was C5H6N3O2Cl1 and consisted of four DBEs. The formation of this OP can be explained by a nucleophilic attack of ozone on the carbon-nitrogen double bond and stabilization under oxygen elimination (Figure 4.27, B) [34]. Characteristic neutral losses gained from MS/MS experiments supported the proposed molecular structure 2-methyl-4-chloro-5-amino-pyridazine-3,6-dione (Figure 4.27, A). For example, the neutral loss of a methyl group (*m/z* 160.9988) indicates that the OP still contains the unmodified methyl group from M-DPC.

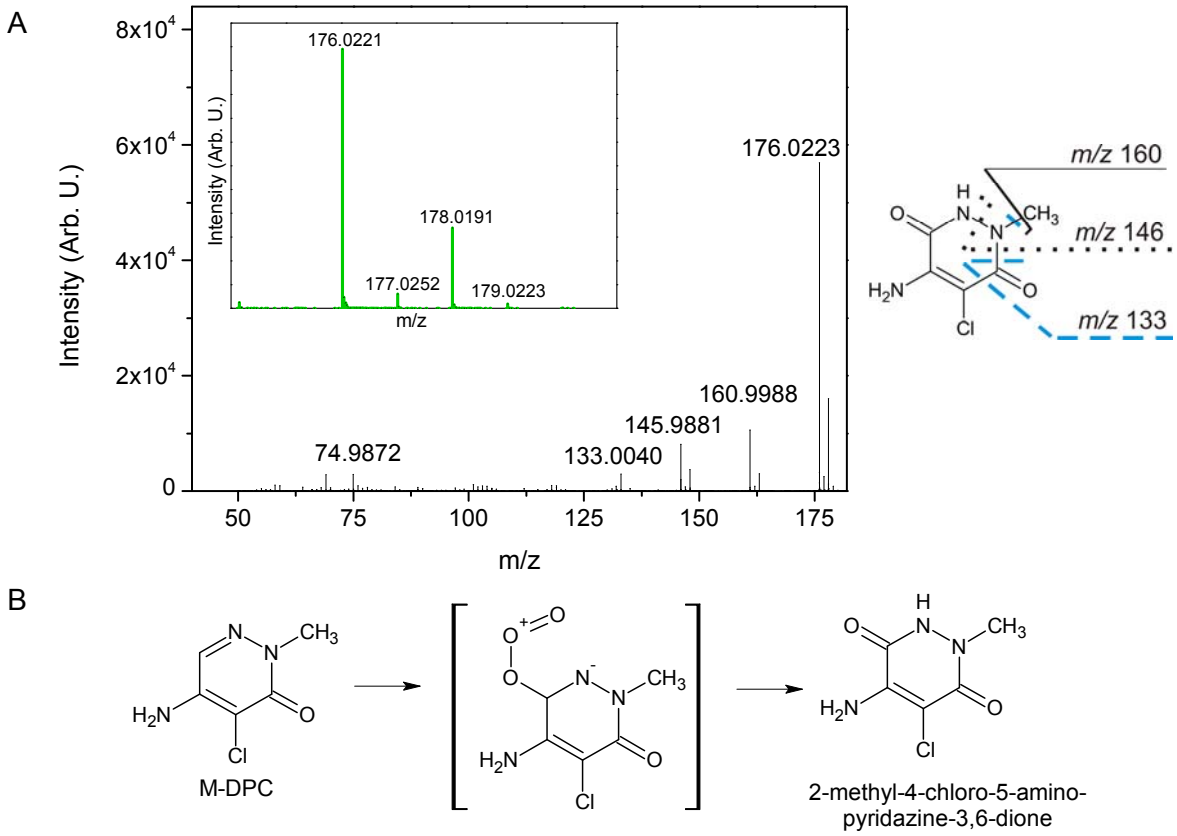

Figure 4.27: (A) Characteristic isotopic pattern of a chlorine-containing compound and its MS/MS spectrum (*m/z* 176.0221) with the proposed structure for OP 9 based on major product ions. (B) Proposed formation mechanism of OP 9 2-methyl-4-chloro-5-amino-pyridazine-3,6-dione via nucleophilic attack of ozone on the carbon-nitrogen double bond of M-DPC.

4.3.7 Desphenyl-chloridazon (OP 10)

OP 10 eluted after 10 min with the fragment ion at *m/z* 146.0116 measured in positive ionization mode. The empirical formula for the uncharged molecule was proposed as

C4H4N3O1Cl1. OP 10 was confirmed as DPC with a commercial standard (agreement in retention time, exact mass, isotopic pattern and product ions, Figure 4.28). A possible explanation for the formation of DPC is the oxidation of the methyl group to an aldehyde moiety and further oxidation and elimination as formic acid. IC-CD measurements (see section 4.3.8) confirmed the formation of formic acid during the experiments.

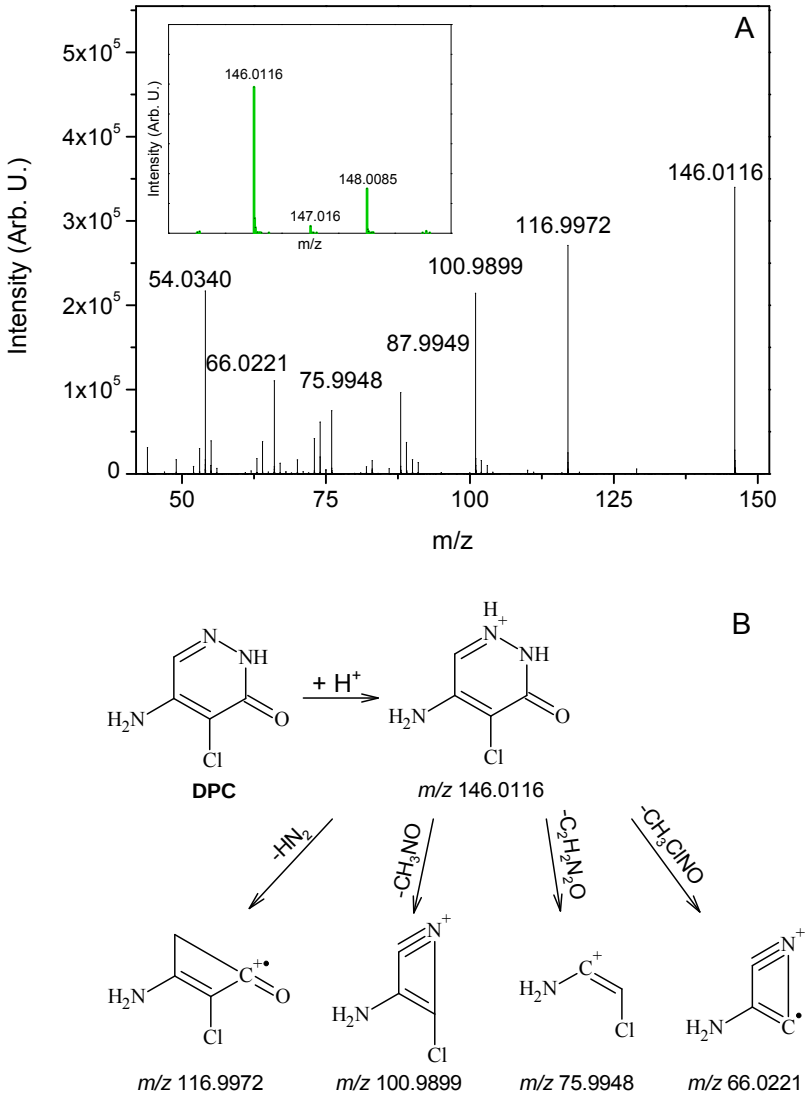

Figure 4.28: (A) Characteristic isotopic pattern for OP 10, desphenyl-chloridazon, containing a chlorine atom and its MS/MS spectrum. (B) Proposed structures for the product ions.

4.3.8 Small organic compounds

Several peaks could be separated by IC followed by conductivity detection (Figure 4.29). Three OPs, namely acetic acid (I), formic acid (II) and oxalic acid (III) could be identified with a standard based on identical retention times. The formation of these OPs indicates that excessive ozone application results in a further oxidation of the previously identified OPs.

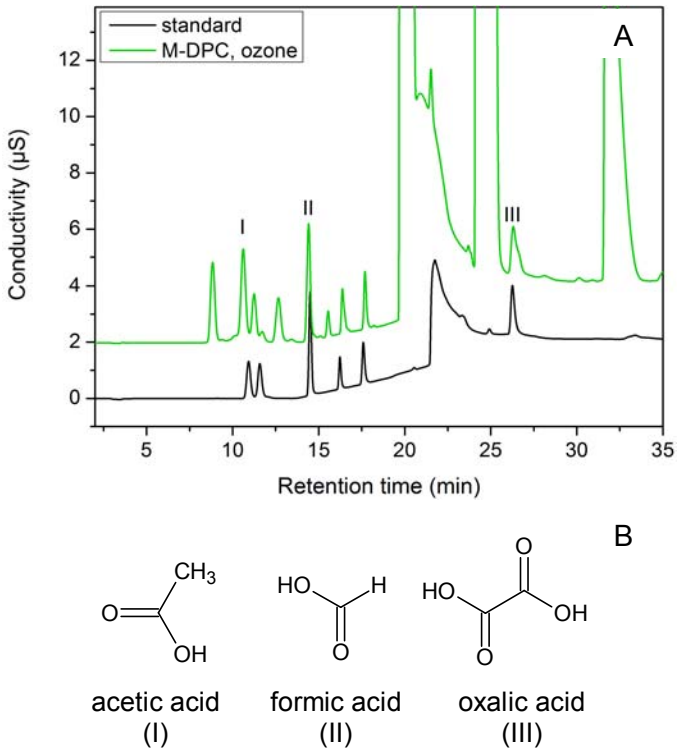

Figure 4.29: (A) IC chromatograms of an ozone-treated sample and identification with a standard mixture containing acetic acid (I), formic acid (II) as well as oxalic acid (III). (B) structures of the identified OPs.

4.3.9 Oxidation products of M-DPC identified in drinking water

Analyses of ozone-treated drinking water samples spiked with 1 mM M-DPC enabled the assessment of the transferability of the results gained from experiments performed in MilliQ water to natural water matrices. The experiments showed that most OPs were formed in both waters and only differed in concentrations (compare Figure 4.18 A and Figure 4.30). For example, OP 1 is present in both matrices with similar concntrations. OP 3 as major OP in MilliQ water is also detectable in drinking water, though to a slightly lower extent. The unidentified OP 4 formed in MilliQ water is not formed in drinking water. Also OP 6 (2-methyl-pyridazine-3,4,5-trione) was only detected in experiments performed in MilliQ water. The OP 4b in drinking water was also formed in MilliQ water, though due to the lower formation rate still has to be identified. However, OPs 5 and 7 to 10 were all formed in both matrices and hence the OPs identified in MilliQ water represent a good overview on OPs formed during ozonation of M-DPC in natural water matrices.

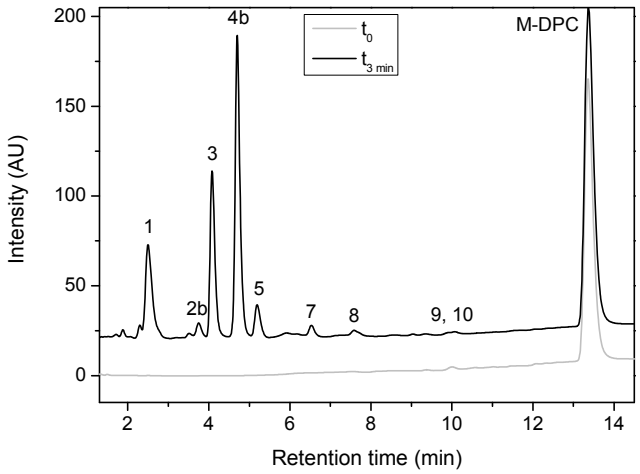

Figure 4.30: Chromatographic separation (λ = 250 nm) of M-DPC and its OPs formed in an ozone-treated drinking water sample.

Table 4.14: Retention times, UV maxima, MS and MS/MS ions gained from methyl-desphenyl-chloridazon, its primary OPs (A) and the synthesized reference compounds (B). Mass error differences were calculated as the deviation of the measured *m/z* from the calculated exact *m/z* and were mainly smaller than 1 ppm.

Peak No./ OP No.	Proposed products	Reference standard	Retention time	UV maxima	Ionization mode	Observed fragment ions MS	MS/MS	Calculated mass to charge ratio	Mass error
A			min	nm	+/-	*m/z*	*m/z*	*m/z*	ppm
Mother compound	M-DPC	Yes	13.8	200, 225, 280	+	160.0272	145.0036, 130.0053, 116.9977, 87.9952	160.0272	0.43
OP 1	CM-MHA	No	2.3	217, 250	-	173.0206	112.9863, 102.0206, 101.0365	173.0204	0.89
OP 3	M-OA-HEA	No	3.9	260	- (+)	172.0364 (174.0509)	129.0199, 100.0524, 85.0306 (157.0242, 156.1382, 142.1225, 129.0294, 85.0399, 70.0655)	172.0364 (174.0509)	0.56 (0.16)
OP 5	C5H5N3O3	No	5.1	242	+	156.0403	-	156.0404	0.25
OP 6	2-Methyl-pyridazine-3,4,5-trione	No	6.1	222, 265	+	141.0295	113.0344, 70.0654, 58.0291, 44.0980	141.0295	0.14
OP 7	5-Amino-4-hydroxy-pyridazine-3-one	Yes	6.6	220, 270	+ (-)	128.0454 (126.0313)	110.0349, 100.0508, 85.0396, 83.0244, 57.0449	128.0455 (126.0309)	0.08 (2.90)
OP 8	1-Methyl-6-azauracil	No	7.7	204, 272	-	126.0314	41.9	126.0309	4.23
OP 9	2-Methyl-4-chloro-5-amino-pyridazine-3,6-dione	No	9.8	230, 277	+	176.0221	160.9985, 145.9876, 133.0040, 74.9872	176.0221	0.13
OP 10	DPC	Yes	10.4	198, 224, 278	+	146.0116	116.9980, 100.9901, 87.9949, 73.9911, 66.0218, 54.0345	146.0116	0.06
B			min	nm	+/-	*m/z*	*m/z*	*m/z*	ppm
Synthesis product 1	2-Methyl-4,5-dihydroxy-pyridazine-3-one	-	13	216, 288	+	143.0451	125.0342, 70.0653, 58.0291, 47.0448, 44.0495	143.0451	0.21
Synthesis product 2	5-Amino-4-hydroxy-pyridazine-3-one	-	6.6	220, 270	+	128.0454	110.0350, 100.0509, 85.0395, 83.0244, 57.0449	128.0455	0.15

4.3.10 Summary and discussion of the oxidation pathway for M-DPC

When M-DPC is treated with ozone several reaction mechanisms, such as electrophilic substitution or 1,3-dipolar cycloaddition to the carbon-carbon double bond [35,50] or nucleophilic attack at the carbon-nitrogen double bond [34,59], can be expected. The proposed reaction pathway for M-DPC (Figure 4.31) is able to explain the identified oxidation products by applying these mechanisms. Generally, a broad spectrum of OPs is formed and can be split into three groups depending on the oxidation pathway by which they are formed. The first pathway is through the attack of ozone via 1,3-dipolar cycloaddition, the second via nucleophilic attack on the carbon-nitrogen double bond and the third via the oxidation of the methyl group (Figure 4.31). Of these three possibilities the predominant reaction pathway seems to follow the first route where the double bond situated between C4 and C5 of the pyridazine ring is attacked by ozone. Depending on how the ozonide stabilizes, this results in the formation of three primary OPs, namely 2-methyl-pyridazine-3,4,5-trione, M-OA-HEA and 1-methyl-6-azauracil. Oxidation of the carbon-nitrogen double bond (situated between C6 and N1) or of the methyl group in position 2 of the pyridazine ring can also be observed, but are of minor relevance. Excessive ozone present in the samples results in further decomposition of the identified OPs forming small carbonic acids such as formic acid and oxalic acid. As M-DPC is oxidized to DPC, ongoing oxidative conditions will result in its oxidation and in the formation of OPs already described for the oxidation of DPC in section 4.1.

When regarding the preferred site of primary ozone attack on substituted aromatic ring systems, the reaction behavior described here agrees with findings in literature. For example, in the case of m-cresol the ozonation initially takes place at the benzene ring resulting in the formation of a catechol followed by cleavage of the ring and formation of first aldehydes and then carbonic acids, whereas the methyl group is only oxidized in following steps [47]. When comparing the reaction of ozone with DPC and M-DPC an attack of ozone on the carbon-nitrogen double bond was only observed during ozonation of M-DPC. Furthermore, another difference is the formation of two chlorine-containing OPs during ozonation of M-DPC, whereas no chlorine-containing OPs could be detected during ozonation of DPC. The main analogies when comparing OP formation are in the formation of the compounds 2-methyl-pyridazine-3,4,5-trione and 1-methyl-6-azauracil from M-DPC and pyridazine-3,4,5-trione and 6-azauracil from DPC. Hence, the mechanisms applicable for the formation of 2-methyl-pyridazine-3,4,5-trione and 1-methyl-6-azauracil are also assignable for pyridazine-3,4,5-trione and 6-azauracil, respectively, from DPC .

When considering the environmental relevance, the proposed oxidation pathway generally provides a representative overview on the OPs formed during ozonation of M-DPC in

drinking water. However there is no toxicological data available for any of the identified OPs. With regard to M-DPC concentrations in waters used for drinking water production, which range in the lower µg/L level, the concentrations of OPs arising from the ozonation of M-DPC can be expected to be in the ng/L range.

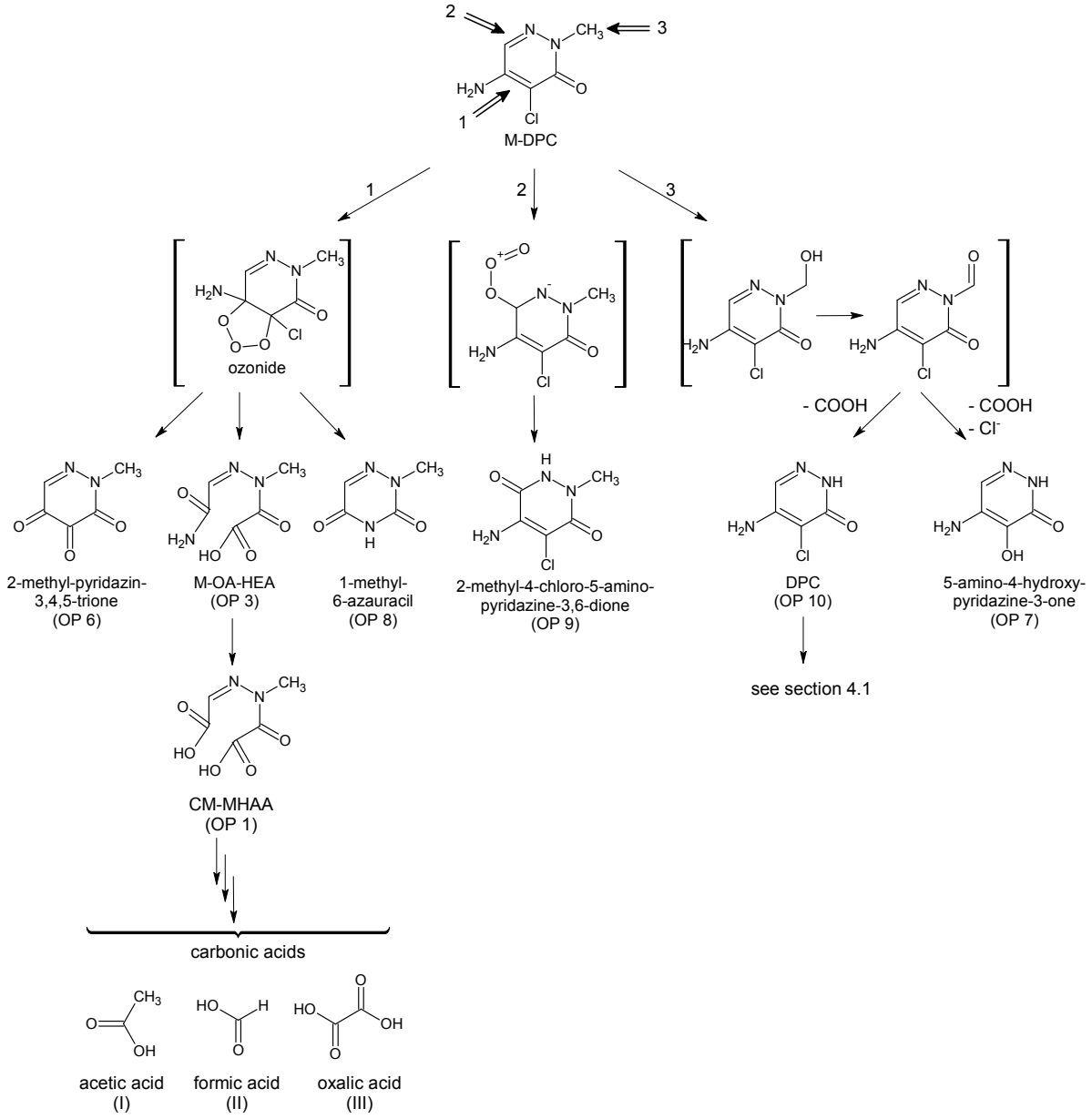

Figure 4.31: Proposed oxidation pathway for methyl-desphenyl-chloridazon (M-DPC) via three sites of primary ozone attack.

5 Summary

Adverse effects have been reported for oxidation products (OPs) of micropollutants formed during ozonation, a step in drinking water treatment, and therefore interest in the identification of these compounds has increased in recent years. Due to their high polarity and persistency, the two metabolites desphenyl-chloridazon (DPC) and methyl-desphenyl-chloridazon (M-DPC), which are formed from the herbicide chloridazon through biological transformation processes in the environment, can frequently be found in surface waters and groundwaters in Germany. However, there is no information available about their possible oxidation products. The present work for the first time investigated the structural elucidation of oxidation products from DPC and M-DPC, reaction mechanisms involved in their formation and possible overall oxidation pathways. Furthermore, the formation of an identified OP that is potentially harmful for humans and the environment was studied under environmentally relevant concentrations and waterworks conditions to evaluate the risk arising from the ozonation of waters containing DPC and M-DPC.

In general, the identification of OPs was performed by combining the application of known ozonation mechanisms from literature to the structures of DPC and M-DPC with lab-scale ozonation experiments and the analysis of the ozone-treated samples using different analytical instruments such as HPLC-DAD-Q-ToF-MS, GC-MS and IC-CD. With this approach, structures for numerous OPs could be proposed and the majority of these were confirmed by standard compounds.

In experiments for structural identification of OPs, 1 mM solutions of DPC and M-DPC in MilliQ water were used and ozone concentrations ranged in the higher mg/L level to ensure that the concentrations of the OPs formed were above the detection limits. To analyze OP formation in natural waters and under environmentally relevant conditions analyte concentrations ranged between 10 µg/L and 100 µg/L and ozone concentrations between 0.5 mg/L and 2 mg/L.

Desphenyl-chloridazon (DPC)

From the oxidation experiments with DPC it was possible to identify eight OPs of which one was the analog OP to 2-methyl-pyridazine-3,4,5-trione formed from M-DPC, namely pyridazine-3,4,5-trione. Further primary OPs were identified as 1,2-dihydro-1,2,4-triazine-3,6-dione and 6-azauracil. A mechanism explaining the formation of 6-azauracil was proposed. Initially, ozone attacks the carbon-carbon double bond in the pyridazine ring of DPC via the first steps of the Criegee mechanism. However, in contrast to the classical Criegee mechanism, the intermediate stabilized after opening of the ozonide under elimination of

formylchloride and formation of a new 1,2,4-triazine ring. This unusual formation mechanism demonstrates that the presence of amino and keto groups in the molecule enables the formation of new ring systems during ozonation.

For 6-azauracil, several adverse effects on plants, animals and humans have been described in literature. For example, 6-azauracil is a known inhibitor of enzymes involved in the synthesis of RNA bases and is also capable of inhibiting flowering in some plants. Furthermore, 6-azauracil is a growth inhibitor for a great number of microorganisms and classified as highly hazardous to water. Because of these effects and due to its high formation yield of up to 20 mol%, the fate of 6-azauracil was further investigated in two respects. Firstly, the OPs arising during ozonation of 6-azauracil were studied, and secondly the extent of 6-azauracil formation under environmentally relevant concentrations in natural water matrices was determined.

The ozonation of 6-azauracil resulted in the formation of 5-hydroxyhydantoin, which again consists of a new ring system. Its formation mechanism can be described in a similar way to that of 6-azauracil. 5-Hydroxyhydantoin in turn was oxidized to parabanic acid which hydrolyzed to oxaluric acid. Oxaluric acid then degraded to oxamic acid, oxalic acid and oxamide. Hence, the complete pathway for the ozonation of 6-azauracil and its OPs ending in mineralization was identified. Through the identification of these OPs and their oxidation pathway it was clarified that oxidation of 6-azauracil results in the formation of uncritical, mostly instable substances.

To investigate the formation of 6-azauracil in natural water matrices, drinking water and river water, were spiked with 100 µg/L DPC and treated with 0.5 mg/L and 2 mg/L of ozone. Through these experiments, the formation of 6-azauracil in natural water matrices was confirmed. The maximum formation of 6-azauracil is reached when DPC is almost fully removed from the samples. Then the concentration of 6-azauracil in the samples decreases. Depending on the ozone dose applied, 6-azauracil was either in its formation maximum or fully removed through ongoing oxidation. In these experiments the maximum 6-azauracil formation was determined as approximately 2 mol% of the initial DPC concentration, which is around an order of magnitude lower than in MilliQ water and could be explained through competing reactions, such as radical reaction, occurring in natural waters. Because of the low formation of 6-azauracil in natural water matrices, an SPE enrichment method was established and validated which enabled the trace analysis of both DPC and 6-azauracil. By applying the SPE method to samples spiked with 10 µg/L DPC and 0.5 mg/L ozone it was shown that 6-azauracil was also formed in drinking water in environmentally relevant concentrations. The maximum formation of 6-azauracil was determined as 3.6 mol% (0.3 µg/L) of the initial DPC concentration.

Methyl-desphenyl-chloridazon (M-DPC)

It was possible to identify ten OPs formed during ozonation of M-DPC. These OPs can be divided into three groups depending on the primary site of ozone attack and thus on the oxidation pathway. The first site of ozone attack is the carbon-carbon double bond via 1,3-dipolar cycloaddition, the second is the carbon-nitrogen double bond via nucleophilic attack of the ozone molecule and the third is the methyl group. Of these three possibilities the predominant reaction pathway seems to follow the first route, whereas the oxidation of the carbon-nitrogen double bond and of the methyl group was found to be of minor relevance.

It was shown that for the first reaction route the instable ozonide stabilized under formation of three OPs. A mechanism for the formation of the first OP, 2-methyl-pyridazine-3,4,5-trione, was proposed. The initial attack of ozone on the carbon-carbon double bond in M-DPC, based on the classical Criegee mechanism, was followed by the formation of an epoxide and stabilization under formation of 2-methyl-pyridazine-3,4,5-trione. Furthermore, the OPs 1-methyl-6-azauracil and (2*Z*)-2-[2-methyl-2-(oxoacetyl)-hydrazinylidene]-ethanamide (M-OA-HEA) were identified. M-OA-HEA in turn was further oxidized to [(2Z)-2(carboxymethylidene)-1-methylhydrazinyl]oxoacetic acid (CM-MHAA). The second pathway resulted in the formation of 2-methyl-4-chloro-5-amino-pyridazine-3,6-dione, the only chlorinated OP besides DPC formed through oxidation of M-DPC. Desphenyl-chloridazon (DPC) and 5-amino-4-hydroxy-pyridazine-3-one were formed via the third reaction route which involved the oxidation of the methyl group. Further oxidation by an excess of ozone resulted in the decomposition of the identified OPs and in the formation of small carbonic acids, such as formic acid, acetic acid and oxalic acid.

The present work shows that by combining chemical expertise on reaction mechanisms with state-of-the-art analytical techniques, for example HPLC-DAD-Q-ToF-MS, an identification of oxidation products and reaction pathways of environmentally relevant micropollutants is feasible.

6 Glossary

Artificially recharged groundwater / Infiltration: Groundwater is enriched through artificial percolation of for example surface water via basins, suction wells or horizontal percolation lines.

Biocide: (derived from Greek *bios* life and *caedere* Latin kill) Biocide is an umbrella term including pesticides. The products included are preparations which serve, by chemical or biological means, to deter, render harmless or destroy pests (like moths, woodworm, mice etc). The aim is to prevent damage to foods, consumer products, construction materials (wood) and other products.

Collision induced dissociation (CID): In mass spectrometry collision induced dissociation is a term describing a mechanism to fragment molecular ions in the gas phase. During CID the ion of interest is selected with a mass analyzed and then subjected to collisions with neutral atoms such as nitrogen. Through the analyses of the resulting fragment ions conclusions regarding the chemical structure of the molecules can be drawn.

Double bond equivalent: Double bond equivalents (DBEs) explain the correlation between empirical formula, double bonds and rings in a molecule. For simple molecules it is calculated as the sum of carbon which counts two, nitrogen which counts one and hydrogen which count minus one. Oxygen does not influence the calculation. Benzene for example consists of three double bonds and one ring which make four double bonds in total. This correlation is a useful tool in the prediction of structures to known empirical formulas.

Groundwater: Water which fills underground openings in the earth crust and follows gravity. It is generated through percolated rainfall which has long percolation way and residence time in the underground.

Hill reaction: This reaction was first demonstrated by Robert Hill in 1939. In this reaction illuminated chloroplasts produce oxygen when they are incubated in the presence of an artificial electron acceptor such as ferricyanide. The reaction is a property of photosystem II.

Inert: Compounds that dissolved in water do not show a decrease in concentration over the time and do not react with other compounds are defined as inert compounds.

In-source collision induced dissociation: Through the application of high voltages in the ionization chamber a pre-fragmentation in the chamber can be achieved. This enables to perfom MS^3 experiments through further CID in the collision cell.

Instable: Compounds that dissolved in water show a decrease in concentration over the time are defined as instable compounds.

Isomer: Structural isomers consist of the same elemental composition but the atoms are arranged differently. Stereo isomers principally have the same structure but differ in their steric configuration.

Mechanism: A mechanism describes in detail how two molecules react with each other, especially how the electrons are transferred and bond broken or created.

Metabolite: Metabolites are defined as compounds were the mother compound (here the pesticide) was modified by biological transformation processes.

> **Non-relevant Metabolite**: Metabolites that show no or far lower activity compared to the pesticide and no other toxicity are termed non-relevant and therefore concentration levels of up to 10 µg/L in drinking waters are accepted according to the Plant Protection Ordinance. The Drinking Water Ordinance gives no details regarding the classification in relevant and non-relevant metabolites.
>
> **Relevant Metabolite**: Metabolites that still show activity similar to the pesticide or other toxicity are termed relevant and therefore concentration levels of up to 1 µg/L in drinking waters are accepted according to the Plant Protection Ordinance.

Oxidation pathway: An oxidation pathway describes the chronological formation of oxidation products (analytically confirmed) without going into the underlying mechanisms.

Oxidation product: Oxidation products are defined as compounds formed through oxidative processes such as ozonation or chlorination. Oxidation products are a subdivision of transformation products.

Pathway: see oxidation pathway.

Pesticide: (derived from Latin *pestis* plage and *caedere* Latin kill) Substances intended to repel, kill, or control any species designated a "pest" including weeds, insects, rodents, fungi, bacteria, or other organisms. The family of pesticides includes herbicides, insecticides, rodenticides, bacteria and fungicides.

Plant protection product: Pesticides used to protect plants from pests and diseases or control unwanted plants (weeds).

Pseudo first order kinetic: If the reactant A is present in excess during a reaction of A and B to P ($A + B \rightarrow P$) its concentration during the reaction only changes to a small extent. Hence, the concentration of A is almost constant and the influence on the reaction rate can be accounted for with the help of a constant of proportionality (k'). k' can be determined from the half-live $t_{1/2}$ with the equation $k' = (\ln 2)/(t_{1/2})$.

R_{ct} value: The ratio of hydroxyl radicals to ozone is described by the R_{ct} value. This value varies between 10^{-6} and 10^{-9} during the treatment of water with ozone.

Riverbank filtrate: Surface water that naturally infiltrates via riverbanks and riverbed.

Spring water: Groundwater which appears through free incline, although it differs form the "real" groundwater regarding its formation mechanism, its nature and its form of catchment.

Stable: Compounds that dissolved in water do not show a decrease in concentration over the time are defined as stable compounds. If a reactant is present these compounds will undergo a reaction.

Surface water: Water from standing or flowing above-ground waters especially from reservoirs, lakes, rivers but also from seawater. The character/composition of surface waters strongly differs in terms of time and location particularly depending on the type and utilization of the catchment area.

Transformation product: Compounds that are formed through abiotic processes, such as oxidation and reduction processes or photodegradation as well as ozonation of chlorination. Oxidation products are a sub-group of transformation products.

7 References

[1] Statistisches Bundesamt. Öffentliche Wasserversorgung und Abwasserbeseitigung 2004. Statistisches Bundesamt. Wiesbaden. 2006.

[2] Mehlhorn H. Wasserversorgung der Zukunft - Gedanken zu Wettbewerb und Qualität. Wissensdurst, Bodensee - Wasserversorgung. 2008. 3, 14-29.

[3] Mutschmann J and Stimmelmayr F. Taschenbuch der Wasserversorgung. Vieweg, Springer Fachmedien Wiesbaden GmbH. 2002. 13 ed, chapter 4.

[4] Wienand I. Entwicklung eines GIS- und QRA-basierten Wassersicherheitsplans (WSP) als ein Instrument des Ressourcenschutzes in Trinkwassereinzugsgebieten. Mathematisch-Naturwissenschaftlichen Fakultät der Rheinischen Friedrich-Wilhelms-Universität Bonn. 2006.

[5] Bannick C, Engelmann B, Fendler R, Frauenstein J, Ginzky H, Hornemann C, Ilovan O, Kirschbaum B, Penn-Bressel G, Rechenberg J, Richter S, Roy L and Wolter R. Bundesministerium für Umwelt, Naturschutz und Reaktorsicherheit (BMU). Reihe Umweltpolitik, Grundwasser in Deutschland. 2008.

[6] DIN 2000:2000-10: Zentrale Trinkwasserversorgung - Leitsätze für Planung, Bau, Betrieb und Instandhaltung der Versorgungsanlagen - Technische Regel des DVGW. Beuth-Verlag. 2000.

[7] Technische Regeln - Arbeitsblatt: DVGW-W 202. Techniche Regeln Wasseraufbereitung (TRWA) - Planung, Bau, Betrieb und Instandhaltung von Anlagen zur Trinkwasseraufbereitung. 2010.

[8] Han B, Runnells T, Zimbron J and Wickramasinghe R. Arsenic removal from drinking water by flocculation and microfiltration. Desalination. 2002. 145, 293-298.

[9] Seitz W, Jiang J, Weber WH, Lloyd BJ, Maier M and Maier D. Removal of iodinated X-ray contrast media during drinking water treatment. Environmental Chemistry. 2006. 3, 35-39.

[10] Van der Bruggen B and Vandecasteele C. Removal of pollutants from surface water and groundwater by nanofiltration: overview of possible applications in the drinking water industry. Environmental Pollution. 2003. 122, 435-445.

[11] Watson BM and Hornburg CD. Low-energy membrane nanofiltration for removal of color, organics and hardness from drinking water supplies. Desalination. 1989. 72, 11-22.

[12] Geiges M and Kiefer J. Struktur der Trinkwasserversorgung Deutschlands sowie Darstellung der bei der Trinkwasseraufbereitung eingesetzten Verfahren und besonderer Berücksichtigung des Einsatzes von Ozon. Literaturstudie Teil 1. TZW-Umfrage 2011.

[13] Hofmann O, Hoyer O, Schoenen D and Wricke B. Desinfektion. Jekel M., Gimbel R., Ließfeld R. (Hrsg.): Wasseraufbereitung - Grundlagen und Verfahren. 19, 765-790. München, Wien, Oldenbourg Industrieverlag.(2004).

[14] Umweltbundesamt (UBA). Liste 1 der Aufbereitungsstoffe und Desinfektionsverfahren gemäß § 11 Trinkwasserverordnung 2001.

[15] Ormad MP, Miguel N, Claver A, Matesanz JM and Ovelleiro JL. Pesticides removal in the process of drinking water production. Chemosphere. 2008. 71, 97-106.

[16] Ternes TA, Meisenheimer M, McDowell D, Sacher F, Brauch HJ, Haist-Gulde B, Preuss G, Wilme U and Zulei-Seibert N. Removal of pharmaceuticals during drinking water treatment. Environmental Science & Technology. 2002. 36, 3855-3863.

[17] Verordnung über die Behandlung von Lebensmitteln mit Elektronen-, gamma- und Röntgenstrahlen, Neutronen oder ultravioletten Strahlen. Lebensmittelbestrahlungsverordnung vom 14.12.2000 (BGBl. I S. 1730), die zuletzt durch Artikel 7 der Verordnung vom 13.12.2011 (BGBl. I S. 2720) geändert worden ist.

[18] Hua G and Reckhow DA. Comparison of disinfection byproduct formation from chlorine and alternative disinfectants. Water Research. 2007. 41, 1667-1678.

[19] Ternes TA, Stumpf M, Müller J, Haberer K, Wilken RD and Servos M. Behavior and occurrence of estrogens in municipal sewage treatment plants - I. Investigations in Germany, Canada and Brazil. Science of the Total Environment. 1999. 225, 81-90.

[20] Buser HR, Poiger T and Müller M D. Occurrence and fate of the pharmaceutical drug diclofenac in surface waters: Rapid photodegradation in a lake. Environmental Science & Technology. 1998. 32, 3449-3456.

[21] Buser HR, Poiger T and Müller MD. Occurrence and environmental behavior of the chiral pharmaceutical drug ibuprofen in surface waters and in wastewater. Environmental Science & Technology. 1999. 33, 2529-2535.

[22] Reddersen K, Heberer T and Dünnbier U. Identification and significance of phenazone drugs and their metabolites in ground- and drinking water. Chemosphere. 2002. 49, 539-544.

[23] Hirsch R, Ternes TA, Haberer K, Mehlich A, Ballwanz F and Kratz KL. Determination of antibiotics in different water compartments via liquid chromatography-electrospray tandem mass spectrometry. Journal of Chromatography A. 1998. 815, 213-223.

[24] Hirsch R, Ternes TA, Haberer K and Kratz KL. Occurrence of antibiotics in the aquatic environment. Science of the Total Environment. 1999. 225, 109-118.

[25] Ternes TA. Occurrence of drugs in German sewage treatment plants and rivers. Water Research. 1998. 32, 3245-3260.

[26] Fang Y, Karnjanapiboonwong A, Chase DA, Wang J, Morse, AN and Anderson T A. Occurrence, fate, and persistence of gemfibrozil in water and soil. Environmental Toxicology and Chemistry. 2012. 31, 550-555.

[27] Adler P, Steger-Hartmann T and Kalbfus W. Vorkommen natürlicher und synthetischer Östrogener Steroide in Wässern des süd- und mitteldeutschen Raumes. Acta hydrochimica et hydrobiologica. 2001. 29, 227-241.

[28] Belfroid AC, Van der Horst A, Vethaak AD, Schäfer AJ, Rijs GBJ, Wegener J and Cofino WP. Analysis and occurrence of estrogenic hormones and their glucuronides in surface water and waste water in The Netherlands. Science of the Total Environment. 1999. 225, 101-108.

[29] Putschew A, Wischnack S and Jekel M. Occurrence of triiodinated X-ray contrast agents in the aquatic environment. Science of the Total Environment. 2000. 255, 129-134.

[30] Seitz W, Weber WH, Jiang JQ, Lloyd BJ, Maier M, Maier D and Schulz W. Monitoring of iodinated X-ray contrastmedia in surface water. Chemosphere. 2006. 64, 1318-1324.

[31] Andreozzi R, Marotta R, Pinto G and Pollio A. Carbamazepine in water: persistence in the environment, ozonation treatment and preliminary assessment on algal toxicity. Water Research. 2002. 36, 2869-2877.

[32] Camel V and Bermond A. The use of ozone and associated oxidation processes in drinking water treatment. Water Research. 1998. 32, 3208-3222.

[33] McDowell D, Huber M, Wagner M, von Gunten U and Ternes TA. Ozonation of carbamazepine in drinking water: Identification and kinetic study of major oxidation products. Environmental Science & Technology. 2005. 39, 8014-8022.

[34] Riebel AH, Erickson RE, Abshire CJ and Bailey PS. Ozonation of carbon-nitrogen double bonds. I.Nucleophilic attack of ozone. Journal of the American Chemical Society. 1960. 82, 1801-1807.

[35] Decoret C, Royer J, Legube B and Dore M. Experimental and theoretical studies of the mechanism of the initial attack of ozone on some aromatics in aqueous medium. Environmental Technology Letters. 1984. 5, 207-218.

[36] Lide, DR. CRC Handbook of Chemistry and Physics. 2012. 92nd ed (Internet Version).

[37] Glaze WH. Reaction products of ozone: a review. Environmental Health Perspectives. 1986. 69, 151-157.

[38] Hoigné J and Bader H. Rate constants of reactions of ozone with organic and inorganic compounds in water - II. Water Research. 1983. 17, 185-194.

[39] Hoigné J and Bader H. Rate constants of reactions of ozone with organic and inorganic compounds in water - I. Water Research. 1983. 17, 173-183.

[40] Hoigné J and Bader, H. The role of hydroxyl radical reactions in ozonation processes in aqueous solutions. Water Research. 1976. 10, 377-386.

[41] Sierka RA and Amy GL. Catalytic effects of ultraviolet light and/or ultrasound on the ozone oxidation of humic acid and trihalomethane precursors. Ozone Science Engineering. 1985. 7, 47-62.

[42] Staehelin J and Hoigne J. Decomposition of ozone in water: Rate of initiation by hydroxide ions and hydrogen peroxide. Environmental Science & Technology. 1982. 16, 676-681.

[43] Staehelin J, Buehler RE and Hoigne J. Ozone decomposition in water studied by pulse radiolysis. 2. Hydroxyl and hydrogen tetroxide (HO4) as chain intermediates. The Journal of Physical Chemistry. 1984. 88, 5999-6004.

[44] Legube B, Guyon S and Doré M. Ozonation of Aqueous Solutions of Nitrogen Heterocyclic Compounds: Benzotriazoles, Atrazine and Amitrole. Ozone: Science & Engineering. 1987. 9, 233-246.

[45] Rosal A, Rodríguez A, Perdigón-Melón JA, Petre A, García-Calvo E, Gómez MJ, Agüera A and Fernández-Alba AR. Degradation of caffeine and identification of the transformation products generated by ozonation. Chemosphere. 2009. 74, 825-831.

[46] Turhan K and Uzman S. Removal of phenol from water using ozone. Desalination. 2008. 229, 257-263.

[47] Valsania MC, Fasano F, Richardson SD and Vincenti M. Investigation of the degradation of cresols in the treatments with ozone. Water Research. 2012. 46, 2795-2804.

[48] Elovitz MS, Kaiser HP and von Gunten U. Hydroxyl radical/ozone ratios during ozonation processes. II. The effect of temperature, pH, alkalinity, and DOM properties. Ozone: Science & Engineering. 2000. 22, 123-150.

[49] Elovitz MS and von Gunten U. Hydroxyl radical/ozone ratios during ozonation processes. I. The R_{ct} concept. Ozone: Science & Engineering. 1999. 21, 239-260.

[50] Criegee R. Mechanism of ozonolysis. Angewandte Chemie, International Edition. 1975. 14, 745-752.

[51] White HM and Bailey PS. Ozonation of aromatic aldehydes 1. The Journal of Organic Chemistry. 1965. 30, 3037-3041.

[52] Bailey PS. The reactions of ozone with organic compounds. Chemical Reviews. 1958. 58, 925-1010.

[53] Gould JP and Weber WJ. Oxidation of phenols by ozone. Water Pollution Control Federation. 1976. 48, 47-60.

[54] Mvula E and von Sonntag C. Ozonolysis of phenols in aqueous solution. Organic & Biomolecular Chemistry. 2003. 1, 1749-1756.

[55] Ramseier MK and von Gunten U. Mechanisms of phenol ozonation - Kinetics of formation of primary and secondary reaction products. Ozone: Science and Engineering. 2009. 31, 201-215.

[56] Eisenhauer HR. The ozonization of phenolic wastes. Water Pollution Control Federation. 1968. 40, 1887-1899.

[57] Singer PC and Gurol MD. Dynamics of the ozonation of phenol - I. Experimental observations. Water Research. 1983. 17, 1163-1171.

[58] Kuo CH and Huang CH. Aqueous phase ozonation of chlorophenols. Journal of Hazardous Materials. 1995. 41, 31-45.

[59] Erickson RE, Andrulis PJ, Collins JC, Lungle ML and Mercer GD. Mechanism of ozonation reactions. IV. Carbon-nitrogen double bonds. The Journal of Organic Chemistry. 1969. 34, 2961-2966.

[60] Erickson RE and Myszkiewicz TM. Mechanism of ozonation reactions. Nitrones. The Journal of Organic Chemistry. 1965. 30, 4326-4327.

[61] Bachman GB and Srawn KG. Ozone oxidation of primary amines to nitroalkanes. The Journal of Organic Chemistry. 1968. 33, 313-315.

[62] Bailey PS and Keller JE. Ozonation of amines. III. t-Butylamine. The Journal of Organic Chemistry. 1968. 33, 2680-2684.

[63] Bailey PS, Carter TP and Southwick LM. Ozonation of amines. VI. Primary amines. The Journal of Organic Chemistry. 1972. 37, 2997-3004.

[64] Bailey PS, Michard DA and Kashhab AI. Ozonation of amines. II. The competition between amine oxide formation and side-chain oxidation. The Journal of Organic Chemistry. 1968. 33, 2675-2680.

[65] Bailey PS, Keller JE and Carter TP. Ozonation of amines. IV. Di-tert-butylamine. The Journal of Organic Chemistry. 1970. 35, 2777-2782.

[66] Bailey PS, Lerdal DA and Carter TP. Ozonation of nucleophiles. 9. Tertiary amines. The Journal of Organic Chemistry. 1978. 43, 2662-2664.

[67] Bailey PS, Southwick LM and Carter TP. Ozonation of nucleophiles. 8. Secondary amines. The Journal of Organic Chemistry. 1978. 43, 2657-2662.

[68] Erickson RE, Bakalik D, Richards C, Scanlon M and Huddleston G. Mechanism of Ozonation Reactions. II. Aldehydes. The Journal of Organic Chemistry. 1966. 31, 461-466.

[69] Martinez RI. The mechanism of O_3-aldehyde reactions. International Journal of Chemical Kinetics. 1982. 14, 237-249.

[70] Voukides AC, Konrad KM and Johnson RP. Competing mechanistic channels in the oxidation of aldehydes by ozone. The Journal of Organic Chemistry. 2009. 74, 2108-2113.

[71] Batterbee J and Bailey P. Ozonation of carbon-hydrogen bonds. Anthrone. The Journal of Organic Chemistry. 1967. 32, 3899-3903.

[72] Giamalva DH, Church DF and Pryor WA. Kinetics of ozonation. 5. Reactions of ozone with carbon-hydrogen bonds. American Chemical Society. 1986. 108, 7678-7681.

[73] Nangia PS and Benson SW. Thermochemistry and kinetics of ozonation reactions. Journal of the American Chemical Society. 1980. 102, 3105-3115.

[74] Giamalva DH, Church DF and Pryor WA. Kinetics of ozonation. 6. Polycyclic aliphatic hydrocarbons. The Journal of Organic Chemistry. 1988. 53, 3429-3432.

[75] Ikehata K and El-Din MG. Aqueous pesticide degradation by ozonation and ozone-based advanced oxidation processes: A review (Part I). Ozone: Science & Engineering. 2005. 27, 83-114.

[76] Ikehata K, Naghashkara NJ and El-Dina MG. Degradation of aqueous pharmaceuticals by ozonation and advanced oxidation processes: A review. Ozone: Science & Engineering. 2006. 28, 353-414.

[77] Ikehata K, El-Din MG and Snyder SA. Ozonation and advanced oxidation treatment of emerging organic pollutants in water and wastewater. Ozone: Science & Engineering. 2008. 30, 21-26.

[78] Schmidt CK and Brauch HJ. *N,N*-dimethylsulfamide as precursor for *N*-nitroso-dimethylamine (NDMA) formationupon ozonation and its fate during drinking water treatment. Environmental Science & Technology. 2008. 42, 6340-6346.

[79] Weber WH, Seitz W and Schulz W. Nachweis der Metaboliten Desphenyl-chloridazon und Methyl-desphenyl-chloridazon in Oberflächen-, Grund- und Trinkwasser. Vom Wasser. 2007. 105, 7-14.

[80] Bonnet JL, Bonnemoy F, Dusser M and Bohatier J. Assessment of the potential toxicity of herbicides and their degradation products to nontarget cells using two microorganisms, the bacteria Vibrio fischeri and the ciliate tetrahymena pyriformis. Environmental Toxicology. 2007. 22, 78-91.

[81] Farré M, Asperger D, Kantiani L, González, S., Petrovic, M., and Barceló, D. Assessment of the acute toxicity of triclosan and methyl triclosan in wastewater based on the bioluminescence inhibition of vibrio fischeri. Analytical and Bioanalytical Chemistry. 2008. 390, 1999-2007.

[82] Bhargava HN and Leonard PA. Triclosan: Applications and safety. American journal of infection control.1996. 243, 209-218.

[83] Coogan MA, Edziyie RE, La Point TW and Venables BJ. Algal bioaccumulation of triclocarban, triclosan, and methyl-triclosan in a North Texas wastewater treatment plant receiving stream. Chemosphere. 2007. 67, 1911-1918.

[84] Coogan MA and Point TWL. Snail bioaccumulation of triclocarban, triclosan, and methyltriclosan in a north texas, usa, stream affected by wastewater treatment plant runoff. Environmental Toxicology and Chemistry. 2008. 27, 1788-1793.

[85] Bundesamt für Verbraucherschutz und Lebensmittelsicherheit (BVL). Metaboliten von Pflanzenschutzmittel-Wirkstoffen im Sickerwasser von Lysimeter- oder Feldversickerungsstudien. 2008.

[86] European Food and Safety Authority (EFSA). Conclusion on the peer review of tolylfluanid EFSA Scientific Report. 2005. 29, 1-76.

[87] Von Gunten U, Salhi E, Schmidt CK and Arnold WA. Kinetics and mechanisms of N-nitrosodimethylamine formation upon ozonation of N,N-dimethylsulfamide-containing waters: bromide catalysis. Environmental Science & Technology. 2010. 44, 5762-5768.

[88] Magee PN and Barnes JM. The production of malignant primary hepatic tumours in the rat by feeding dimethylnitrosamine. British Journal of Cancer. 1956. 10, 114-122.

[89] Scanlon B. N-Nitroso compounds analysis and formation. Chromatographia. 1973. 6, 444.

[90] Bundesamt für Verbraucherschutz und Lebensmittelsicherheit (BVL): Wiederruf der Zulassung für Tolylfluanid. http://www.bvl.bund.de/DE/04_Pflanzenschutzmittel/01_Aufgaben/02_ZulassungPSM/01_ZugelPSM/03_Widerrufe/psm_ZugelPSM_widerrufe_node.html (accessed 26.05.2012).

[91] Bundesamt für Verbraucherschutz und Lebensmittelsicherheit (BVL): Absatz an Pflanzenschutzmitteln in der Bundesrepublik Deutschland Ergebnisse der Meldungen gemäß § 19 Pflanzenschutzgesetz für das Jahr 2009. http://www.bvl.bund.de/DE/04_Pflanzenschutzmittel/01_Aufgaben/02_ZulassungPSM/01_ZugelPSM/03_Widerrufe/psm_ZugelPSM_widerrufe_node.html (accessed 19.09.2011).

[92] Qasem JR. Chemical weed control in seedbed sown onion (Allium cepa L.). Crop Protection. 2006. 25, 618-622.

[93] Corbett JR, Moreno C and Arruga MV. The biochemical mode of action of pesticides. Academic Press, London. 1984. 2 ed, 50-92.

[94] Cremlyn RJ. Pesticides: Preparation and mode of action. John Wiley and Sons, Chichester. 1978. Chapter 2.

[95] Castle RN and Seese W. Imidazo[4,5-d]pyridazines. I. Synthesis of 4,7-disubstituted derivatives. The Journal of Organic Chemistry. 1958. 23, 1534-1538.

[96] Castle RN. The Chemistry of heterocyclic compounds - Pyradizines, John Wiley and Sons. 1973. Vol 28.

[97] Gierig M. Ergebnisse der Untersuchungen von PSM-Metaboliten in Grund- und Oberflächenwasser Bayerns. Fachtagung des Bayerischen Landesamtes für Umwelt am 18. und 19.11.2008. Pflanzenschutzmittel-Metaboliten. Vorkommen und Bewertung. 26-34.

[98] Buttiglieri G, Peschka M, Froemel T, Mueller J, Malpei F, Seel P and Knepper TP. Environmental occurrence and degradation of the herbicide n-chloridazon. Water Research. 2009. 43, 2865-2873.

[99] Schneider B. Ergebnisse von Metaboliten im Grundwasser in Baden-Württemberg. Fachtagung des Bayerischen Landesamtes für Umwelt am 18. und 19.11.2008. Pflanzenschutzmittel-Metaboliten. Vorkommen und Bewertung. 35-40.

[100] Richtlinie 91/414/EWG des Rates vom 15.07.1991 über das Inverkehrbringen von Pflanzenschutzmitteln.

[101] Richtlinie 98/83/EG des Rates vom 03.11.1998 über die Qualität von Wasser für den menschlichen Gebrauch.

[102] Pflanzenschutzmittelverordnung in der Fassung der Bekanntmachung vom 09.03.2005 (BGBl. I S. 734), die zuletzt durch Artikel 3 § 7 des Gesetzes vom 13.12.2007 (BGBl. I S. 2930) geändert worden ist.

[103] Trinkwasserverordnung vom 21.5.2001 (BGB. I S. 959) in der Fassung der Bekanntmachung vom 28.11.2011(BGBl. I S.2370).

[104] Corsten K. Zulassung von Pflanzenschutzmitteln in Deutschland. Fachtagung des Bayerischen Landesamtes für Umwelt am 18. und 19.11.2008. Pflanzenschutz-mittel-Metaboliten. Vorkommen und Bewertung. 10-15.

[105] European Commission. Guidance Document on the Assessment of the Relevance of Metabolites in Groundwater. Sanco/221/2000 – rev 10, 25.02.2003.

[106] Umweltbundesamt (UBA). Trinkwasserhygienische Bewertung stoffrechtlich "nicht relevanter" Metaboliten von Wirkstoffen aus Pflanzenschutzmitteln im Trinkwasser. Empfehlung des Umweltbundesamtes nach Anhörung der Trinkwasserkommission der Bundesministeriums für Gesundheit beim Umweltbundesamt. Bundesgesundheitsblatt - Gesundheitsforschung - Gesundheitsschutz. 2008, 51, 797-801.

[107] Umweltbundesamt (UBA). Bundesinstitut für Risikobewertung (BfR): Gesundheitliche Orientierungswerte (GOW) für nicht relevante Metaboliten (nrM) von Wirkstoffen aus Pflanzenbehandlungs- und Schädlingsbekämpfungsmitteln 2011, 51, 797-801. www.umweltdaten.de/wasser/themen/trinkwassertoxikologie/tabelle_gow_nrm.pdf (accessed: 15.08.2012).

[108] DIN 38408-G3-3:2011-4: Deutsche Einheitsverfahren zur Wasser. Abwasser und Schlammuntersuchung. Gasförmige Bestandteile (Gruppe G) - Teil 3: Bestimmung von Ozon (G3). Beuth-Verlag. 2011.

[109] Bader H and Hoigné J. Determination of ozone in water by the indigo method. Water Research. 1981. 15, 449-456.

[110] DIN EN 1484:1997-08: Wasseranalytik - Anleitung zur Bestimmung des gesamten organischen Kohlenstoffs (TOC) und des gelösten organischen Kohlenstoffs (DOC). Deutsche Fassung EN 1484-1997. Beuth-Verlag. 1997.

[111] DIN 38404-3:2005-07: Deutsche Einheitsverfahren zur Wasser-, Abwasser- und Schlammuntersuchung - Physikalische-chemische Kenngrößen (Gruppe C) - Teil 3: Bestimmung der Absorption im Bereich der UV-Strahlung, Spektraler Absorptionskoeffizienten (C3). Beuth-Verlag. 2005.

[112] DIN EN ISO 7887:2012-04: Wasserbeschaffenheit - Untersuchung und Bestimmung der Färbung (ISO 7887:2011). Deutsche Fassung EN ISO 7887:2011. Beuth-Verlag. 2011.

[113] Hapeman CJ, Anderson BG, Torrents A and Acher AJ. Mechanistic investigations concerning the aqueous ozonolysis of bromacil. Journal of Agricultural and Food Chemistry. 1997. 45, 1006-1011.

[114] Dowideit P and von Sonntag C. Reaction of ozone with ethene and its methyl- and chlorine-substituted derivatives in aqueous solution. Environmental Science & Technology. 1998. 32, 1112-1119.

[115] Andrews JC and Sell IT. The properties and interrelationship of oxaluric and parabanic acids. Archives of Biochemistry and Biophysics. 1955. 56, 405-411.

[116] Andreozzi R, Insola A, Caprio V and D'Amore MG. Ozonation of 1, 1' dimethyl, 4,4' bipyridinium dichloride (paraquat) in aqueous solution. Environmental Technology. 1993. 14, 695-700.

[117] Acero J, Stemmler K and von Gunten U. Degradation kinetics of atrazine and its degradation products with ozone and OH radicals: A predictive tool for drinking water treatment. Environmental Science & Technology. 2000. 34, 591-597.

[118] Freireich EM, Frei E, Holland JF, Pinkel D, Selawry O, Rothberg H, Haurani F, Taylor R and Gehan EA. Acute leukemia. studies of 6-azauracil evaluation of a new chemotherapeutic agent in patients with "Advanced Refractory". Blood. 1960. 16, 1268-1278.

[119] Shnider BI, Frei E, Tuohy JH, Gorman J, Freireich J, Brindley CO and Clements J. Clinical studies of 6-azauracil. Cancer Research. 1960. 20, 28-33.

[120] Handschumacher RE and Welch AD. Microbial studies of 6-azauracil, an antagonist of uracil. Cancer Research. 1956. 16, 965-969.

[121] Welch AD, Handschumacher RE and Jaffe JJ. Studies on the pharmacology of 6-azauracil. Journal of Pharmacology & Experimental Therapeutics. 1960. 129, 262-270.

[122] Ross C. Metabolism of 6-azauracil and its incorporation into RNA in the cocklebur. Phytochemistry. 1964. 3, 603-607.

[123] Bonner J and Zeevaart JA. Ribonucleic acid synthesis in bud an essential component of floral induction in xanthium. Plant Physiology. 1962. 37, 43-49.

[124] Merck, Produktinformationen zu 6-Azauracil. http://www.merckmillipore.com/germany/chemicals/6-azauracil/MDA_CHEM-841156/p_hwWb.s1LETQAAAEWnOEfVhT (accessed 22.08.2012).

[125] Sigma-Aldrich, Sicherheitsdatenblatt zu 6-Azauracil gemäß Verordnung (EG) Nr. 1907/2006, Version 4.0 Überarbeitet am 27.02.2010. http://www.sigmaaldrich.com/MSDS/MSDS/DisplayMSDSPage.do?country=DE&language=de&productNumber=A1757&brand=SIGMA&PageToGoToURL=http%3A%2F%2Fwww.sigmaaldrich.com%2Fcatalog%2Fproduct%2Fsigma%2Fa1757%3Flang%3Dde (accessed 22.08.2012).

[126] DIN 32645:2008-11: Chemische Analytik - Nachweis-, Erfassungs- und Bestimmungsgrenze unter Wiederholbedingungen - Begriffe, Verfahren, Auswertung. Beuth-Verlag. 2008.

8 Appendix

8.1 Water parameters

Due to the fact that waters vary in their composition drinking water from Karlsruhe and river waterfrom the river Rhine were compared regarding their components (Table 8.1). Differences especially in calcium and sulfate concentrations between drinking water and river water can be noted. In river water the concentration of calcium only lay by 10 % compared to drinking water from Karlsruhe. Sulfate concentrations in drinking water lay by 73 mg/L whereas river water showed concentrations of 5.5 mg/L.

Table 8.1: Water parameters of drinking water from Karlsruhe and water from the river Rhine.

Water parameter	Drinking water	River water
Fluoride (µg/L)	0.07	0.09
Chloride (mg/L)	20	9.5
Bromide (mg/L)	0.04	0.05
Bicarbonate (mg/L)	350	170
Nitrate (mg/L)	6.0	4.0
Sulfate (mg/L)	73	5.5
Phosphate (mg/L)	<0.01	0.18
Calcium (mg/L)	115	10.7
Magnesium (mg/L)	12	1.5
Potassium (mg/L)	2.0	4.9
Sodium (mg/L)	12	5.1
Alkalinity (mmol/L)	0.784	0.061
Acid capacity (mmol/L)	5.23	2.79
Conductivity (mS/m)	67.8	46.9
$SAC_{254\ nm}$ (m^{-1})	<0.1	3.9
$SAC_{436\ nm}$ (m^{-1})	<0.1	0.2
TOC (mg/L)	<0.2	1.9
pH value	7.20	7.95

8.2 Supplementary information to the results section

Ozone stability in water is crucially influenced by its pH value and hence experiments were performed to characterize the ozone stability with varying pH values in drinking water and in MilliQ water. Experiments in drinking water at five different pH values (6, 7, 8, 8.5 and 9) each spiked with 2 mg/L ozone reveal its influence on ozone decomposition (Figure 8.1, A) which in all cases follow first order kinetics (Figure 8.1, B). In MilliQ water ozone is relatively stable and only shows a slight decrease in concentration after 45 min of reaction time. Ozone decomposition in drinking water is faster, the influence of varying pH values in the range of 6 to 8 is negligible and after 45 min the ozone concentration ranges around 40 % of the initial value. An increase in pH value starts to show effects from 8.5 and upwards. A pH value of 9 results in a total decomposition of ozone after 45 min. The stability of ozone can be correlated to the reactions occurring in waters. When ozone is stable in waters less radicals are present and therefore it can be assumed that the predominant reactions will be through direct attack of ozone. When, in contrary, ozone is decomposed more radicals are present and the reactions occur faster.

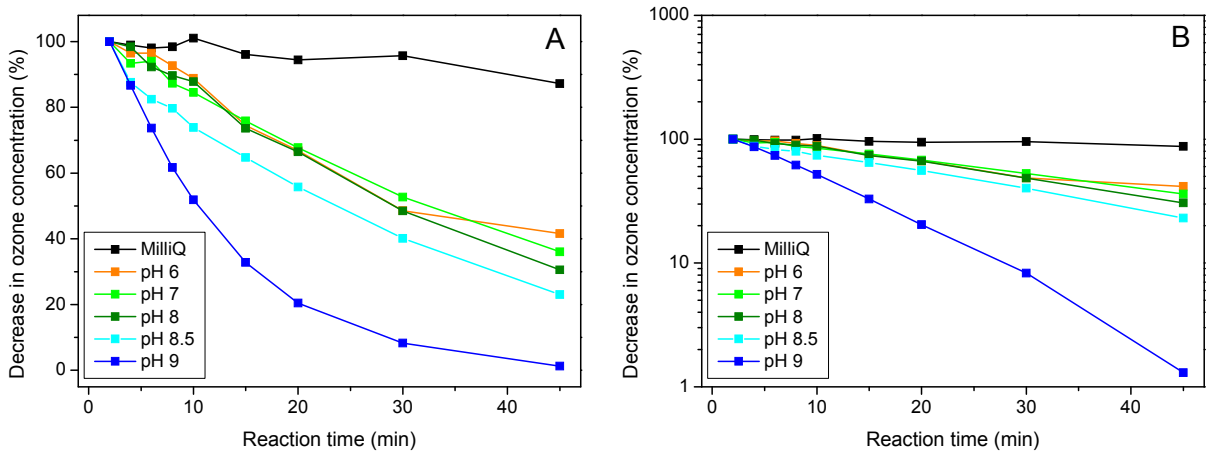

Figure 8.1: (A) Decrease of ozone concentration in demineralized water and drinking water at different pH values over time and (B) logarithmic scale of the decomposition over time.

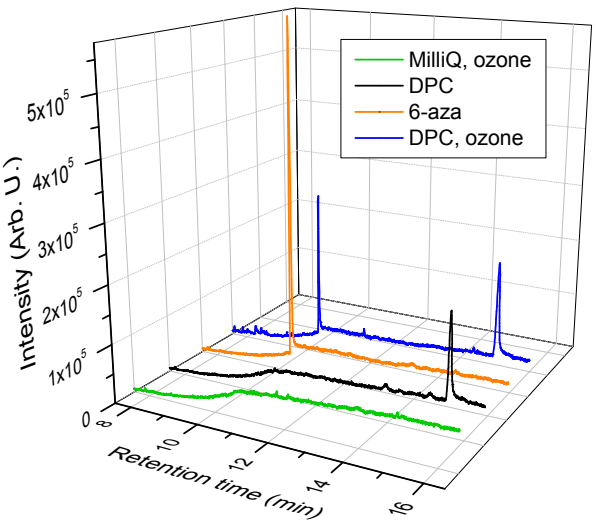

Figure 8.2: TIC of the standards DPC and 6-azauracil (6-aza) as well as the ozone-treated sample DPC and MilliQ water treated with ozone as a blank all measured with GC-MS and electron impact (EI) mode.

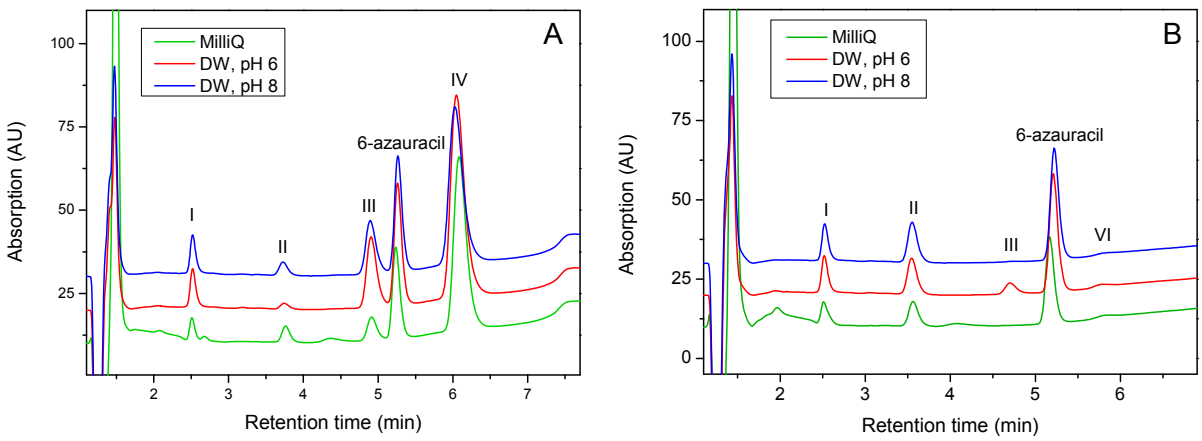

Figure 8.3: (A) UV chromatograms (λ = 220 nm) of 6-azauracil and ozone-treated samples in drinking water (DW) and MilliQ water immediately after ozonation and (B) after 24 h. The peaks were identified as 5-hydroxyhydantoin (I), oxaluric acid (II), parabanic acid (III) and N-(nitrosocarbamoyl)-2-oxoacetamide (IV).

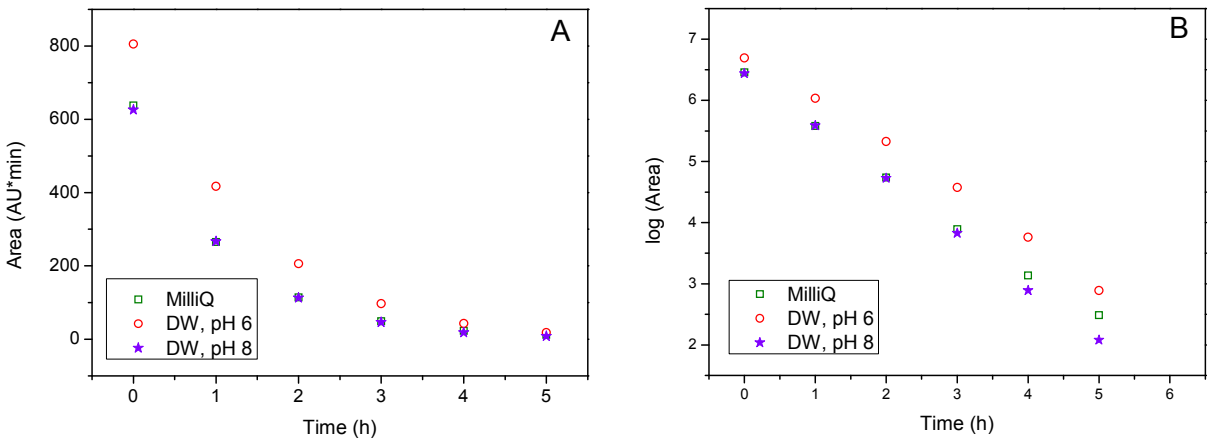

Figure 8.4: (A) Decomposition of the instable OP IV in drinking water (DW) and MilliQ water. Decrease in area (λ = 220 nm) and of the area of the fragment ion at *m/z* 144.0051 over time. (B) Logarithmic scale of the decomposition over time.

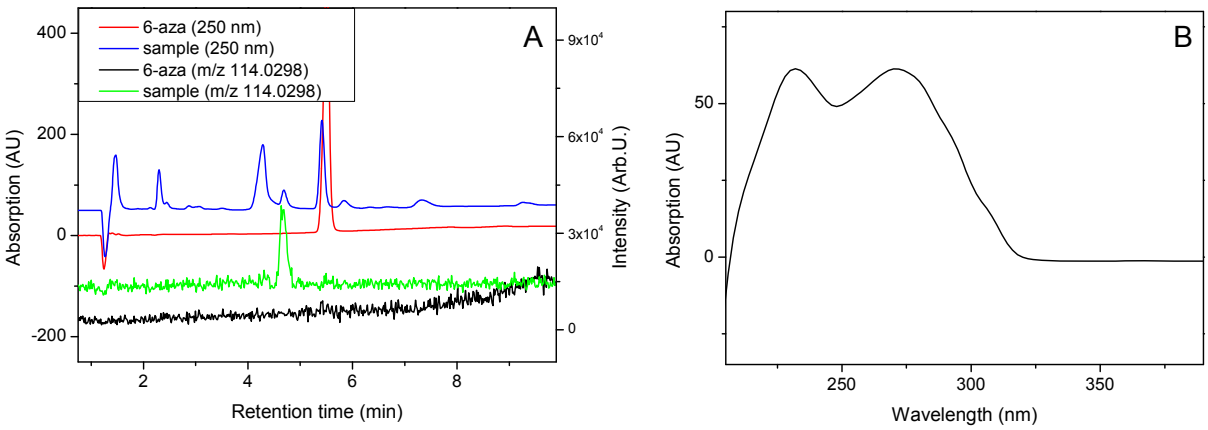

Figure 8.5: (A) UV chromatograms and EIC (*m/z* 114.0298) of 6-azauracil and an ozone-treated DPC sample. The isomer to 6-azauracil eluting after 4.3 min retention time can be detected in positive ionization mode. (B) UV spectrum of iso-6-azauracil.

Table 8.2: Influence of sample concentration and enrichment volume on recoveries for DPC, 6-azauracil and 5-hydroxyhydantoin (5-OH). All samples were reconstituted in 100 µL MilliQ water except samples with * which were reconstituted in 300 µL and samples with ** in 500 µL; n=3.

c (nM)	DPC (µM)			6-azauracil (µM)			5-OH (µM)		
Prior SPE	Enrichment volume (mL)			Enrichment volume (mL)			Enrichment volume (mL)		
	20	50	100	20	50	100	20	50	100
5	0.4	1.0	1.8	0.3	0.5	0.5	0.1	0.1	0.1
10	0.8	1.9	4.2*	0.6	1.2	1.2*	0.2	0.2	<LOD*
20	1.6	4.0**	8.5**	1.2	2.0**	2.5**	0.3	<LOD**	<LOD**

Table 8.3: Analyte stability depending on water matrix and pH value. DW, drinking water; MQ, MilliQ water; 5-OH, 5-hydroxyhydantoin; n=1.

Analyte	pH 3		pH 7		pH 10	
	MQ	DW	MQ	DW	MQ	DW
DPC (%)	120	120	120	110	120	120
6-Azauracil (%)	140	140	120	130	130	140
5-OH (%)	140	140	100	20	30	10

Table 8.4: Analyte stability in drinking water in the presence of sulfite. MV, mean value; RSD, relative standard deviation; n=2.

	DPC	6-Azauracil
MV (µM)	0.487	0.497
RSD (%)	1	0
Recovery (%)	97	99

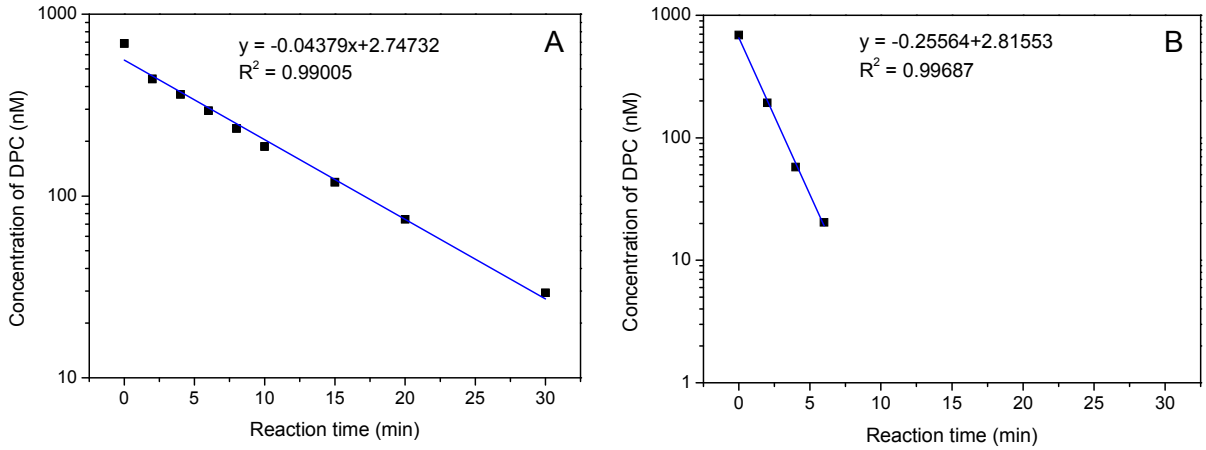

Figure 8.6: (A) Logarithmic scale presentation of the elimination of 100 µg/L DPC spiked with 0.5 mg/L ozone and (B) spiked with 2 mg/L ozone. Both transformations follow pseudo first order kinetics.

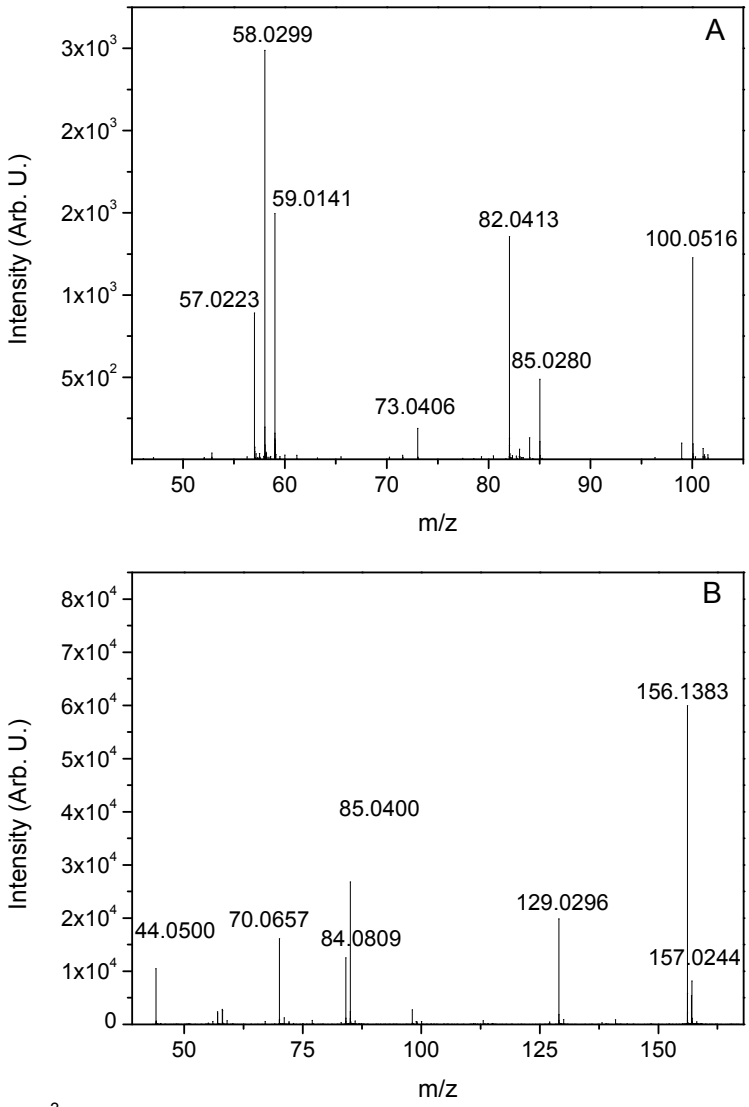

Figure 8.7: (A) MS^3 spectra of OP 3 in negative ionization mode for the fragment ion at *m/z* 100.0516 and (B) in positive mode for the fragment ion at *m/z* 157.0244.

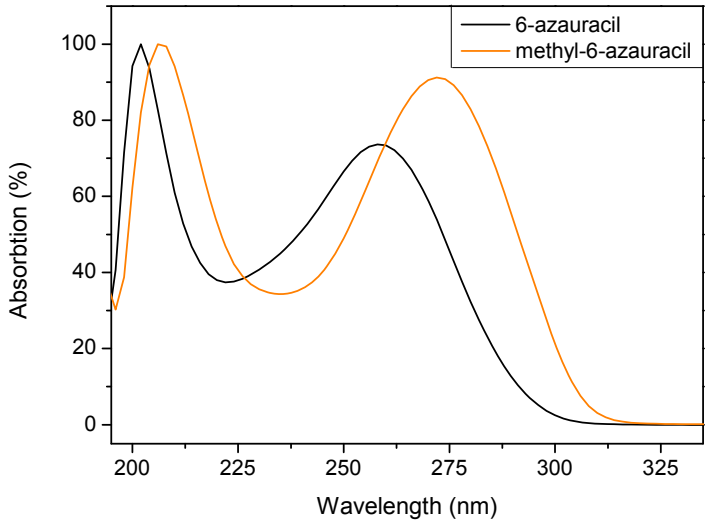

Figure 8.8: Comparison of the UV spectum of 1-methyl-6-azauracil in the ozone-treated sample of M-DPC with the maxima at 207 nm and 272 nm and the UV spectum of 6-azauracil detected in the ozone-treated sample of DPC with the maxima at 205 nm and 258 nm.

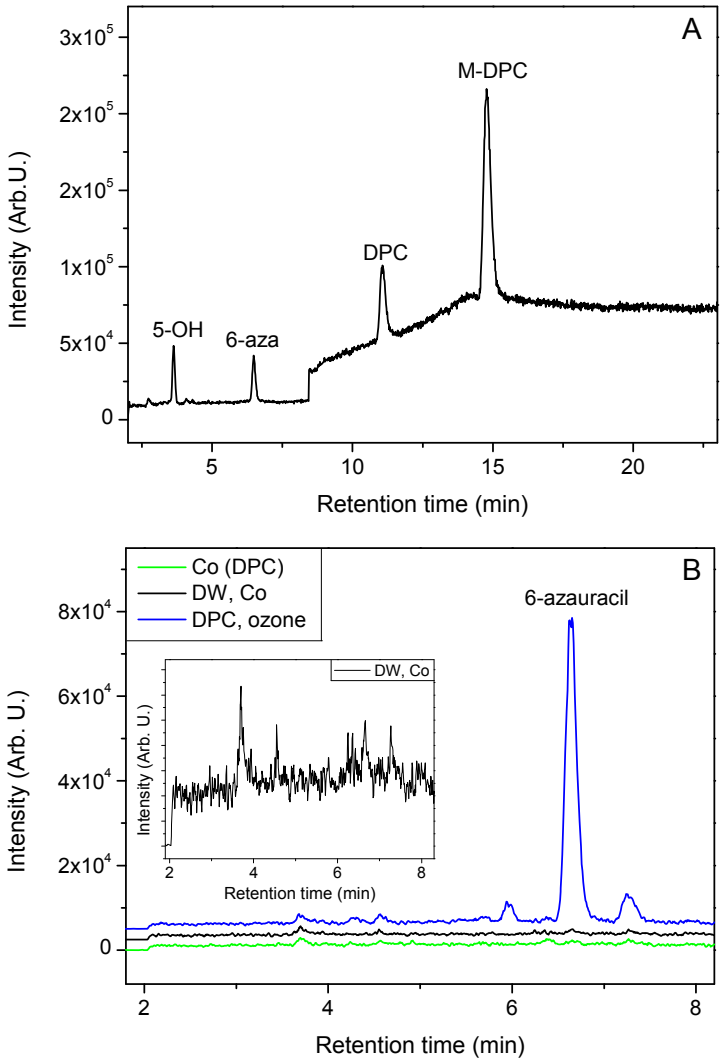

Figure 8.9: (A) Representative spectrum of the chromatographic separation of M-DPC, DPC, 6-azauracil (6-aza) and 5-hydroxyhydantoin (5-OH). (B) Representative chromatogram of 6-azauracil and blanks after SPE enrichment.

List of Publications

N. Schatz, O. Happel and D. Richter. Oxidation des Tolylfluanidmetaboliten N,N-Dimethylsulfamid (DMS).Mitteilungen Umweltchemie Ökotoxikologie 4/2011, 88-89.

N. Schatz, B. Körner, D. Richter, S. E. Kulling and H.-J. Brauch. Ozonation of the chloridazon metabolite desphenyl-chloridazon in water: Oxidation products and reaction pathways (submitted).

N. Schatz, D. Richter, S. E. Kulling and H.-J. Brauch. Ozonung von Desphenyl-chloridazon in Trinkwasser: Bildung von 6-Azauracil. Vom Wasser 3/2012 (accepted).

N. Schatz, D. Richter, S. E. Kulling and H.-J. Brauch. Identification of ozonation products from methyl-desphenyl-chloridazon using high-performance liquid chromatography quadrupole time-of-flight mass spectrometry (submitted).

List of Conference Contributions

Oral presentations:

N. Schatz, D. Richter, H.-J. Brauch and S. E. Kulling, Ozonung von Desphenyl-chloridazon in der Trinkwasseraufbereitung: Reaktionsmechanismen, Oxidationsprodukte und Reaktionspfade. Wasser 2012 - Jahrestagung der Wasserchemischen Gesellschaft Neu-Ulm, 14.-16. Mai 2012.

Poster presentations:

N. Schatz, S. Skrbek, B. Watzl and C. E. Rüfer, Zellulären Aufnahme von Anthocyanen in vitro. 38. Deutscher Lebensmittelchemikertag 2009 Berlin, 14.-16. September 2009.

N. Schatz, O. Happel and H.-J. Brauch, Untersuchungen zum Einfluss von Bromid auf die Umsetzung von N,N-Dimethylsulfamid (DMS) zu N,N-Dimethylnitrosamin (NDMA) während der Ozonung. Wasser 2010 - Jahrestagung der Wasserchemischen Gesellschaft Bayreuth, 10.-12. Mai 2010.

N. Schatz, O. Happel and H.-J. Brauch, Identification of reaction intermediates (RI) and transformation products from *N,N*-dimethylsulfamide (DMS) during ozonation. TransCon 2010 Centro Stefano Franscini, Monte Verità, Ascona, Switzerland, on 12.-17. September 2010.

N. Schatz, O. Happel and H.-J. Brauch, Bromidinduzierte N,N-Dimethylnitrosamin (NDMA)-Bildung bei der Ozonung von N,N-Dimethylsulfamid (DMS). 39. Deutscher Lebensmittelchemikertag 2010 Stuttgart-Hohenheim, 20.-22. September 2010.

N. Schatz, B. Körner, D. Richter, H.-J. Brauch and S. E. Kulling, Ozonation of Chloridazon Metabolites: Identification of Oxidation Products and Transformation Pathways. ICCE 2011 - 13th EuCheMS International Conference on Chemistry and the environment, ETH Zurich, Switzerland, 11.-15. September 2011.

N. Schatz, O. Happel, H.-J. Brauch and S. E. Kulling, Pflanzenschutzmittel-Metabolite nach der Ozonung: Was bleibt? Wasser 2011 - Jahrestagung der Wasserchemischen Gesellschaft Nordeney, 30. Mai-1. Juni 2011.

Nina Jane Schatz

Essenweinstraße 42a, 76131 Karlsruhe

Email: nina.schatz@gmx.de

Date of birth: 12/03/1984 Place of birth: Reutlingen

Curriculum Vitae

Education

2009 – 2012

- PhD thesis at the Water Technology Center (TZW) Karlsruhe in cooperation with the Dept. of Safety and Quality of Fruit and Vegetables at the Max Rubner-Institute Karlsruhe and the Dept. of Chemistry and Biosciences at the Karlsruhe Institute of Technology

2003 –2009

- Academic studies of Food Chemistry at the University of Karlsruhe (TH Karlsruhe)
  Diploma thesis in the Dept. of Safety and Quality of Fruit and Vegetables at the Max Rubner-Institut Karlsruhe
  Topic: Determination of the cellular uptake of anthocyanes *in vitro*
- Degree in Food Chemistry
  First and second part of State Examination for Food Chemists

2000 – 2003

- Hermann-Gundert-Schule Calw
  (Sixth Form College for economics)
  Qualification: General qualification for university entrance

1995 – 2000

- Secondary school Wildberg

1990 – 1995

- Primary school Neubulach

Internship

2006

- Quality Management
  Lindt & Sprüngli Aachen

Acknowledgements

Special thanks go to Prof. Dr. Sabine Kulling from the Max Rubner-Intitut (MRI) for her interest in my thesis, her unceasing support and guidance, and especially for her faith in me and my abilities.

I would like to thank Prof. Dr. Manfred Metzler from the Karlsruher Institut für Technologie (KIT) for his friendly interest in this thesis and for agreeing to act as a co-examiner.

Prof. Dr. Heinz-Jürgen Brauch from the Technologiezentrum Wasser (TZW) is acknowledged for offering me the possibility to do my PhD work in his department and for the creative freedom during my work.

I would like to thank Dr. Doreen Richter for her assistance and support during the last three years, her motivating words and encouragement and for the relaxing time during our lunchbreaks.

Thanks go to Dr. Frank Sacher for his time, the helpful discussions in all matters and especially for his full support during the last weeks of completing my thesis.

Special thanks go to Michael Wenz for his interest in my experiments, his help with solving analytical challenges and for passing on his knowledge to me. I would like to thank Sabine Mertineit for familiarizing me with the ozonation apparatus and her assistance during experiments. I would also like to thank Michael Merklinger for his help. Thanks go to Birgit Körner for her assistance during GC-MS measurements and to Brigitte Raue for her assistance during IC-CD analyses.

I would further like to thank my colleagues from the technological department Sibylla Nordwig-Krauß, Ralf Schäfer and Hans Groß for the pleasant moments in the lab. Furthermore, I thank Andrea Wagner, Sabine Mertineit and Martin Tröster for the time in our office.

Thanks go to Martin Kreutzer for the many phone calls, analytical advice and for being there for me.

Above all I want to greatly thank my family for their unceasing help, understanding, their motivation and their belief in me!